5-2012

Biological Mechanisms And Clinical Implications Of Bcr-Abl-Induced Mitochondrial Oxidative Stress And Cell Survival In Chronic Myeloid Leukemia

Hui Zhang

1. Introduction

1.1 Oxidative Stress and Cancer Progression.

Cancer progression has been viewed as an evolved adaptation of normal cells to a sustained cancer stress microenvironment by succeeding matched gene mutations and cellular non-genetic alterations. Cellular adaptive consequences result in multiple malignant phenotypes, including self-sufficiency in growth signals, insensitivity to anti-growth signals, evading apoptosis, limitless replicative potential, sustained angiogenesis and tissue invasion and metastasis, which are known as six hallmarks of cancer. [1] In the past decade, another two emerging hallmarks have been added to this list, known as reprogramming of energy metabolism and evading immune destruction. [2]

Oxidative stress is defined as an imbalance of the pro-oxidant antioxidant ratio and is characterized as an increase in reactive species (RS). RS are the essential components of cellular redox system and play multiple roles in human physiology and pathology, including two main groups – ROS (derived from oxygen, such as superoxide ($O_2^{-}\cdot$), hydrogen peroxide (H_2O_2), hydroxyl radical ($\cdot OH$)) and RNS (containing nitrogen, such as nitric oxide ($NO\cdot$) and peroxynitrite (-ONOO)). [3] Oxidative stress has been implicated in cancer development through modifying cellular structure, gene expression and enzyme function. [4,5] The etiological study of cancer has indicated that oxidative DNA lesions are correlated with the tumor related gene mutations. [6,7] However, some cancer pathological studies also argued that the increase of oxidative DNA lesions, such as 8-OH-G, is not sufficient to cause malignancy. [6,7] In non-malignant cells, the

elevated level of cellular oxidative DNA lesions may also cause apoptosis or cytotoxicity. In addition, cellular DNA repair process plays an important role for maintain genome stability through limiting the elevated oxidative DNA lesions. A previous study indicated that RS could also impair cellular DNA repair machinery and result in the accumulation of DNA mutations. [8] Besides the direct genetic modification, studies have also demonstrated the crucial role of RS in mediating the tumorigenic function of some non-genotoxic carcinogens.[9] These findings suggested that oxidative stress plays an important role in cancer signal transduction. Further, tumorigenesis studies have demonstrated that RS is required to mediate downstream pathway activation of oncogenes and functional inactivation of tumor suppressors. [10,11] Because persistent oxidative stress can induce various cellular damages, RS also serves as a stress source to trigger cell adaptation and select the malignant seeds leading to abnormal cell growth and survival. [12] Besides regulating cell survival, RS functions as microenvironment stimuli that reprograms cell energy or redox metabolism, and causes Warburg effect or the enhanced content of the detoxification factor glutathione (GSH) in malignant cells. [13]

1.1.1 Reactive Species Induce Modification of Biological Molecules.

According to chemical electron status, RS are divided into two groups, radical and non-radical species. Free radical RS refer to those with an unpaired electron, which have high free energy and are very reactive. Superoxide ($O_2^{-}\cdot$), hydroxyl radical (·OH) and nitric oxide (NO·) are three main cellular radical RS. RS that possess all-paired electrons are called non-radical RS and have a strong

oxidizing capacity. Hydrogen peroxide (H_2O_2) and peroxynitrite (-ONOO) are two main non-radical RS. Among these RS, $O_2^{-}\cdot$ and NO· are two main direct byproducts of cell metabolism which are regulated by subsequent cellular redox reactions. [14] In general, RS can induce damage, oxidation and nitration on cell molecules.

The oxidative DNA lesions are the most common effects of RS. Besides the direct modification on DNA (8-OH-G), RS also induce nucleotide base oxidation and generate pre-mutagenic lesions, such as 8-OH-dGTP and 2-OH-dATP. [15] These oxidized DNA precursors are incorporated into cell genome DNA by DNA polymerase, and further cause cell mutagenesis. [16] This observation was also supported by studies in which activation of MTH1 was shown to hydrolyze and suppress the accumulation of oxidized nucleotides and decrease the rate of tumor formation in aged mice. [17,18] In addition to direct genetic modification, RS are also shown to be correlated with DNA methylation, an epigenetic code suppressing gene expression. The increase of DNA methylation is commonly coincident with increased pro-oxidants or down-regulation of antioxidants. [19-21] Furthermore, the impairment of cellular DNA repair system by RS plays a crucial role in the development of genome instability. DNA strand break rejoining and base excision repair are the main cellular repair machineries protecting DNA against oxidative damage with the reductive environment being important for these processes. [8] Elevated cellular RS, such as H_2O_2, create a pro-oxidant intracellular microenvironment, attenuate the cellular DNA repair activity, and lead to the accumulation of un-repaired gene mutations. [22]

Additionally, RS such as ·OH and NO·, also induce post-translational modifications on protein products. [23,24] RS-induced reversible modifications, such as disulfide bond formation, are largely involved in cell signaling transduction; while RS-induced irreversible modifications, such as carbonylation, are mainly viewed as the oxidative stress-induced protein damage or cellular oxidative stress sensors. [24,25] There are several groups of amino acid residues that have been reported mutated or modified by RS in tumor cells, including sulfur-containing amino acids, carbonylation targeting amino acids and the phosphorylation site residues of proteins. [26,27] Cysteine is a common RS-sensitive sulfur-containing amino acid, which derives multiple oxidative stress-generated products. Mild and moderate oxidative stress result in the reversible cysteine modification, such as S-Nitrosylation, glutathionylation Cys-SH, intra- or inter-disulphide bond formation Cys-S-S-Cys, mixed disulphide Cys-S-S-glutathione and sulfenic acid Cys-SOH. These types of modifications may alter protein conformations and reversibly inhibit or activate enzymes, such as p53, Ras and Akt. Excessive oxidative stress promotes irreversible oxidized products which permanently change the protein activation, such as sulphinic acid Cys-SO_2H and sulphonic acid Cys-SO_3H. In addition, carbonylation is also a common irreversible event caused by excessive oxidative stress and leads to damaging alterations to protein functions. RS induce direct oxidative carbonyl formation of lysine, arginine, proline and threonine. Lysine, cysteine and histidine can also undergo carbonylation through interaction with the lipid and glycation oxidative products. In addition, methionine is another sulfur-containing amino acid,

oxidized to methionine sulfoxide by RS. This reversible modification is important for the regulation of calmodulin, which is an essential calcium regulatory protein. [28] Furthermore, tyrosine phosphorylation induced by RS is an important process that regulates cellular kinase activity and functions in multiple-type tumors and leukemia. Intra-disulfide bond formation in tyrosine kinase protein, such as c-ABL, interrupts the protein kinase activity through regulation of the stability of tyrosine phosphorylation. [29] The nitration of tyrosine, a reversible modification caused by RNS (nitrogen containing RS) prevents phosphorylation and suppresses protein activation, as evidenced by studies of JNK and PKC. [28] Furthermore, the irreversible oxidative modification Tyr–Tyr crosslink Di-Tyr induced by excessive oxidative stress blocks the phosphorylation-mediated regulation at tyrosine. [30]

Cellular lipids are highly diverse, interacting with proteins to form plasma membranes mediating cellular signal transduction, and are also sensitive to oxidative stress. The most common RS-mediated lipid modification is lipid peroxidation which leads to conformation alteration and oxidative degradation of lipids. [31] During lipid peroxidation, lipids transfer electrons or lose allylic hydrogens to RS generating fatty acid radicals, lipid peroxides or cycling peroxides. This process mainly affects polyunsaturated fatty acids, which contain multiple double bonds and act as the reactive hydrogen donors. The entire process includes two main steps: initiation and propagation. Highly reactive RS, such as ·OH and –ONOO, can react with lipids and produce unstable primary fatty acid radicals. After initiation, the primary fatty acid radicals react with

molecular oxygen and further generate unstable peroxyl-fatty acid radicals. The peroxyl-fatty acid radicals may react with other fatty acids to form new fatty acid radicals and lipid peroxides or just cyclic peroxides. This process is a continuous cycle due to the new fatty acid radical formation which subsequently changes the cellular lipid conformation. Cellular antioxidants, especially the phospholipid hydroperoxide glutathione peroxidase, can scavenge lipid radicals and terminate the lipid peroxidation chain reaction. The deficiency of such cellular antioxidants results in an elevated lipid peroxidation or damage of cellular membrane structures, and subsequently activates cellular stress-sensitive signaling pathway.[31]

1.1.2 Reactive Species Function in Tumor Growth Signal Transduction.

Studies have identified that RS can function as signal transduction factors that promote cell growth. [1] Cell mitogenic growth factors, such as PDGF and TGFα, can promote mitosis through the activation of receptor kinase pathway, notably PDGFR/Ras/MAPK pathway. This pathway has been demonstrated as a redox sensitive pathway. [32] RS play a role in activated phosphorylation of tyrosine kinase receptor and Ras through protein thiol modification, and further stimulate the downstream MAPK pathway activation. [32] In addition, RS induce the oxidative inactivation of a specific phosphatase, which inhibits this pathway that promotes the dephosphorylation of the kinases. [32] Signal transduction mediated by RS has also been reported in a study of tumor-related angiogenesis. Angiogenesis, the process of the new blood vessel formation, plays an essential role in tumor progression and metastasis. Tumor cell-secreted VEGF stimulates

the activation of endothelial cells and promotes angiogenesis. During this process, RS function in up-regulating the VEGF expression and mediate the activated of VEGFR downstream pathway. [33] HIF-1 is the important transcription factor to up-regulate VEGF expression in response to hypoxia. [34] HIF-1 is a heterodimer of HIF-1α and HIF-1β. HIF-1α is localized in the cytosol and undergoes an oxygen-mediated degradation process. RS molecules, such as $O_2^{-}\cdot$ and H_2O_2, block such degradation process and stabilize HIF-1α. The stabilized HIF-1α translocates to the nucleus to bind with HIF-1β to trigger the transcription activity of HIF-1, and up-regulates VEGF expression as well. In endothelial cells, VEGFR2 is the crucial VEGF receptor to mediate tumor cell-stimulated tube formation. RS, especially $O_2^{-}\cdot$ derived from cellular NADPH oxidase, inhibit the tumor suppressor protein tyrosine phosphatases PTEN, and stimulate the auto-phosphorylation-mediated activation of VEGFR2. [33] Besides angiogenesis, RS is also involved in regulating integrins during metastasis. Integrins are a group of cell surface transmembrane heterodimeric receptor proteins, consisting of two non-covalently bound glycoprotein α and β. RS promote integrin expression and further stimulate the communication between tumor cells and extracellular matrix.[35] The ligand binding affinity of integrins is regulated by the disulfide formation between α and β glycoproteins, which is a redox-sensitive process and depends on the levels of RS. [35] In addition, a late stage of tumorigenesis is linked to extra-cellular matrix degradation, which is an essential process for endothelial cells migration into the tumor tissue. Matrix metalloproteinase (MMP) cooperates with integrins regulating cell invasion and

metastasis. [5] MMPs are secreted from tumor cells and phagocytes (especially macrophages). [36] RS and RS-sensitive growth factors are also involved in regulating MMP expression. A study has shown that RS promote cellular MMP9 expression. Also, VEGF can up-regulate MMP1 and MMP2. [37,38]

Besides the function in promoting cell growth, RS also function as a stress source to promote cellular redox-sensitive survival machinery activation, such as activating cell survival transcription factors, stimulating kinase pathways and altering cellular metabolism. [28] Moderate levels of RS promote cell survival through activation of transcription factors, such as NFκB, Nrf2 and HIF-1, as well as kinase pathways, such as PI3K/Akt pathway. [28] NFκB mainly responds to mitochondria derived RS, and up-regulates anti-apoptotic factors and survival antioxidants, such as IAPs and SOD2. [28] Nrf2 mainly responds to the ER stress and exogenous carcinogens, and promotes the expression of the acute stress-induced antioxidants and cellular detoxification factors, such as HO-1 and glutathione (GSH) system factors. [28] HIF-1 mainly responds to the cellular oxygen status, such as hypoxia, and stimulates the expression of angiogenesis factors and energy-generating enzymes, such as VEGF and glycolysis pathway enzymes. [28] Besides the above transcription factors, PI3K/Akt kinase pathway is another crucial survival pathway involved in the cellular oxidative stress response. The survival function of PI3K/Akt pathway is mainly through up-regulation of BCL-2 family anti-apoptotic factors, and inactive phosphorylation of cellular pro-apoptotic factors or cell death signal mediators, such as BAD and ASK1. [28]

1.1.3 Reactive Species Disrupt Cell Cycle and Evades Cell Death.

In normal cells, multiple anti-growth signals maintain the cellular quiescent status and regulate the homeostasis process that responds to the external or intrinsic stress stimuli. Tumorigenic stress may also force the benign cells into cell cycle arrest or apoptosis. Malignant cells are believed to derive from the pre-malignant ones which successfully disrupt the normal cell cycle regulation and escape from the stress-induced cell death. [1] RS are linked to this process and serve as the stress source to promote malignancy transformation.

At the molecular level, pRb and p53 play important roles in regulating cell cycle and function as tumor suppressors. Disruption of pRb or p53 is a key step for tumor progression. Mammalian pRb and its relatives are the mediators of the multiple cell arrest signals. Hyper-phosphorylation of pRb blocks cell cycle by inhibiting the E2F transcription factors which control the expression of genes involved in the normal cell cycle, especially from G1 to S stage. [39] The pRb pathway cooperates with mitogenic signaling pathways to promote intracellular RS generation. The increased RS activate PKCδ, which promotes the further elevation of RS, and forms a RS-PKCδ feedback loop. [40] This RS-PKCδ loop is not only involved in inhibition of cell proliferation but also in induction of cell survival. In addition, a previous in vitro study has suggested that pRb is regulated by protein oxidation through oxidation of the specific methionine to methionine sulfoxide. [41] This modification alters the serine phosphorylation of pRb induced by kinases and disrupts the regulating function of pRb in cell cycle. Similar to pRb, p53, another crucial factor that regulates cell proliferation, is also

regulated by RS, but in a more complicated process. Responding to the different levels of cellular oxdative stress, p53 promotes various biological consequences, such as DNA repair, senescence and apoptosis. [5] The expression of several crucial antioxidants is regulated by p53 at transcriptional level, including GPX1, catalase and SOD2. [42] Additionally, p53 is also involved in the regulation of cellular RS generation machineries, such as mitochondrial respiratory chain. Conversely, function of p53 is also regulated by RS-mediated protein modification. Protein phosphorylation induces controversy effects on p53 depending on the RS level.[43] There are ten cysteine residues localized in p53 DNA binding region. RS could alter the p53 conformation by modifying these cysteine residues. Such structure alterations cause the similar effects of p53 mutations, and attenuate the p53 DNA binding activity. One study has shown the potential malignant biological consequences induced by p53 cycteine residue oxidations. Using an in vivo mouse model, researchers have observed that interruption of redox-directed regulation of Cys173, 235 or 239 of p53 caused complete loss of p53 tumor suppressor function as well as gained oncogenic function. [44] This study showed the potential malignant biological consequences induced by p53 cycteine residue oxidations.

Taken together, the cellular oxidative stress plays important roles in cancer progression through induction of genome instability, interruption of cell growth and promotion of cell survival. RS not only cause DNA mutations that activate proto-oncogene or inhibit tumor suppressor, but also mediates malignant signal transduction through various biological modifications (Figure 1).

Figure 1. Biological functions of oncogene-induced ROS. The direct effects from ROS and the relative biological consequences in malignant cells are listed.

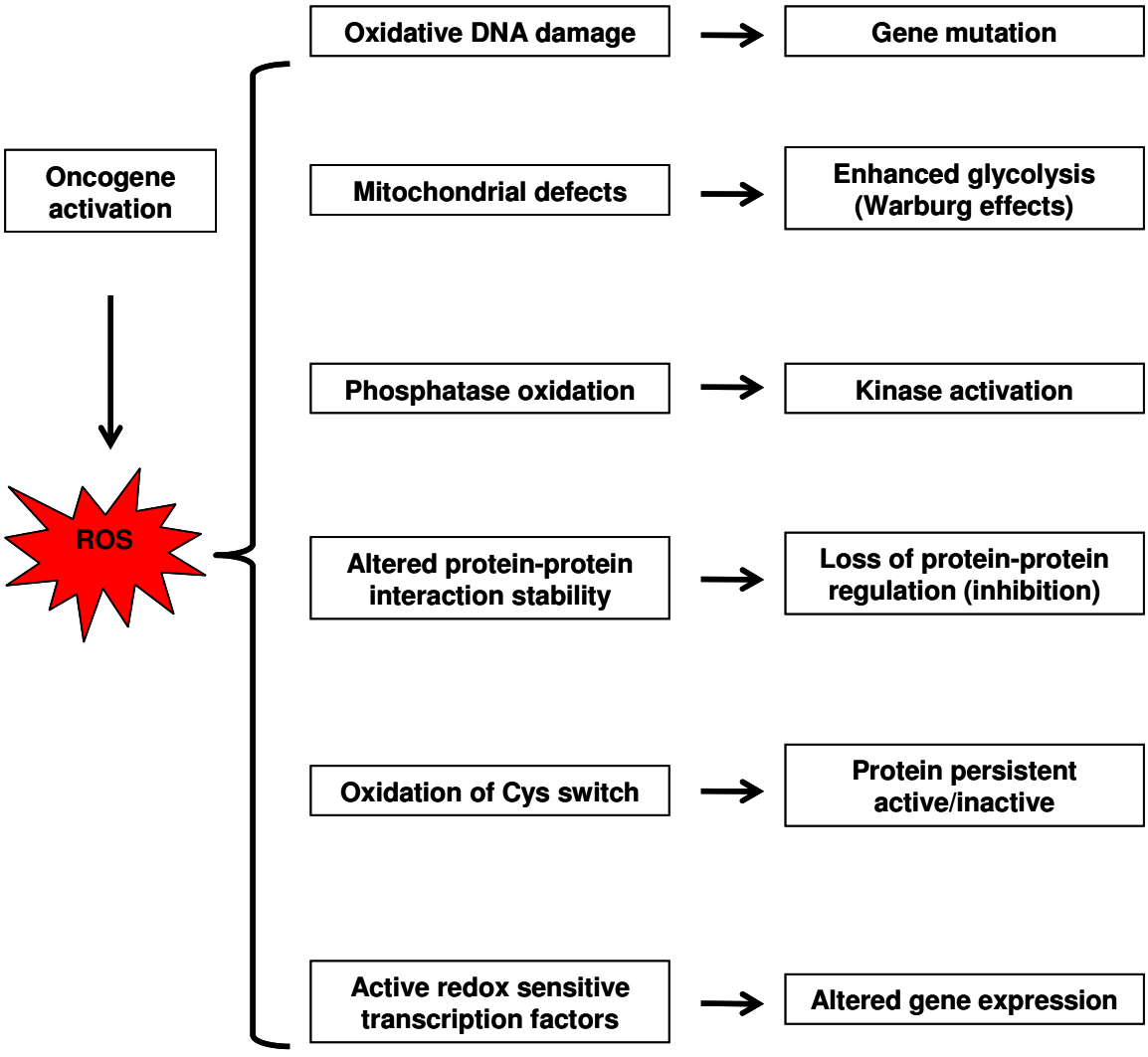
Oncogene activation
ROS
Oxidative DNA damage
Gene mutation
Mitochondrial defects
Enhanced glycolysis (Warburg effects)
Phosphatase oxidation
Kinase activation
Altered protein-protein interaction stability
Loss of protein-protein regulation (inhibition)
Oxidation of Cys switch
Protein persistent active/inactive
Active redox sensitive transcription factors
Altered gene expression

1.2 BCR-ABL Positive CML and Oxidative Stress.

Chronic myeloid leukemia (CML) causes abnormal growth and survival of myeloid precursor cells in the bone marrow and blood. CML represents approximately 15-20% of all adult leukemia, and often occurs during or after middle-age. CML is grouped into chronic, accelerated and blast crisis phases. The chromosome 9/22 translocation (Philadelphia chromosome, Ph) has been identified in about 95% CML cases. Bcr-Abl fusion gene as the result of Ph chromosome encodes a tyrosine kinase oncoprotein, which is constitutively active and functions distinctly from the endogenous c-ABL. (Figure 2) [45-47] The association between CML malignancy progression and BCR-ABL activation has been demonstrated in vitro and in vivo. [48-50] There are several variants of BCR-ABL oncoprotein, including 230 kD, 210 kD and 190 kD isoforms. The 210 kD BCR-ABL (b2a2 or b3a2) is well studied and is linked with the development of CML through suppression of normal hematopoiesis and promotion of abnormal cell survival in hematopoietic progenitor cells. [51,52]

Figure 2. The formation of Ph Chromosome and *BCR-ABL* fusion gene. *BCR* locates on chromosome 22. *ABL* locates on chromosome 9. Chromosome 9/22 translocation generates Ph chromosome and *BCR-ABL* fusion gene.

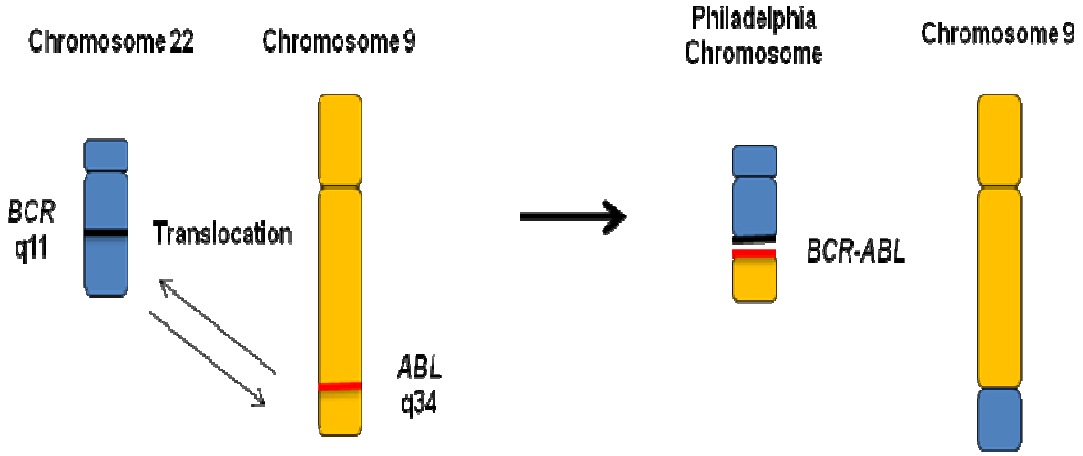
Chromosome 22
Chromosome 9
Philadelphia Chromosome
Chromosome 9
BCR
q11
Translocation
ABL
q34
BCR-ABL

1.2.1 BCR-ABL Induces Cellular ROS Elevation.

The elevation of cellular oxidants plays an important role in malignancy initiation and progression by creating a favorable environment for cancer and leukemia cell. [53-57] Superoxide ($O_2^{-}\cdot$) and hydrogen peroxide (H_2O_2) are the two most abundant stable forms of intracellular ROS. Mitochondria and cellular membrane bound NADPH oxidases (NOXs) are key sites for ROS generation in leukemia cells. The accumulation of the intracellular $O_2^{-}\cdot$ and H_2O_2 is mainly regulated by superoxide dismutases (SODs) and glutathione peroxidases (GPXs). [14] The oxidative environment results in a self-perpetuating process and induces tumorigenesis-associated gene mutations by DNA damage. In addition, oxidative stress also induces protein modifications and activates the carcinogenesis-related transcription factors or kinases.

The increased oxidative DNA damage and the elevated intracellular ROS production have been observed in BCR-ABL transformed cells, which can be abrogated by the treatment of BCR-ABL kinase inhibitor or ROS scavenging agents. [58-60] The consistent genetic and redox alterations have been found in human CML primary cells compared with normal bone marrow cells from healthy donors. [58,59,61] Furthermore, the mechanistic study of BCR-ABL-induced ROS elevation has demonstrated that BCR-ABL-induced ROS increase is associated with phosphorylation at Tyr-177 residue of BCR-ABL, activation of PI3K pathway, up-regulation of cellular glucose metabolism and elevation of mitochondrial respiratory chain activity. [60,62,63]

1.2.2 ROS and BCR-ABL Activation.

The kinase activity of BCR-ABL is related with its tyrosine residue phosphorylation status, which is negatively regulated by protein tyrosine phosphotases (PTPase) through dephosphorylation. Previous studies have demonstrated that H_2O_2 induces the same effective inhibition of PTPase as PTPase inhibitor pervanadate in non-malignancy human megakaryocytic cell MO7e. The inhibition of PTPase by H_2O_2 can enhance phosphorylation and tyrosine kinase activity of proto-oncogene c-ABL. [62] These results have indicated that ROS may contribute to the constitutively tyrosine kinase phosphorylation of BCR-ABL by suppressing PTPase-mediated protein dephosphorylation. Besides regulating PTPase activity, ROS has been shown to stabilize tyrosine phosphorylation of BCR-ABL through generation of protein intra-disulfide bond formation. [64] In addition, clinic and laboratory studies have identified that the elevated cellular ROS contributes to the generation of tyrosine kinase inhibitor-resistant mutants by promoting oxidative DNA damage of native BCR-ABL in CML cells. [59]

1.2.3 BCL-XL Mediates Cell Death Resistance in BCR-ABL Cells.

BCR-ABL functions in evading apoptosis and promoting abnormal survival in CML cells. [65] B-cell lymphoma-extra large (BCL-XL) is a crucial downstream survival factor of BCR-ABL. [66,67] BCL-XL enhances cell survival through suppressing the activation of pro-apoptotic factors. [68] In addition, BCL-XL has been found to attenuate growth factor withdrawal or CD95 activation-induced cell death by preventing the depletion of cellular GSH. [69,70] High intracellular GSH

content is the crucial metabolic cofactor for the development of drug-resistance and abnormal cell survival. [71-73] One recent study has identified that over-expression of BCL-XL may cause the dramatic increase of cellular GSH through activation of pentose phosphate pathway. [74] A previous study has demonstrated that BCR-ABL promotes BCL-2 independent anti-apoptotic function through up-regulating BCL-XL. [75] Inhibition of BCR-ABL by ABL kinase inhibitor CGP 57148 (Imatinib) induces severe cell death along with the down-regulation of BCL-XL in CML cell line K562. Over-expression of BCL-XL in parental K562 cells prevents CGP 57148-induced cell death. [76] BCR-ABL-induced BCL-XL up-regulation is mainly mediated by signal transducer and activator of transcription 5 (STAT5). [77] The cytokine-independent and kinase-dependent constitutive activation of STAT5 has been demonstrated in CML cells. [78] Previous studies have identified that both SH2 domain and SH3 domain proline-rich binding sites of BCR-ABL are required for the activation of STAT5.[79] Additionally, hematopoietic cell kinase (Hck) interacts with BCR-ABL SH2 and SH3 domains as a downstream activation kinase of BCR-ABL. The activation of Hck leads to the phosphorylation of STAT5B on Tyr699 residue and stimulates the activation of STAT5. [80] Intriguingly, two recent studies have indicated that both IL-3R/JAK2 dependent and independent regulation play important roles in up-regulating BCL-XL in BCR-ABL-expressing cells. [81] The elevation of cellular ROS may also be involved in mediating up-regulation of BCR-ABL, because previous studies have demonstrated that the increase of cellular ROS can mediate the activation of STATs in non-BCR-ABL cells, including STAT1, STAT3 and STAT5. [82,83]

Additionally, BCL-XL repressor, interferon consensus sequence binding protein (ICSBP) is also dramatically down-regulated in chronic stage CML patients. [84,85] Taken together, it is suggested that BCL-XL is a specific BCR-ABL downstream survival factor activated through multiple modes of regulation.

1.2.4 Glutathione Redox Buffer System.

Glutathione (GSH) is a ubiquitous small thiol peptide at mM range concentrations, and functions as the essential intracellular redox buffer factor in mammalian cells. [73] Under normal physiological condition, cellular ROS scavenging function mainly depends on GSH metabolism. GSH functions as the substrate for the reduction of H_2O_2 to H_2O by GPXs. GSH oxidized product GSSG is recycled back to the reduced form of GSH by glutathione reductase (GR). [86] GPX1 is the most abundant intracellular GPX enzyme and plays a key role to scavenge H_2O_2. [87] Therefore, both intracellular GSH content and GPX1 activity are important for maintaining proper cell redox balance. Cellular GSH content is associated with GSH synthesis, transport and distribution. Two key enzymes, γ-Glutamyl-cysteine synthetase (GCLC) and glutathione synthase (GSS) catalyze GSH synthesis using glutamate, cysteine and glycine as substrates. [88] The intracellular and extracellular GSH transport and distribution are regulated by Gluathione-S-transferases (GSTs) and membrane GSH efflux pumps. [89]

1.2.5 Clinical Application of BCR-ABL Targeting Inhibitors.

In the past few years, BCR-ABL targeting inhibitors have been developed for the chemotherapy of CML. [90] Imatinib mesylate (Gleevec) has shown high

clinical response rate and represents the first generation of BCR-ABL tyrosine kinase inhibition reagents. Due to its good selectivity, Imatinib has become the front-line reagent for CML. [91,92] This merit of Imatinib has been demonstrated by both a long term randomized clinical study and the successful clinical trial of higher dose Imatinib in CML therapy. [93-95] However, only about 65-75% of early stage CML patients respond to Imatinib. Moreover, more advanced stage of CML are resistant to Imatinib. In addition, a set of BCR-ABL mutants have been identified to cause Imatinib-refractory CML in patients. These mutants result in the three-dimensional structure alteration at the kinase activation site, and induce constitutive kinase activity due to the decrease in Imatinib affinity. [96-99] In order to overcome Imatinib-resistance, the second generation BCR-ABL tyrosine kinase inhibitors have been developed. Dasatinib (BMS0354825), one of these second generation inhibitors, has been approved for the treatment of CML by the FDA. Clinical trials have demonstrated that Dasatinib effectively eliminates various Imatinib-resistant mutants except the one harboring BCR-ABL-T315I mutation. [100-102] The limitations of BCR-ABL inhibitor reagents have inspired the development of alternative therapeutic strategies dependent on the further understanding of drug resistance in CML. [103,104]

2. Hypothesis and Specific Aims

The major goal of this study is to understand the role of BCR-ABL in inducing persistent intracellular oxidative stress in CML. Oxidative stress occurs with an overabundance of ROS, and results in cell differentiation or apoptosis under normal physiological conditions. Previous studies have demonstrated that BCR-ABL promotes malignancy development along with the increases of cellular and mitochondrial ROS generation. However, the essential survival factors protecting CML cells against oxidative stress are still unclear. The increase of ROS generally triggers the antioxidant response which protects against apoptosis through activation of intracellular redox enzymes. But, are there any unique cell survival machineries responsive to oxidative stress in malignant cells? This is a question worthy of further investigation. Previous studies have found that several molecular factors functioning in antioxidant enzyme expression are dysfunctional in BCR-ABL cells, such as FOXO3, ATM/ATR and P53. [105-107] Consistently, some antioxidant enzymes specifically responsive to intracellular H_2O_2 accumulation are decreased in some BCR-ABL positive patients or cultured human CML cells, such as GPX1 and catalase. [92,108] It is worth noting that some transcription factors responding to oxidative stress are up-regulated or activated in BCR-ABL cells, such as STAT5 and NF-κB. [77,109] Furthermore, their downstream anti-apoptotic factors are over-expressed in BCR-ABL cells, such as BCL-XL and BCL2. [75,110] These findings suggest that BCR-ABL may render cells to be more dependent on anti-apoptotic factors rather than antioxidant enzymes in tolerating intra- or extra-cellular oxidative stress. Taken

together, **I hypothesize that BCR-ABL induces mitochondrial oxidative stress, while protecting against oxidative stress-induced CML cell apoptosis through up-regulation of BCL-2 family survival factors.**

To address the above hypothesis, I will investigate the following specific aims in this study:

Aim 1: Identifying the function of glucose metabolism in BCR-ABL-induced mitochondrial oxidative stress. Previous studies have indicated that glucose metabolism is important for mitochondrial ROS increase in cells stably transfected with BCR-ABL. [60,62,63] Whether such biological alterations are either initial changes induced by BCR-ABL or late adaptations to malignant signals is still unknown. Therefore, the BCR-ABL inducible model will be used to evaluate the correlation between glucose metabolism and mitochondrial ROS level.

Aim 2: Investigating the role of BCL-2 and BCL-XL in protecting CML cell against oxidative stress-induced apoptosis. Up-regulation of BCL-2 and BCL-XL in leukemia has been identified by numerous studies. [75,110] BCL-XL is the direct downstream survival factor of BCR-ABL through activation of STAT5. BCL-2 functions in malignant development, and mediates BCR-ABL-independent Imatinib-resistance in some CML patients. [111] In addition, the heterogeneous BCL-XL and BCL-2 has been observed in CML cells. The goal of this specific aim is to identify the dominant survival factors responsive to oxidative stress in CML. To achieve this goal, BCR-ABL inducible cells, CML cells with differentially expressing levels of BCL-XL and BCL2, genetically modified BCL-XL or BCL-2 expressing cells and BCR-ABL stable transformed cells will be used. The initial

survival factor responsive to BCR-ABL induction will be evaluated. The sensitivity of oxidative stress-induced apoptosis and the biological alterations of mitochondria will be tested in the cells with differential level of BCL-XL and BCL-2 expression.

Aim 3: Testing the cell killing effects of redox modulating agents in CML. BCR-ABL-induced ROS elevation plays an important role in malignancy development. On the other hand, such enhanced ROS accumulation might serve as a biochemical basis to preferentially promote cell apoptosis via further oxidative stress induction. BCR-ABL contains multiple redox-sensitive cysteine residues which could be oxidized by ROS and cause protein instability. Previous studies have suggested that modulation of cellular antioxidant GSH content by N-acetylcysteine (NAC, an antioxidant) or BSO (an inhibitor of glutathione synthesis) affects BCR-ABL stability. [112,113] Based on the previous findings, I will use a redox modulating agent, β-phenylethyl isothiocyanates (PEITC, a natural compound found in edible cruciferous vegetables) to target the cellular glutathione (GSH) system and test the cell viability of CML cells. In addition, I will also test redox modulation-induced cell killing effects in cells harboring T315I-BCR-ABL (the most drug-resistant BCR-ABL mutant observed in clinic), T315I-BCR-ABL transformed cells and T315I-BCR-ABL positive patient samples. Furthermore, the effective combination of redox modulating agents and other drugs will be also investigated. CML cells exhibit substantial phenotypic heterogeneity. Certain sub-populations of cells carrying a secondary mutation, such as BCL-2, often escape from primary treatment of Imatinib and enhance

disease recurrence risk. Even under the condition that Imatinib is efficient to inhibit the activation of BCR-ABL, the diseased cells may still survive but become more sensitive to extreme stress. Using a redox modulating agent PEITC as a combination agent may promote massive cell death in such cells. To test this point, I have established a cell model with fluorescence-linked heterogeneous BCL-XL and BCL-2 expression in CML cells. Imatinib or oxidative stress-induced cell death will be investigated in the cells with different BCL-XL and BCL-2 genetic background.

3. Materials and Methods

3.1 Chemicals and Reagents.

Doxycycline, 30% H_2O_2, β-phenylethyl isothiocyanate (PEITC, C_9H_9NS), N-acetyl cysteine (NAC), and bovine catalase were purchased from Sigma-Aldrich (St. Louis, MO). Imatinib mesylate (Gleevec) and ABT737 were purchased from Chemie Tek (Indianapolis, IN). 'Active caspas-3, caspase inhibitors Z-VAD-FMK and Z-DEVD-FMK were obtained from BD Biosciences (San Jose, CA). The proteasome inhibitor MG132 was acquired from EMD biosciences (Calbiochem, San Diego, CA). Drugs were dissolved in DMSO and further diluted with culture medium before use. The final DMSO concentrations in the cell culture medium were less than 0.1% (v/v). Bovine catalase was freshly dissolved in culture media and sterilized by passing through 0.2 μm sterile syringe filter (Corning, NY) before use.'[114]

3.2 Plasmid Transfection.

Human HA-Bcl-XL plasmid was a gift from Dr. Paul Chiao and Dr. Xiangwei Wu (MD Anderson Cancer Center, The University of Texas). Human GFP-Bcl2 plasmid was obtained from Addgene (Cambridge, MA). Tet-on Human Bcl-XL shRNA plasmid was purchased from Thermo Scientific-Open Biosystems (Huntsville, AL). All the transfection reagents were purchased from Life Technologies-Invitrogen (Carlsbad, CA). Cells were starved in serum free media for 8-12 hours, and then seeded at 1E6 cells/ml in six-well plates. Plasmid DNA 2 – 4 μg was diluted by 500 μl Opti-MEM (Invitrogen), and transfected into cells using lipofectamine 2K (Invitrogen). Transfected cells were cultured in serum

free media for another 12 – 24 hours, and then diluted into 2E5cells/ml in culture media with 10% serum. 2 μg G418 (Cellgro, Manassas, VA) was used in the selection for HA-Bcl-XL and GFP-Bcl2 transfected cells. 4 μg Puromycin was used in selection for Tet-on Human Bcl-XL shRNA transfected cells. After one month of selection, the enriched HA-Bcl-XL or GFP-Bcl2 transfected cell pools were tested for the presence of transgene by Western blotting. The enriched Tet-on Human Bcl-XL shRNA transfected cell pool was maintained in tetracycline free media and decrease of BCL-XL in the presence or absence of doxycycline 0.5 – 1.0 μg/ml was tested by Western blotting.

3.3 Cell Lines and Cell Culture.

'All human and murine BCR-ABL positive cells were maintained in RPMI 1640 medium with 10% fetal bovine serum (FBS) at 37℃ in an atmosphere of 5% CO_2 balanced humidified air. K562 cell line expressing the 210 kD BCR-ABL protein was derived from a female myeloid CML patient in blast crisis. [115] KBM5 cell line expressing the 210 kD BCR-ABL protein was derived from a female myeloid CML patient in blast crisis. [116,117] KBM5-T315I was derived from KBM5 by exposing to increasing concentrations of Imatinib leading to the selection of surviving clones harboring T315I mutation. [118] KBM5-T315I cells were routinely maintained in culture medium containing 1 μM Imatinib. In studies where KBM5-T315I cells were compared with the parental KBM5 cells, Imatinib was washed off and KBM5-T315I cells were cultured in drug free medium for several days before the experiments. All the murine cells are gifts from Dr. Ralph Arlinghaus (MD Anderson Cancer Center, The University of Texas). TonB210 cell line was

derived from the murine BaF3 cells by transfection using Tet-on *BCR-ABL*. TonB210 cells were maintained with IL3 at 1.0 – 4.0 ng/ml. The induction of BCR-ABL was through addition of 0.5 – 1.0 µg/ml doxycycline into culture media. 32D-p210 cells were derived from the murine 32D cells by transfection using *BCR-ABL*. Parental 32D cells were maintained with 1.0 – 4.0 ng/ml IL3. BaF3-Bcr-Abl cells and BaF3-Bcr-Abl/T315I cells were derived from the murine BaF3 cells by transfection using *BCR-ABL* or T315I-mutated *BCR-ABL*. [119-121 ،114]

3.4 Isolation of Primary CML Cells.

'Normal lymphocytes and primary CML cells were isolated from fresh peripheral blood samples from health donors and CML patients, respectively, after obtaining informed consent in accordance with a research protocol approved by M. D. Anderson Cancer Center institutional review board (IRB). Patients CML1 and CML2 were at blast crisis stage. Patient CML2 was identified to carry BCR-ABL-T315I mutant. Cells were isolated using gradient centrifugation with Fico/Lite lymphoH (d=1.077, Atlanta Biologicals, Atlanta, GA). After isolation, cells were washed by phosphate-buffered saline (PBS) and suspended in fresh culture medium. All drug treatments started after the cells were pre-cultured for 24 hours. The peripheral blood specimens were obtained from CML patients after proper informed consent under a research protocol approved by IRB of the University of Texas MD Anderson Cancer Center.'[114]

3.5 Measurement of Cellular ROS.

'Cellular ROS contents were measured by incubating the control and experimental cells with 1.0 - 2.5 µM of CM-H_2DCF-DA (Life technologies-

Invitrogen, Carlsbad, CA) for 60 minutes as the chemical probe for ROS. CM-H_2DCF-DA is cell membrane permeable, and once insider cells, reacts with H_2O_2 and other ROS species to generate green fluorescence. The intensity of green fluorescence, reflecting cellular ROS contents, was measured by flow cytometric analysis. ‘[114]

3.6 Measurement of Mitochondrial ROS.

Mitochondrial ROS contents were measured by incubating the control and experimental cells with 1.0 - 2.0 μM of MitoSOX Red (Life technologies-Invitrogen, Carlsbad, CA) for 60 minutes as the chemical probe for mitochondrial ROS. MitoSOX Red is cell membrane permeable, and accumulates in the mitochondria and mainly reacts with superoxide to generate red fluorescence. The intensity of red fluorescence, reflecting mitochondrial ROS contents, was measured by flow cytometry.

3.7 Measurement of Cell Lactate Release.

Cell lactate production during growth was detected by the Accutrend Lactate analyzing system purchased from Roche (Mannheim, DE). Differentially treated cells were incubated in fresh media for 48 hours. Each aliquot of the cultured media was collected at a volume of 30 μl to detect lactate concentration in a range between 0.8 – 22 mM according to manufacturer’s instruction.

3.8 Oxygen Consumption in Whole Cells.

Oxygen consumption in cells was measured by a Clark type oxygen electrode system purchased from Hansatech Instruments (Norfolk, UK). Cells were incubated with different experimental conditions, and then harvested by

centrifugation. The samples were resuspended in air saturated 37℃ media (O_2 21%) and immediately added into the oxygen chamber. The oxygen consumption rate was measured in the sealed off chamber for 15 minutes. Oxygen consumption curves were generated for each experimental condition.

3.9 Measurement of Mitochondrial Membrane Potential.

Mitochondrial membrane potential was assessed by the cationic voltage-sensitive lipophilic dye Rhodamine 123 (Life technologies-Invitrogen, Carlsbad, CA). Cells were incubated with different experimental conditions and labeled with 200 nM Rhodamine 123 for 30 minutes. The fluorescence of Rhodamine 123 in the washed and resuspended samples was measured in channel FL-2 by flow cytometry. The dramatic drop of florescence is indicative of mitochondrial membrane collapse.

3.10 Detection of GFP-BCL2 Mitochondrial Localization.

MitoTracker Red (CMXRos, Life technologies-Invitrogen, Carlsbad, CA), a red fluorescent dye to stain mitochondria in live cells, was used to visualize mitochondria. Mitotracker Red was directly added into cell suspensions at 200 nM for 60 minutes. Total 0.5E5 cells of each sample were collected for cytospin. The slides and filters were placed into appropriate slots in the cytospin. Cells were loaded into chamber and collected onto slide by spin down at 1000 RPM 10 minutes (Shandon Cytospin 2). The samples on slides were washed with cold PBS twice and fixed with 4% paraformaldehyde for 20 minutes. Samples were then coated with Mounting Medium with DAPI purchased from UltraCruz (Santa Cruz, CA), and further analyzed by confocal microscope.

3.11 Isolation of Mitochondria.

Cell pellets were washed with cold PBS, and then resuspended in RSB buffer (10 mM NaCl, 1.5 mM $CaCl_2$, 10 mM Tris-HCl, pH 7.5) to allow cells TO swell for 10 minutes. The pellets were homogenized with a tight-fit glass tissue homogenizer for 10 strokes, and the mixed with 2.5 X MS buffer (525 mM mannitol, 175 mM sucrose, 12.5 mM Tris-HCl, pH 7.5, 12.5 mM EDTA) to the final 1 X MS buffer concentration. Nuclei and unbroken cells were removed from homogenates by centrifugation at 1300 g for 5 minutes twice. The supernatants were transferred to fresh tubes and centrifuged at 17,000 g for 20 minutes to pellet mitochondria fragments. The mitochondria pellets were further washed with 1 X MS buffer three times, and then resuspended in SDS lysis buffer for Western blotting analysis.

3.12 Measurement of Cellular Glutathione.

Two different methods were used to evaluate cellular glutathione. 'In one way, total cellular glutathione contents were measured by using a DTNB-enzyme cycling glutathione assay kit (Cayman Chemical, Ann Arbor, MI). Cell extracts were prepared from the control or drug-treated cells by sonication and deproteinization. The glutathione and DTNB reaction product, yellow colored TNB, was detected by 96-well plate reader at absorbance A414 nm. The cellular glutathione contents were calculated using the standard curve generated in the experiments with parallel standard glutathione samples, and data from each individual experiment were normalized to control (100%).'[114] In the other way, relative cellular glutathione levels were measured by incubating the control and

experimental cells with 200 - 400 nM of CMFDA (Life technologies-Invitrogen, Carlsbad, CA) for 60 minutes as the chemical probe for cellular thiols. CMFDA is cell membrane permeable, and reacts with thiols to generate green fluorescence. The intensity of green fluorescence, mainly reflecting free glutathione contents (98%), was measured by flow cytometry.

3.13 Quantitative Real-Time PCR Analysis for GPX1 Expression.

32D and 32D-p210 cell pellets were collected at the exponential growth stage. Total RNA of each sample was isolated using TRIzol Reagents purchased from Life technologies-Invitrogen (Carlsbad, CA). The first strand cDNA was generated from 1µg total RNA by reverse transcription using SuperScript VILO cDNA Synthesis Kit purchased from Life technologies-Invitrogen (Carlsbad, CA). The mRNA expression file of *Gpx1* was assessed by real-time PCR analysis using SYBR Green PCR Kit purchased from Life technologies-Applied Biosystems (Carlsbad, CA). The primers used in this assay are listed as following: Murine GPX1 forward 5'-CATTGCCTGGAACTTTGAGA-3', reverse 5'-CGATGTCGATGGTACGAAAG-3'; Murine ACTB forward 5'-CTCTTCCAGCCTTCCTTCCT-3', reverse 5'-TGCTAGGGCTGTGATCTCCT-3'.

3.14 Immunoblot Analysis.

'Protein lysates were prepared from the control and drug-treated cells, separated by electrophoresis on 8% to 15% SDS-PAGE, and transferred to nitrocellulose membranes. The molecules of interest were detected using specific antibodies as described previously. Primary rabbit polyclonal antibodies against full length and cleaved BCR-ABL, caspase-3, BCL-2, BCL-XL, GPX-1, MCL-1,

BAX, HSP60, HA, phspho-c-ABL Tyr245 and phospho-FOXO3a Thr32 were obtained from Cell Signaling Technology (Boston, MA). Primary mouse monoclonal antibody against poly (ADP-ribose) polymerase (PARP) was purchased from BD Transduction Laboratories (San Diego, CA). Mitochondrial respiratory chain subunit antibodies were from MitoProfile Total OXPHOS Human WB Antibody Cocktail purchased from MitoSciences (Abcam, Eugene, OR). Actin was probed as a loading control.'[114]

3.15 Cytotoxicity Assays.

Three different methods were used to evaluate the cytotoxic effect of drugs under various experimental conditions. 'Cell viability was determined by 3-(4,5-Dimethylthiazol-2-yl)-2,5-diphenyltetrazolium bromide (MTT) assay [122]. Cells were treated with various concentrations of drugs in 96-well plates for 72 hours, and MTT reagent was added and incubated during the last 4 hours of the drug treatment. After washing off the culture medium, the cell pellets were dissolved in 200 µl DMSO and OD 570nm was quantified using a 96-well plate reader. Drug sensitivity was compared using the cell survival curves and the IC_{50} values, defined as the drug concentration that induced 50% loss of cell viability.'[114] Cell death was also determined by flow cytometric analysis after the cells were stained with propidium iodide (PI) from BD Biosciences Pharmingen (San Diego, CA). After cells were incubated with various experimental conditions as indicated in the figure legends, the samples were stained with PI over night and analyzed by flow cytometry. The red fluorescence generated by intracellular PI is indicative of cell DNA content. The dead cells, presenting a dramatic loss of

DNA, are named as sub-G1 population. The percentage of sub-G1 population in the whole sample represents the status of cell death. Additionally, cell apoptosis was determined by flow cytometric analysis after the cells were double-stained with Annexin-V-FITC and PI, using an assay kit from BD Biosciences Pharmingen (San Diego, CA). After cells were incubated with various experimental conditions as indicated in the figure legends, the samples were stained with Annexin-V/PI. The Annexin-V-FITC only positive cells are pre-apoptosis cells. The Annexin-V-FITC and PI double positive cells are apoptosis cells. The Annexin-V-FITC and PI double negative cells are viable.

3.16 Statistical Analysis.

The flow cytometry results were analyzed by BD FACSCalibur equipped with Becton Dickson CellQuest Pro software (San Jose, CA) and FlowJo (Ashland OR). The comparison between the control and experimental samples were tested for statistical significance by the two-tailed Student's *t*-test. Significance was determined at $p<0.05$ and the 95% confidence interval. Data analysis was performed with PRISM 5.0 (GraphPad, San Diego, CA)

4. Results

4.1 BCR-ABL Promotes Mitochondrial Oxidative Stress through Enhancement of Glucose Metabolism.

4.1.1 Over-expression of BCR-ABL is Correlated with Cellular ROS Increase.

The murine BCR-ABL inducible cell line TonB210 was used to evaluate the level of cellular ROS by probing with DCF-DA. BCR-ABL expression is induced by doxycycline ranging between 0.5 and 1.0 μg/ml. The BCR-ABL non-induced cells served as control and maintained in tetracycline free media with IL3. I further detected BCR-ABL expression and cellular ROS level at the different time points during BCR-ABL induction. BCR-ABL was detected by Western blotting using anti-c-ABL antibody. The total cellular ROS was indicated by the amount of green fluorescence derived from DCF-DA probe. BCR-ABL showed the time-dependent increase during induction at 12, 24 and 36 hour points (Figure 3A). The consistent time-dependent increase of total ROS was also observed in the samples with the increase of BCR-ABL expression (Figure 3B). Based on the above experimental results, this indicates that increase of ROS is correlated with BCR-ABL over-expression.

Figure 3. Over-expression of BCR-ABL is correlated with cellular ROS increase in TonB210 cells. (A) BCR-ABL was induced by 0.5 µg/ml doxycycline in TonB210 cells. (B) Intracellular ROS was detected by flow cytometry using DCF-DA probe in BCR-ABL over-expressing cells.

A

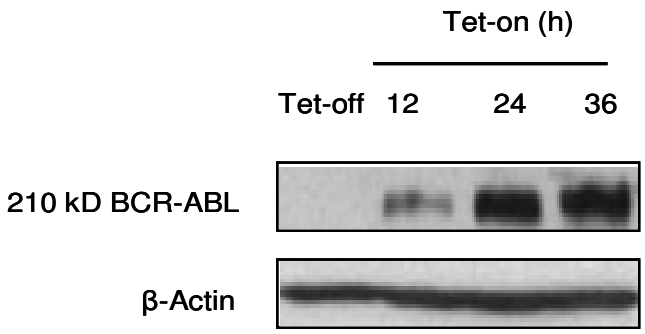
Tet-on (h)
Tet-off
12
24
36
210 kD BCR-ABL
β-Actin

B

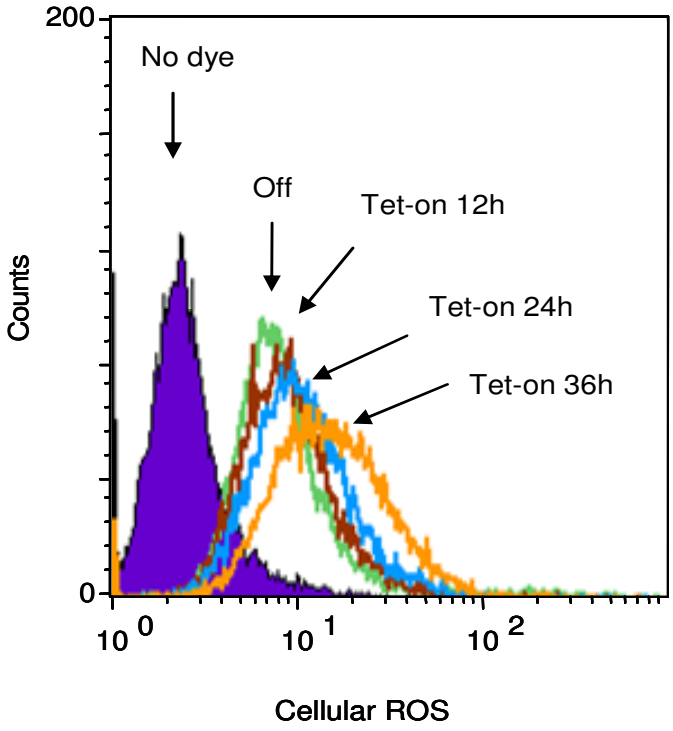
200
No dye
Off
Tet-on 12h
Tet-on 24h
Tet-on 36h
Counts
0
10 0
10 1
10 2
Cellular ROS

4.1.2 Activation of BCR-ABL Causes the Enhancement of Glucose Metabolism.

TonB210 cells were cultured with or without doxycycline for 48 hours. The doxycycline treated cells were either incubated with 5μM Imatinib or not. Cells were cultured with IL3 in order to prevent cell death in parental cells or Imatinib treated BCR-ABL over-expressing cells. The amount of glycolysis end product lactate released from the differentially treated TonB210 cells has been measured. BCR-ABL over-expressing cells showed a significant increase of lactate products (Figure 4, Upper). Furthermore, Imatinib significantly suppressed the enhancement of lactate in BCR-ABL over-expressing cells (Figure 4, Upper) along with the inhibition of BCR-ABL tyrosine kinase activation (Figure 4, Lower). These results suggested that BCR-ABL onco-protein activity is required for the enhancement of cellular glucose metabolism. In addition, no dramatic changes of cell oxygen consumption were observed in BCR-ABL over-expressing cells (Figure 5). This result excludes mitochondria inhibition as the cause of glycolysis activation. Taken together, the above results have identified that the enhancement of glucose metabolism is an early event induced by BCR-ABL through its kinase activity.

Figure 4. Activation of BCR-ABL enhances glucose metabolism in TonB210 cells. The medium lactate product released from differentially treated TonB210 cells was measured. Lactate amount was normalized by cell numbers. Doxycycline 0.8 µg/ml was used to induce BCR-ABL expression for 48 hours. Imatinib 5µM was used to inhibit BCR-ABL tyrosine kinase activity. Active form and total BCR-ABL were detected by Western blotting using phosphor-BCR-ABL and c-ABL antibody. All the samples were cultured in the presence of IL3.

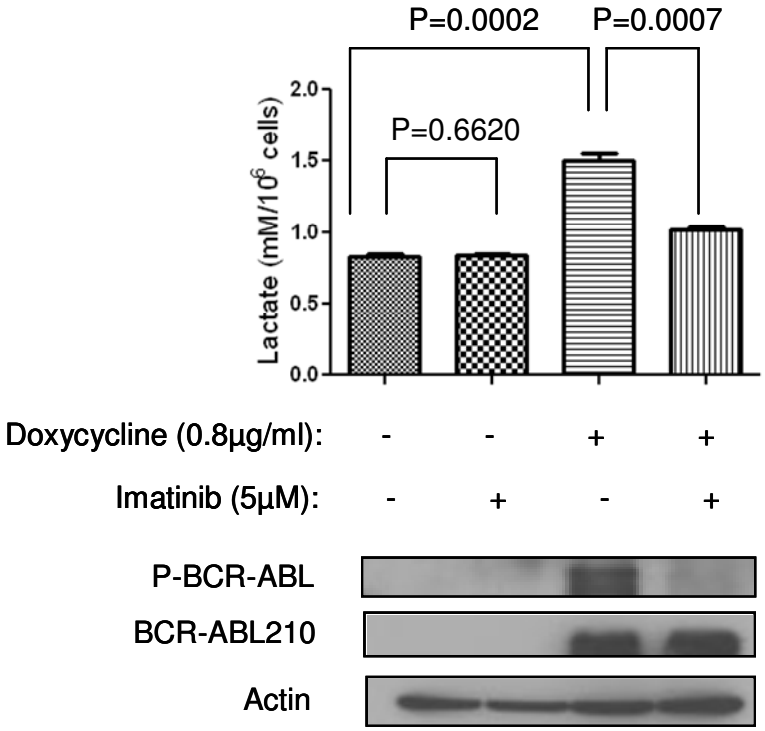
P=0.0002
P=0.0007
P=0.6620
Lactate (mM/10^6 cells)
2.0
1.5
1.0
0.5
0.0
Doxycycline (0.8µg/ml): - - + +
Imatinib (5µM): - + - +
P-BCR-ABL
BCR-ABL210
Actin

Figure 5. No decrease of oxygen consumption rate in BCR-ABL over-expressing cells. Doxycycline 0.5 µg/ml was used to induce BCR-ABL expression in TonB210 cells. Oxygen consumption rate was detected using 8 million cells for each sample. BCR-ABL expressing cells were collected at 12 and 36 hour.

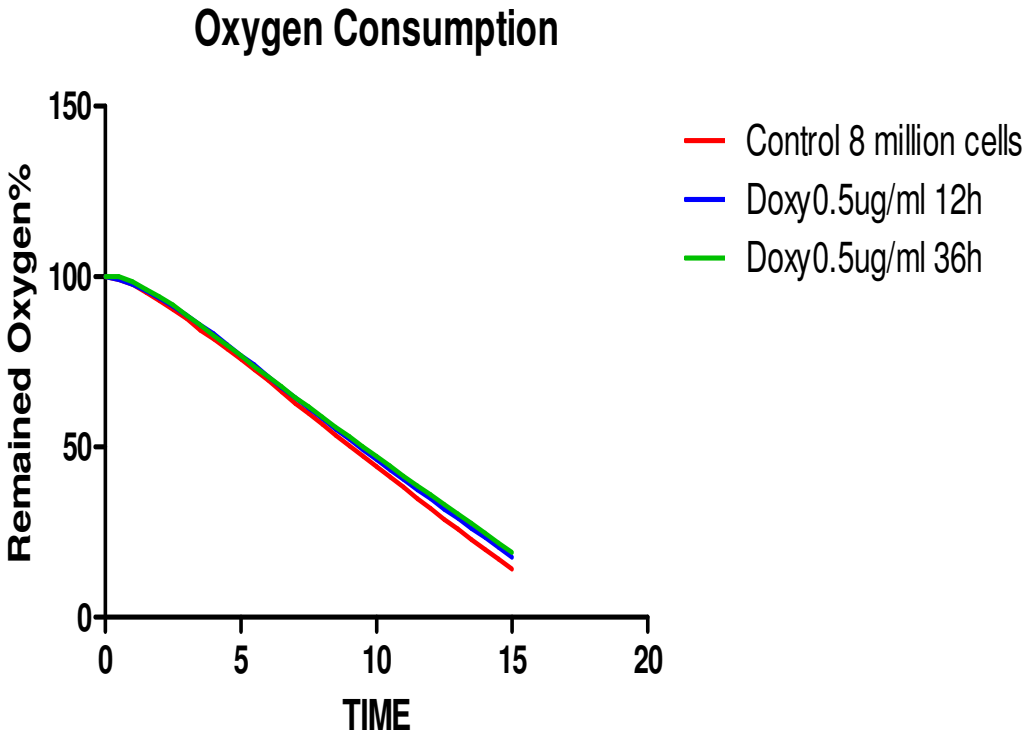
Oxygen Consumption
Remained Oxygen%
150
100
50
0
0
5
10
15
20
TIME
Control 8 million cells
Doxy0.5ug/ml 12h
Doxy0.5ug/ml 36h

4.1.3 Glucose Shortage Results in Decreased Mitochondrial ROS Generation in BCR-ABL Expressing Cells.

The level of cellular ROS and mitochondrial ROS were measured under normal or glucose shortage conditions by probing with DCF-DA and MitoSox Red, respectively. Both cellular and mitochondrial ROS elevations induced by BCR-ABL were suppressed under the glucose shortage conditions (Figure 6). In addition, no dramatic cell death was induced by glucose shortage (Figure 7), which excludes the interruption of cell survival as the cause of ROS decrease. To further prove this point, mitochondrial ROS generation was detected under the glucose shortage conditions in human cultured CML cells. Mitochondrial ROS level was measured in two BCR-ABL positive CML cell lines K562 and KBM5 using MitoSox Red probe. After 20 hour glucose shortage culture, mitochondrial ROS dramatically dropped in both cell lines (Figure 8). In addition, the effects of glucose shortage on cell survival were tested in K562 cells. There was no dramatic cell death caused by 24 hours of glucose shortage (Figure 9, Upper). Just a slight increase of cell death was induced by 48 hour glucose shortage (Figure 9, Lower). Taken together, my results suggested that mitochondrial ROS are highly rely on the glucose nutrient condition, although glucose shortage does not promote potent cell death in BCR-ABL expressing cells.

Figure 6. Glucose shortage decreases BCR-ABL induced cellular and mitochondrial ROS increase in TonB210 cells. Cellular and mitochondrial ROS levels were detected by Using flow cytometry using DCF-DA and MitoSOX Red probes, respectively. Doxycycline 0.8µg/ml was used to induce BCR-ABL expression for 48 hours. Cells were cultured with or without glucose supply. Sample's medians are labeled.

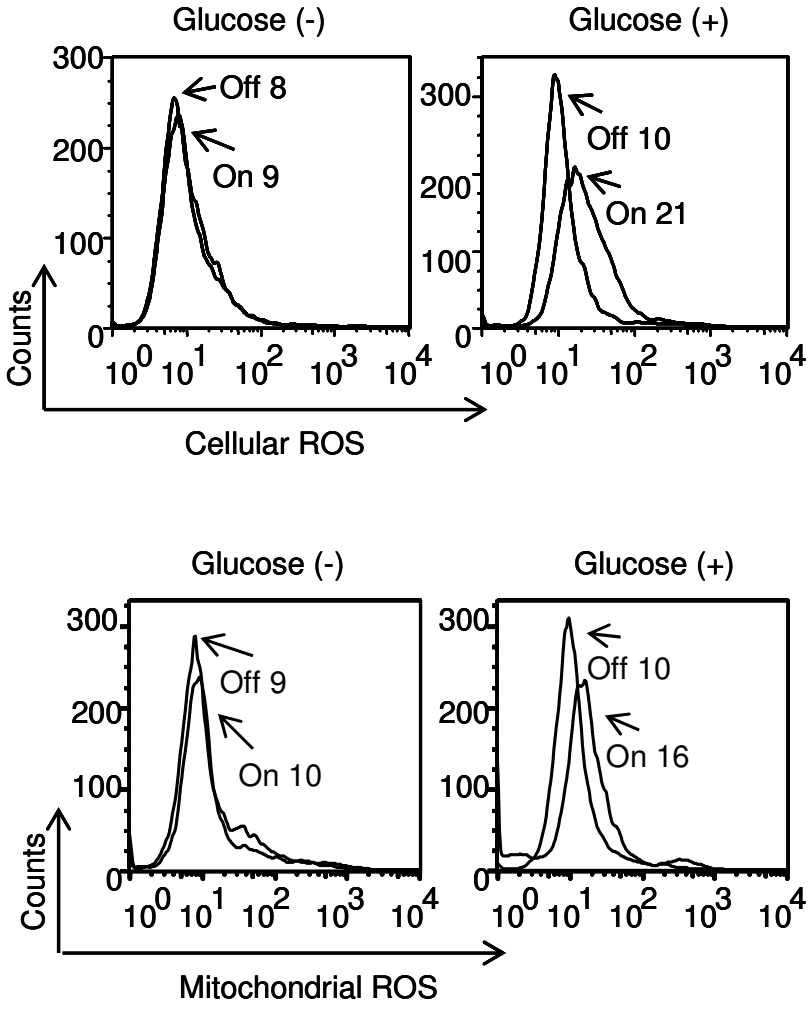
Glucose (-)
Glucose (+)
300
200
100
0
Off 8
On 9
Off 10
On 21
Counts
10^0 10^1 10^2 10^3 10^4
Cellular ROS
Glucose (-)
Glucose (+)
Off 9
On 10
Off 10
On 16
Counts
Mitochondrial ROS

Figure 7. No dramatic cell death induced by 48 hour glucose shortage in TonB210 cells. DNA content was detected by PI staining assay. Doxycycline 0.8 μg/ml was used to induce BCR-ABL expression for 48 hours. Cells were cultured with or without glucose supply for 48 hours. Percentages of sub-G1 population (lethal cell) are labeled.

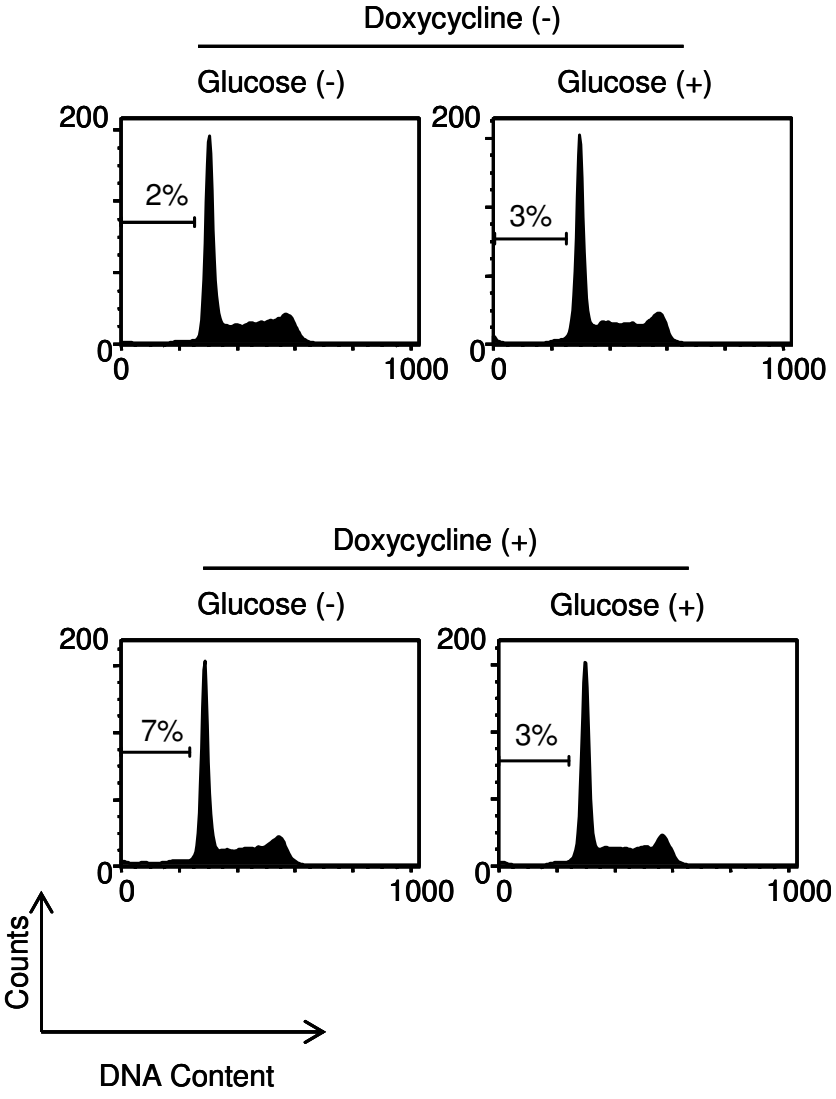
Doxycycline (-)
Glucose (-)
Glucose (+)
200
2%
0
0
1000
200
3%
0
0
1000
Doxycycline (+)
Glucose (-)
Glucose (+)
200
7%
0
0
1000
200
3%
0
0
1000
Counts
DNA Content

Figure 8. Glucose shortage results in mitochondrial ROS decrease in K562 and KBM5 cells. Mitochondrial ROS level was detected by flow cytometry using MitoSOX Red. Cells were cultured with or without glucose supply for 20 hours. Sample's medians are labeled.

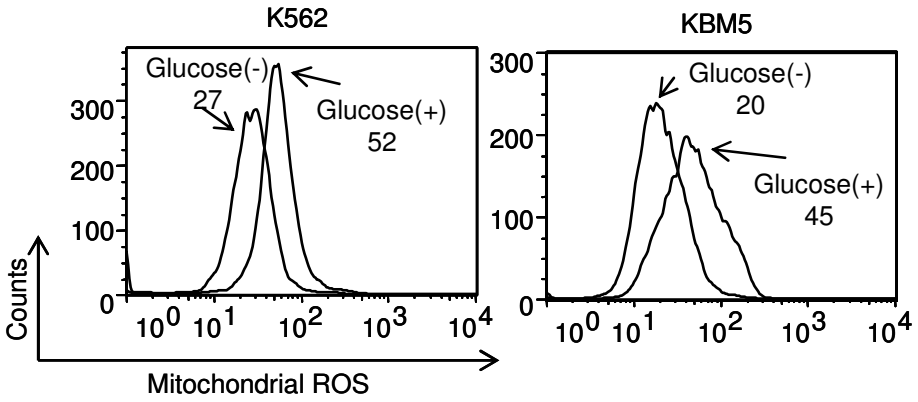
K562
KBM5
Glucose(-)
27
Glucose(+)
52
Glucose(-)
20
Glucose(+)
45
300
200
100
0
10^0 10^1 10^2 10^3 10^4
Counts
Mitochondrial ROS

Figure 9. No dramatic cell death induced by glucose shortage in K562 cells. Cell death was detected by Annexin-V/PI assay. Cells were cultured with or without glucose supply for 24 or 48 hours. Percentages of survival cells are labeled.

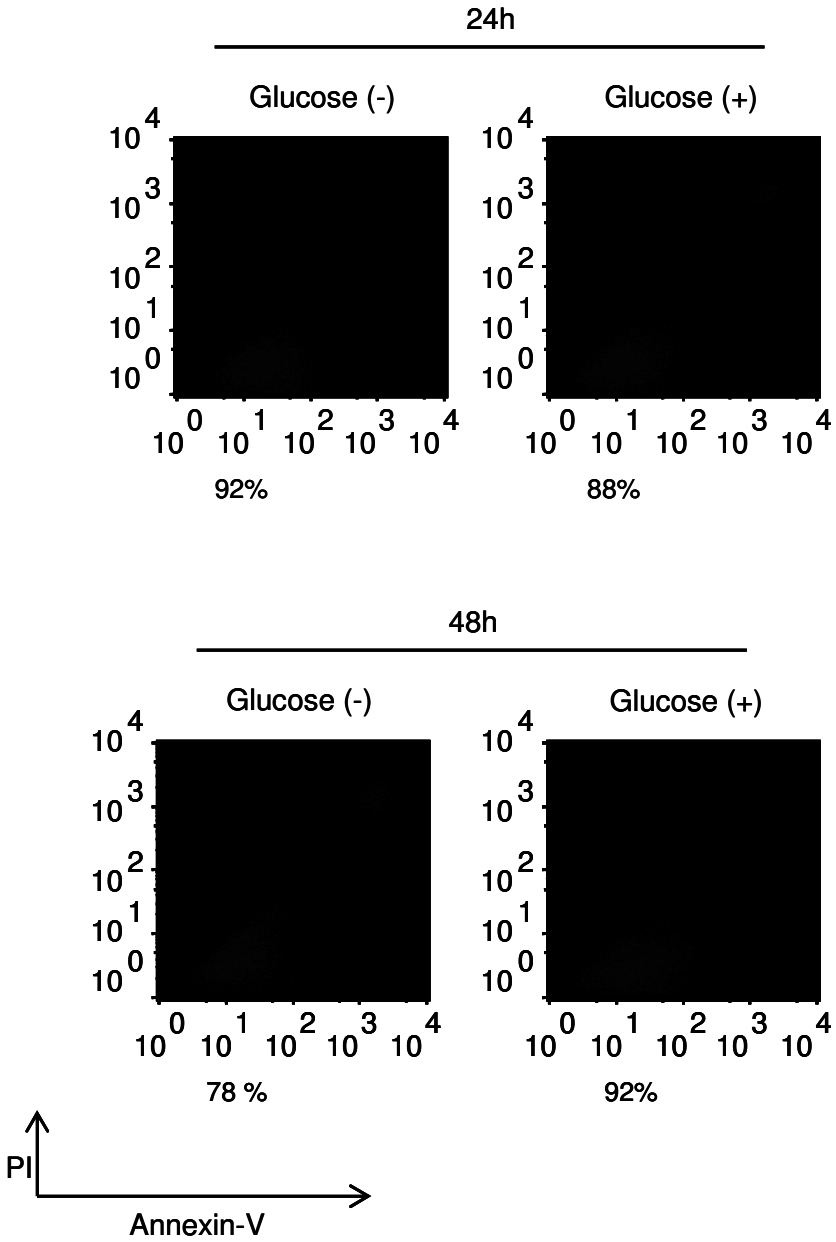
24h
Glucose (-)
Glucose (+)
92%
88%
48h
Glucose (-)
Glucose (+)
78 %
92%
PI
Annexin-V

4.2 BCR-ABL Downstream Survival Factor BCL-XL Plays an Essential Role in Protecting Mitochondria Under Oxidative Stress.

4.2.1 BCL-XL Protects CML Cells Against Oxidative Stress-Induced Apoptosis.

BCR-ABL inducible TonB210 cell model was used to test whether either BCL-XL or BCL-2 is the primary survival factor during BCR-ABL induction. Because TonB210 parental cells were cultured with IL-3, which may promote BCL-XL expression, experimental samples were incubated with low levels of IL-3 at 0.1ng/ml. More specifically, cells were first incubated with doxycycline in the media containing 1.0 – 4.0 ng/ml IL-3. After 48 hours, the IL-3 level was decreased to 0.1ng/ml. After another 12 hours, control and experimental samples were collected. Expression of BCR-ABL, BCL-2 and BCL-XL were then analyzed by Western blotting. BCL-XL but not BCL-2 was dramatically up-regulated by over-expression of BCR-ABL (Figure 10). These results suggested that BCL-XL is an initial survival factor promoted by BCR-ABL. This evidence has also implied that BCL-XL may play an important role in response to BCR-ABL-promoted cellular metabolic alterations, such as oxidative stress. However, both BCL-XL and BCL-2 have been reported to be up-regulated in CML cells. Whether BCL-XL is more essential to protect cells against oxidative stress is still unclear. To further test this point, two human cultured CML cell lines, which express different levels of BCL-XL and BCL-2 were used to compare cell sensitivity to oxidative stress. CML cell line K562 and KBM5 were both established from CML blast crisis patient samples. K562 showed a relatively higher level of BCL-XL but less BCL-2 than KBM5 (Figure 11).

Figure 10. Initial up-regulation of BCL-XL by BCR-ABL. Doxycycline 0.8 µg/ml was used to induce BCR-ABL expression in TonB210 for 48 hours, followed by a decrease of IL-3 to 0.1 ng/ml in the medium. Then medium IL3 level was decreased to 0.1 ng/ml. Cell samples were collected after additional 12 hour Doxycycline incubation. Cell lysates were analyzed by Western blotting for protein expression using c-ABL BCL-XL and BCL-2 antibodies. Actin was used as a loading control.

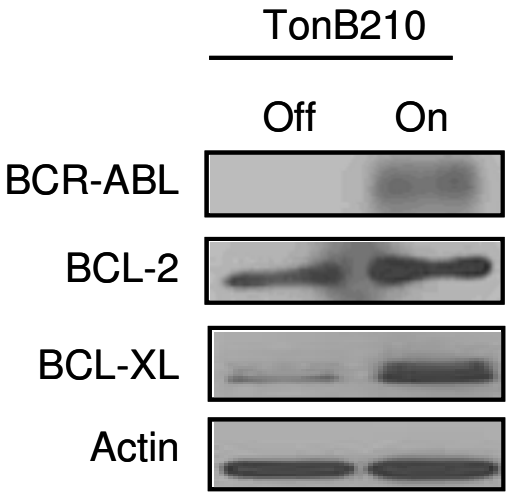
TonB210
Off
On
BCR-ABL
BCL-2
BCL-XL
Actin

Figure 11. Different expression levels of BCL-XL, BCL-2 and antioxidants in K562 and KBM5 cells. Cell lysates was analyzed by Western blotting for protein expression using BCL-XL, BCL-2, MCL-1, GPX-1 and Catalase antibodies. Actin was used as a loading control. The cell lysate of AML cell line HL60 was used as a control to indicate the relative level of BCL-XL, BCL-2, MCL-1 and GPX-1 in CML cells.

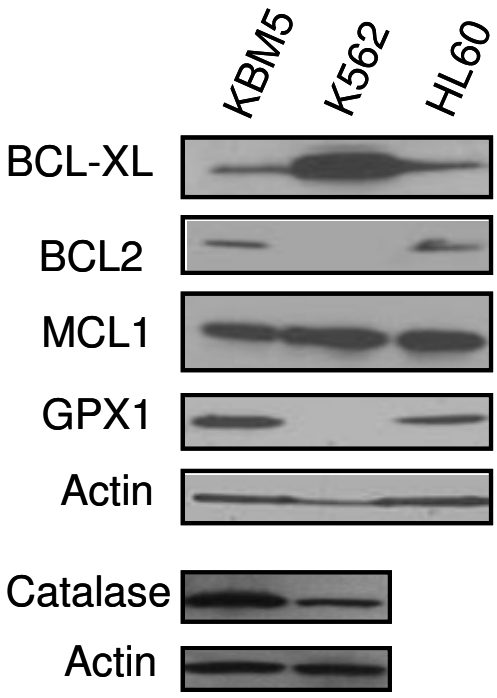
KBM5
K562
HL60
BCL-XL
BCL2
MCL1
GPX1
Actin
Catalase
Actin

It is worthy of noting that antioxidant enzymes GPX1 and catalase, which play major roles in scavenging intracellular ROS products under normal physiological conditions, are both expressed at lower levels in K562 than KBM5 cells (Figure 11). These results suggested a lower antioxidant capacity in K562. To test CML cell sensitivity to oxidative stress, K562 and KBM5 cells were incubated with H_2O_2, a general oxidative stress inducing agent, at 50 μM for 18 hours. In addition, cells were also treated with 0.5 μM Imatinib for 60 hours to test the cell sensitivity of BCR-ABL inhibition. Interestingly, H_2O_2 caused more cell death in KBM5 cells, however, Imatinib promoted more cell killing effects in K562 cells (Figure 12). These results indicated that K562 cells are less sensitive to oxidative stress than KBM5 cells. Therefore, BCL-XL which is highly expressed in K562 cells seems to play a more dominant role in protecting CML cells against oxidative stress than BCL-2. However, these results were generated from the comparison between different cell lines and it is possible that other genetic differences between K562 and KBM5 cells may be also involved. To further clarify the role of BCL-XL in protecting cells against oxidative stress, either BCL-XL expression plasmid or Bcl-XL shRNA plasmid was transfected into cultured human CML cell lines. In this experimental system, I can exclude the impacts derived from genetic background of different cell lines.

Figure 12. K562 is less sensitive to oxidative stress induced apoptosis than KBM5 cells. Cells were treated with 50 μM H_2O_2 or 0.5 μM Imatinib for 18 or 60 hours respectively. Flow cytometry was used to detect cell death by Annexin-V/PI. Percentages of survival cells are labeled.

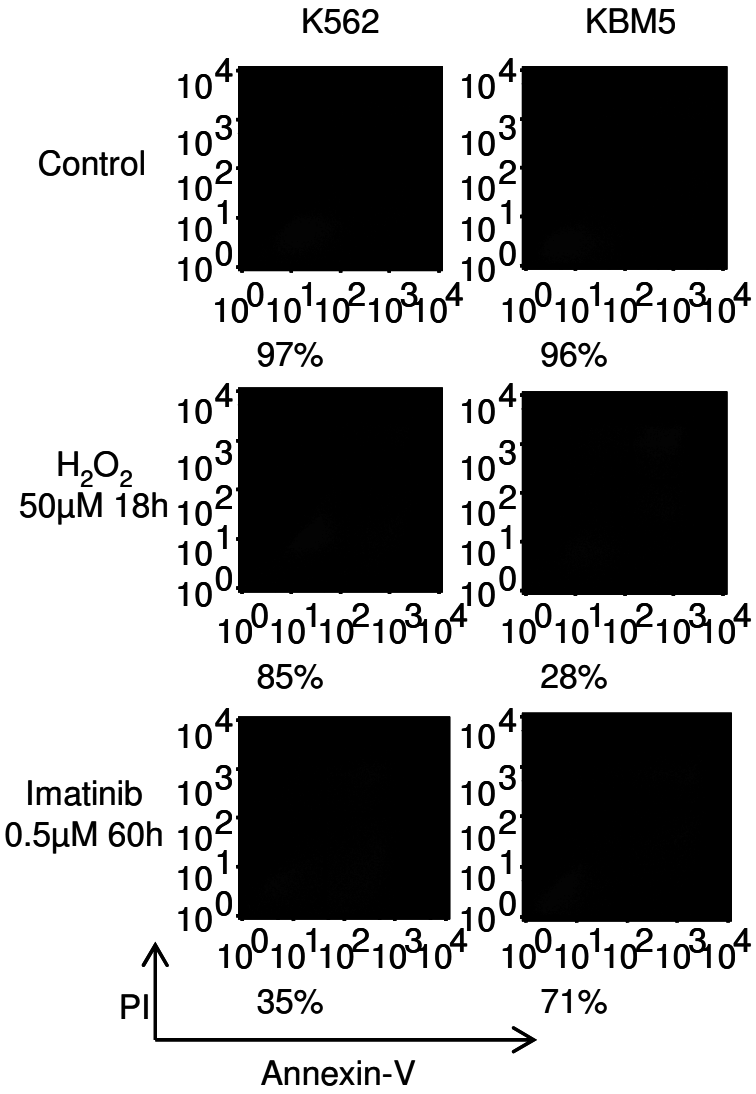
K562
KBM5
Control
H_2O_2
50µM 18h
Imatinib
0.5µM 60h
97%
96%
85%
28%
35%
71%
PI
Annexin-V

KBM5 cells were transfected with a neo'-containing HA tagged human BCL-XL plasmid. The successfully transfected cells were enriched by selector G418 for one month. The selected cell pool was named as KBM5-BCLXL-HA. The over-expressed BCL-XL product was identified by Western blotting using BCL-XL and HA antibodies (Figure 13). KBM5 and KBM5-BCLXL-HA cells were incubated with 50 μM H_2O_2 or 2 μM Imatinib for 24 or 48 hours respectively. Cell death was detected by flow cytometry using Annexin-V-FITC and PI. The increased cell survival of KBM5-BCLXL-HA under treatment of either H_2O_2 or Imatinib was observed (Figure 14). In addition, I used the same approach to generate BCL-XL over-expressing cells from K562, named as K562-BCLXL-HA (Figure 15). K562 and K562-BCLXL-HA cells were treated with 50 μM H_2O_2 or 2 μM Imatinib for 60 hours. Consistent with the results from KBM5 pair cells, the increased cell survival of K562-BCLXL-HA under treatment of either H_2O_2 or Imatinib was also observed (Figure 16). These results have shown that over-expression of BCL-XL in CML cells reduces cell sensitivity to both oxidative stress and Imatinib. Besides these gain of function tests, I further investigated BCL-XL loss of function effects in K562 cells. K562 cells were transfected with RFP linked tet-on inducible Bcl-XL shRNA plasmids. The successful transfected cells were enriched by selector 4 μg/ml puromycin for one month, named as K562-BCLXL-KD. After 4 day doxycycline induced shRNA expression, the BCL-XL level was decreased about 70% (Figure 17). After induction of BCL-XL knock down, cells were treated with 50 μM H_2O_2 for 24 hours. Apoptotic cells were further detected by flow cytometry using Annexin-V-FITC staining assay. The

pre-apoptotic and apoptotic cells indicated as annexin positive were dramatically increased in BCL-XL knocked down cells (Figure 18). Taken together, these results have demonstrated that BCL-XL play an important role in protecting CML cells against oxidative stress.

Figure 13. Over-expression of BCL-XL in KBM5 cells. KBM5 cells were transfected with HA tagged human BCL-XL plasmids. The successful transfected cells were enriched by selector G418 for one month, named as KBM5-BCLXL-HA. The over-expressed product was identified by BCL-XL and HA antibodies. The HA tagged BCL-XL protein showed a higher molecular weight than the endogenous one. Actin was used as a loading control.

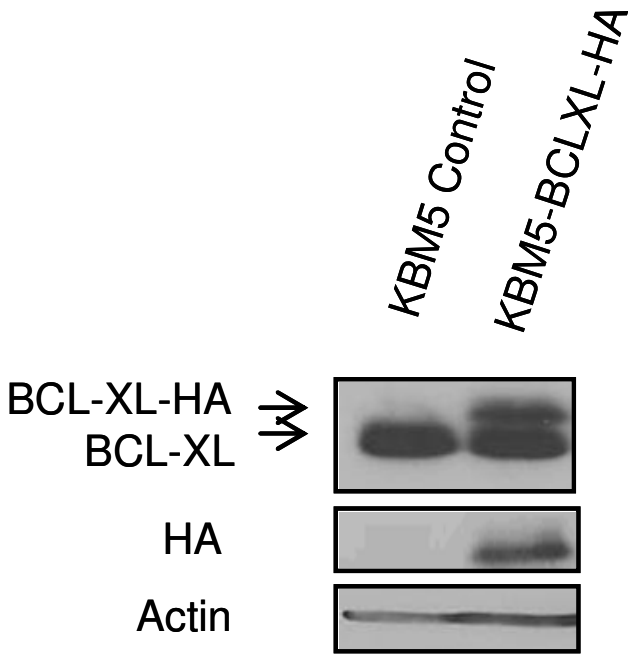
KBM5 Control
KBM5-BCLXL-HA
BCL-XL-HA
BCL-XL
HA
Actin

Figure 14. Over-expression of BCL-XL enhances cell survival under oxidative stress and Imatinib treatment in KBM5 cells. KBM5 and KBM5-BCLXL-HA cells were treated with 50 μM H_2O_2 or 2 μM Imatinib for 24 or 48 hours respectively. Cell viability was detected by Annexin-V/PI assay. Percentages of survival cells are labeled.

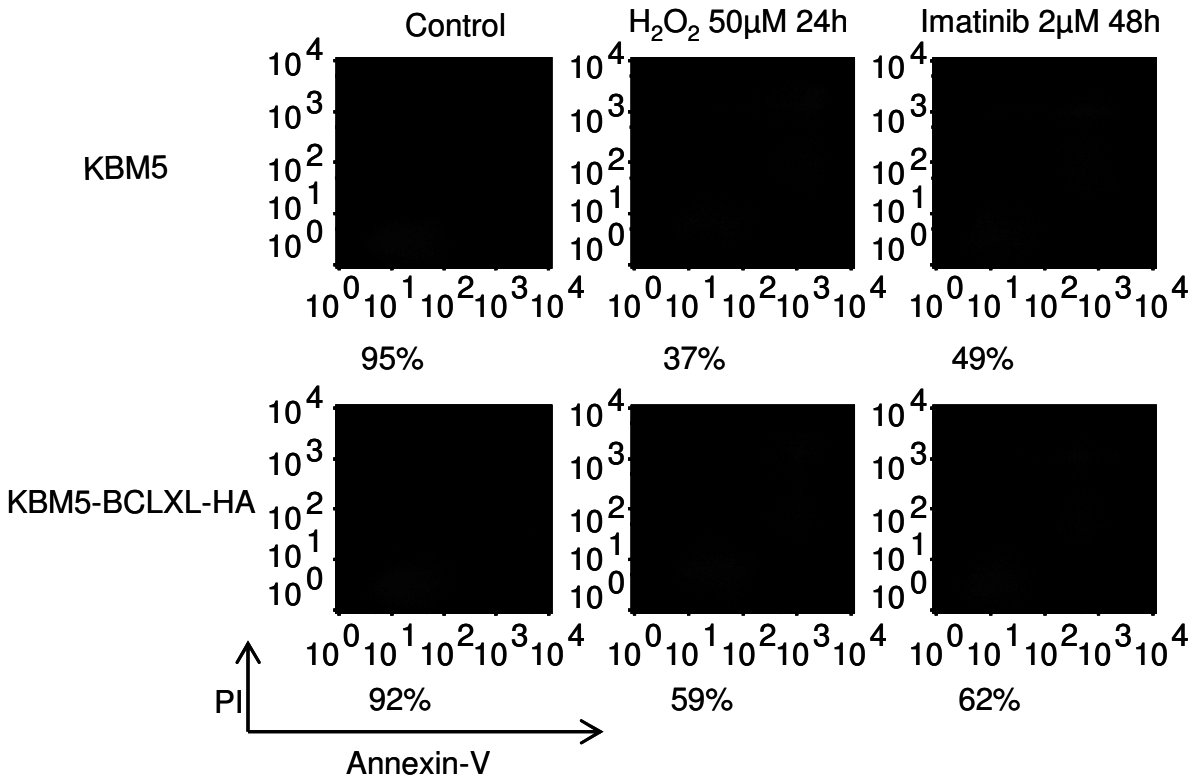
Control
H2O2 50µM 24h
Imatinib 2µM 48h
KBM5
KBM5-BCLXL-HA
95%
37%
49%
92%
59%
62%
PI
Annexin-V

Figure 15. Over-expression of BCL-XL in K562 cells. K562 cells were transfected with HA tagged human BCL-XL plasmids. The successfully transfected cells were enriched by selector G418 for one month, named as K562-BCLXL-HA. The over-expressed product was identified by BCL-XL and HA antibodies. Actin was used as a loading control.

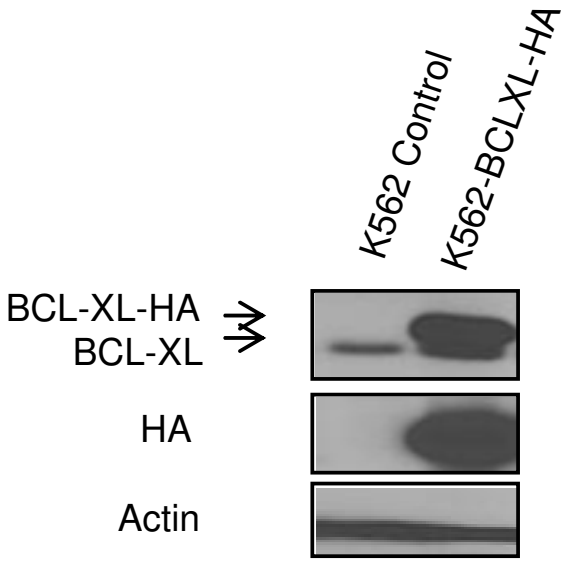
K562 Control
K562-BCLXL-HA
BCL-XL-HA
BCL-XL
HA
Actin

Figure 16. Over-expression of BCL-XL enhances cell survival under oxidative stress and Imatinib treatment in K562 cells. K562 and K562-BCLXL-HA cells were treated with 50 μM H_2O_2 or 2 μM Imatinib for 60 hours. Cell viability was detected by Annexin-V/PI assay. Percentages of survival cells are labeled.

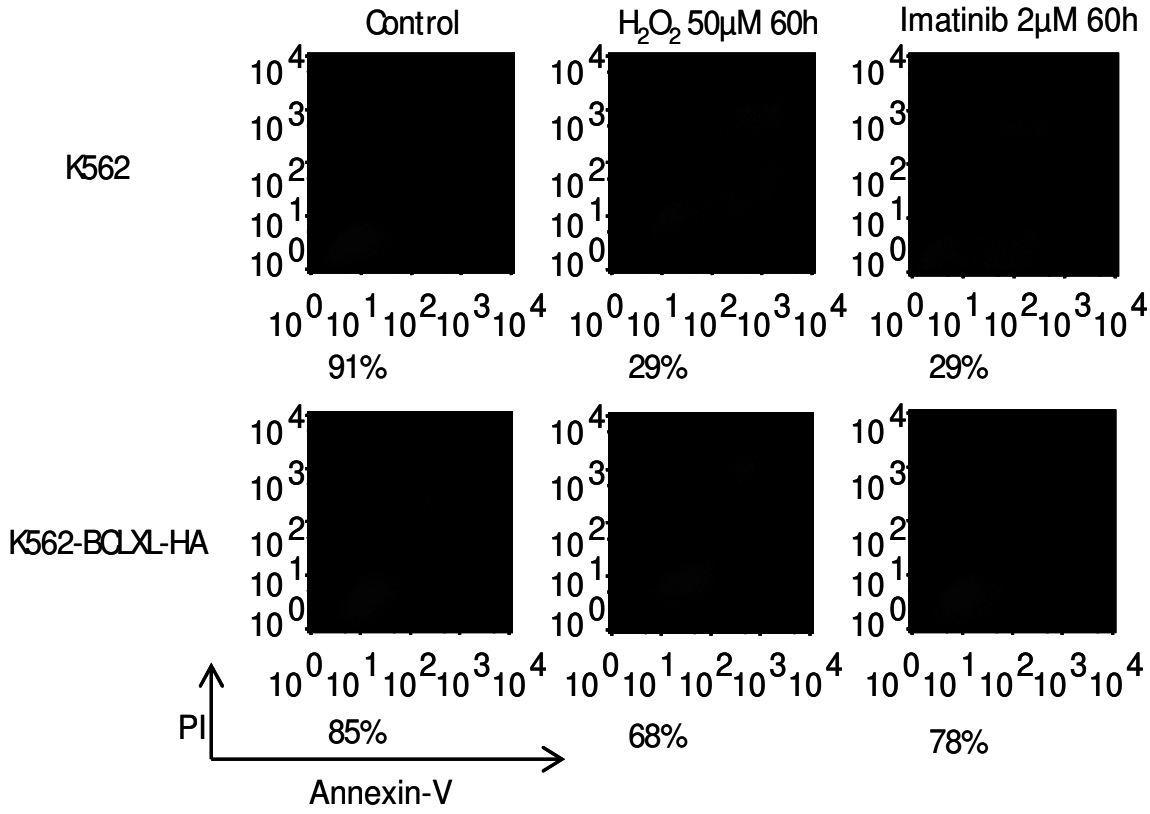
Control
H2O2 50µM 60h
Imatinib 2µM 60h
K562
K562-BCLXL-HA
91%
29%
29%
85%
68%
78%
PI
Annexin-V

Figure 17. Knock-down of BCL-XL in K562 cells. K562 cells were transfected with RFP linked tet-on inducible Bcl-XL shRNA plasmids. The successful transfected cells were enriched by selector puromycin for one month, named as K562-BCLXL-KD. The BCL-XL level was identified by Western blotting using BCL-XL antibody after 4 day shRNA induction by doxycycline treatment. Actin was used as a loading control.

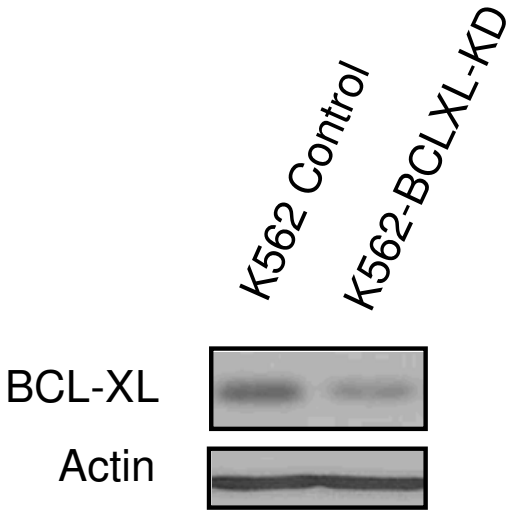
K562 Control
K562-BCLXL-KD
BCL-XL
Actin

Figure 18. Down-regulation of BCL-XL enhances oxidative stress induced apoptosis in K562 cells. Doxycycline-Induced and non-induced BCLXL knock down cells were treated with 50 μM H_2O_2 for 24 hours. Cell apoptosis was detected by Annexin-V (including pre-apoptosis and apoptosis cells). Viable cells are annexin negative, while apoptotic cells are annexin positive. Percentages of gated cells are labeled.

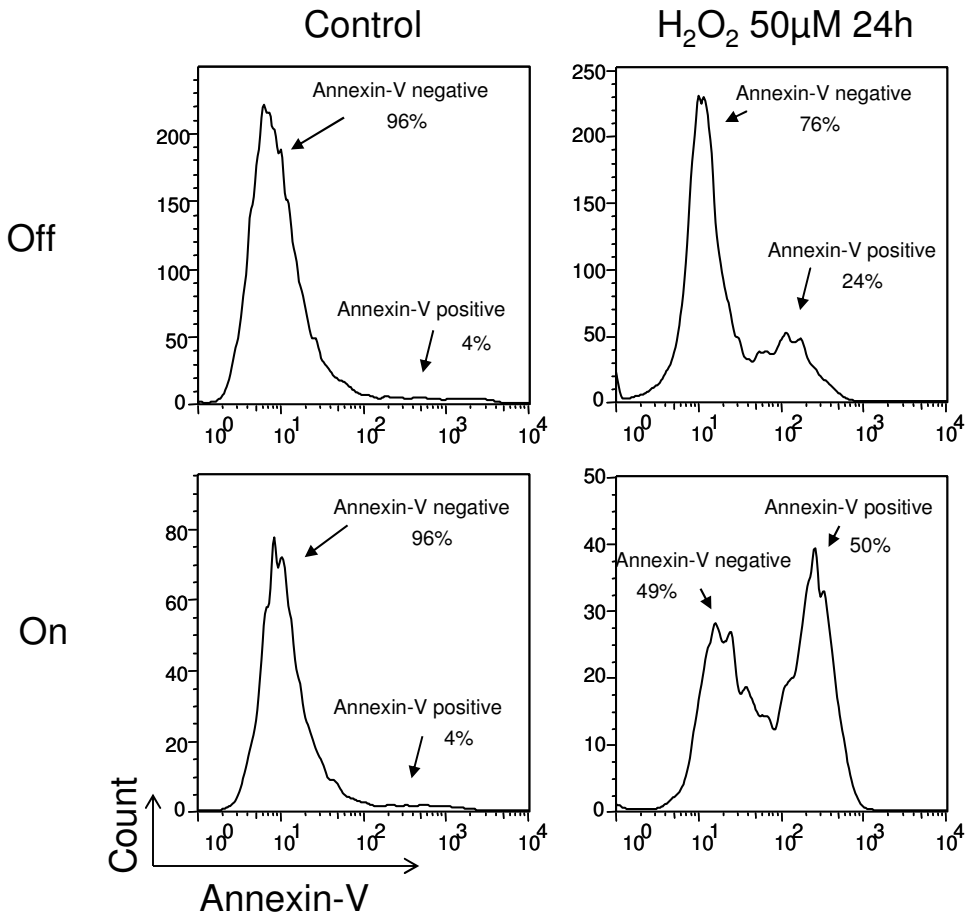
Control
H_2O_2 50µM 24h
Off
On
Annexin-V negative
96%
Annexin-V positive
4%
Annexin-V negative
76%
Annexin-V positive
24%
Annexin-V negative
96%
Annexin-V positive
4%
Annexin-V positive
50%
Annexin-V negative
49%
Count
Annexin-V

4.2.2 BCL-XL but not BCL-2 Prevents Oxidative Stress-Induced Mitochondrial Membrane Potential Collapse.

The above results have shown that KBM5 expresses relatively higher BCL-2, but is more sensitive to oxidative stress-induced apoptosis than K562 (Figure 11, 12). This observation implies that BCL-XL and BCL-2 may be functionally distinct in response to the increased mitochondrial ROS in CML cells. Both BCL-XL and BCL-2 have mitochondrial localization. Previous studies have shown that both BCL-2 and BCL-XL play important roles in the development of CML. BCL-2 especially causes Imatinib resistance in some BCR-ABL positive and BCR-ABL-independent CML cells. Therefore, identification of the differential role of BCL-XL and BCL-2 in response to mitochondrial oxidative stress can help us further understand the biological mechanism of CML progression, and even provide the rationale for the design of novel therapeutic approaches. To achieve these goals, I generated BCL-2 over-expressing cells by transfecting a GFP-fused BCL-2 plasmid into K562 which has low endogenous BCL-2 background. The successfully transfected cells were enriched by G418 selection, and the cell pool was named as K562-BCL2-GFP. Expression of GFP-BCL-2 fusion protein was identified by Western blotting using BCL-2 antibody (Figure 19A). Mitochondria localization of GFP-BCL-2 fusion protein was identified by confocal microscope using MitoTracker Red to indicate mitochondria. The co-localization of GFP and MitoTracker Red showed that a large amount of the over-expressed BCL-2 products were successfully localized to mitochondria (Figure 19B).

Figure 19. Over-expression of BCL-2 in K562 cells. K562 cells were transfected with GFP-fused BCL-2 plasmids. The successfully transfected cells were enriched by selector G418 for one month, named as K562-BCL2-GFP. (A) The over-expressed product was identified by BCL-2 antibodies. The GFP fusion BCL-2 protein showed at a higher molecular weight than the endogenous one. Both K562 and K562-BCLXL-HA were used as negative controls. Actin was used as a loading control. (B) The mitochondria localization of this GFP-BCL-2 fusion protein was identified by confocal microscope (40X) using MitoTracker Red and DAPI indicating mitochondria and nuclei respectively. Cells that showed the co-localization of GFP-BCL-2 (green) and mitochondria (red) are indicated by arrows.

A

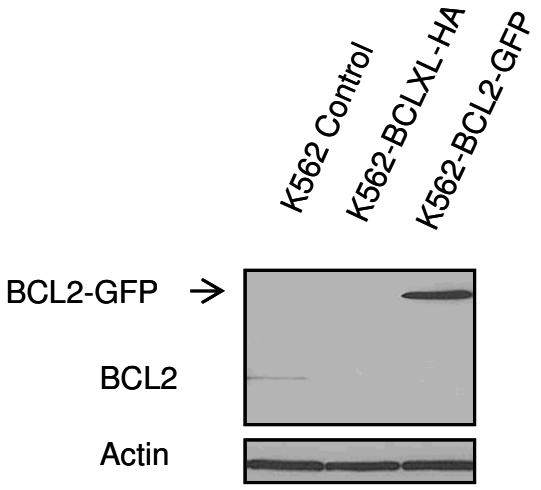
K562 Control
K562-BCLXL-HA
K562-BCL2-GFP
BCL2-GFP
BCL2
Actin

B

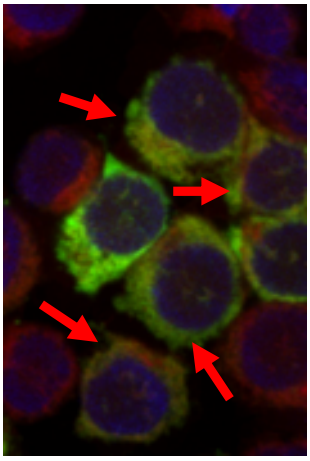
K562-BCL2-GFP: Mito-Tracker Red: DAPI

I further detected cell viability of BCL-XL or BCL-2 over-expressing K562 cells under treatment of H_2O_2 or Imatinib by PI staining assay. The sub-G1 population of each sample indicates the dead cells with decreased DNA contents. After 48 hour treatment, both K562-BCLXL-HA and K562-BCL2-GFP cells showed protection effects against H_2O_2 and Imatinib (Figure 20 Upper). After 72 hour treatment, however, only over-expression of BCLXL protected cells against oxidative stress. In contrast, both over-expression of BCLXL and BCL2 still effectively prevented Imatinib-induced cell death following a 72 hour treatment (Figure 20 Lower). These results have suggested that BCL-2 is equally effective as BCL-XL in protecting cells against inhibitors of BCR-ABL, but is less efficient in preventing oxidative stress induced apoptosis than BCL-XL. This observation is consistent with the results I found in the comparison between KBM5 and K562 (Figure 12). It is suggested that BCL-XL is more efficient to protect cells against oxidative stress than BCL-2, and BCL-2 is more likely to delay oxidative stress induced apoptosis in CML cells. To further address the differential role of BCL-XL and BCL2, I tested the effects of the elevated oxidative stress on mitochondrial membrane potential in CML cells. Following the treatment of 100 μM H_2O_2, cell viability and mitochondrial membrane potential of CML cells were detected by Annexin-V/PI and Rhodamine 123 staining assays respectively. The total cell count including pre-apoptotic and apoptotic cells was matched with the total cell count of cells with collapsed mitochondrial membrane potential (Figure 21). These data indicated that the collapse of mitochondrial membrane potential is an early event and contributes to cell apoptosis. I further

compared oxidative stress induced mitochondrial membrane potential changes between the BCL-XL and BCL-2 differentially expressing cells. K562 was found less sensitive to 50 μM H_2O_2 induced mitochondrial membrane potential collapse than KBM5 (Figure 22). Consistently, BCL-XL but not BCL-2 over-expressing cells prevented 50 μM H_2O_2 induced mitochondrial membrane potential collapses (Figure 23). Taken together, these results have suggested that BCL-XL and BCL-2 differentially protect cells against oxidative stress, and BCL-XL is more efficient in maintaining mitochondrial membrane potential and preventing apoptosis than BCL-2.

Figure 20. BCL-XL is more efficient in protecting cells against oxidative stress than BCL-2. K562, K562-BCLXL-HA and K562-BCL2-GFP cells were treated with 50 μM H_2O_2 or 2 μM Imatinib. Cell death and cell cycle were detected by PI DNA content staining assay following 48 hour treatment (Upper) and 72 hour treatment (Lower). The DNA content low sub-G1 population represents the dead cells.

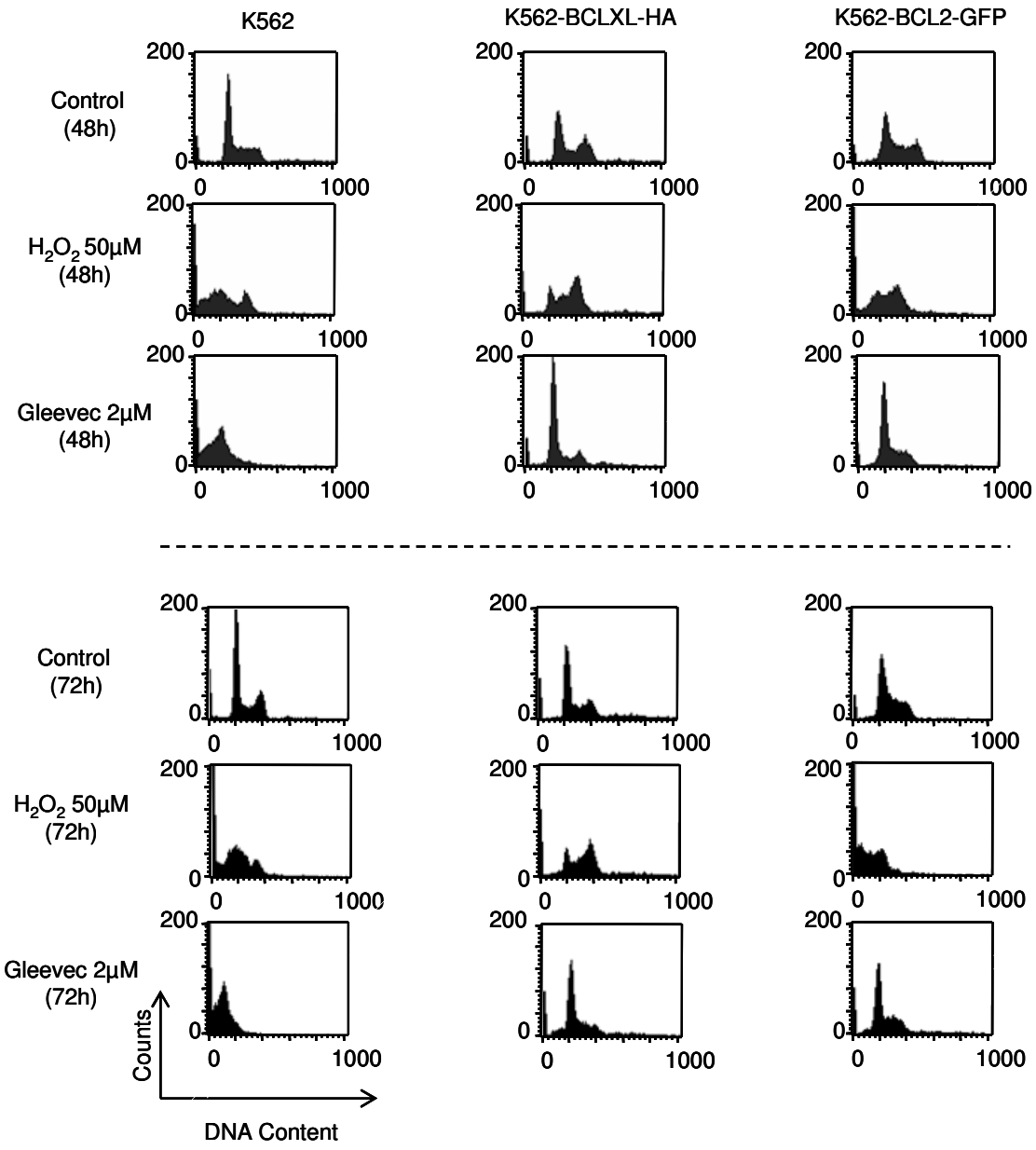
K562
K562-BCLXL-HA
K562-BCL2-GFP
Control (48h)
H2O2 50µM (48h)
Gleevec 2µM (48h)
Control (72h)
H2O2 50µM (72h)
Gleevec 2µM (72h)
200
0
0
1000
Counts
DNA Content

Figure 21. Moderate oxidative stress promotes mitochondrial membrane potential (MMP) collapse and contributes to cell apoptosis in CML cells. K562 cells were treated with 100 μM H_2O_2 for 24 hours. MMP and cell death were detected by Rhodamine 123 and Annexin-V/PI respectively. Decreased Rhodamine 123 fluorescence indicates the MMP collapsed cells. Percentages of MMP collapsed and maintained cells are labeled. Percentages of survival (Lower left), pre-apoptosis (Lower right) and apoptosis (Upper right) are labeled.

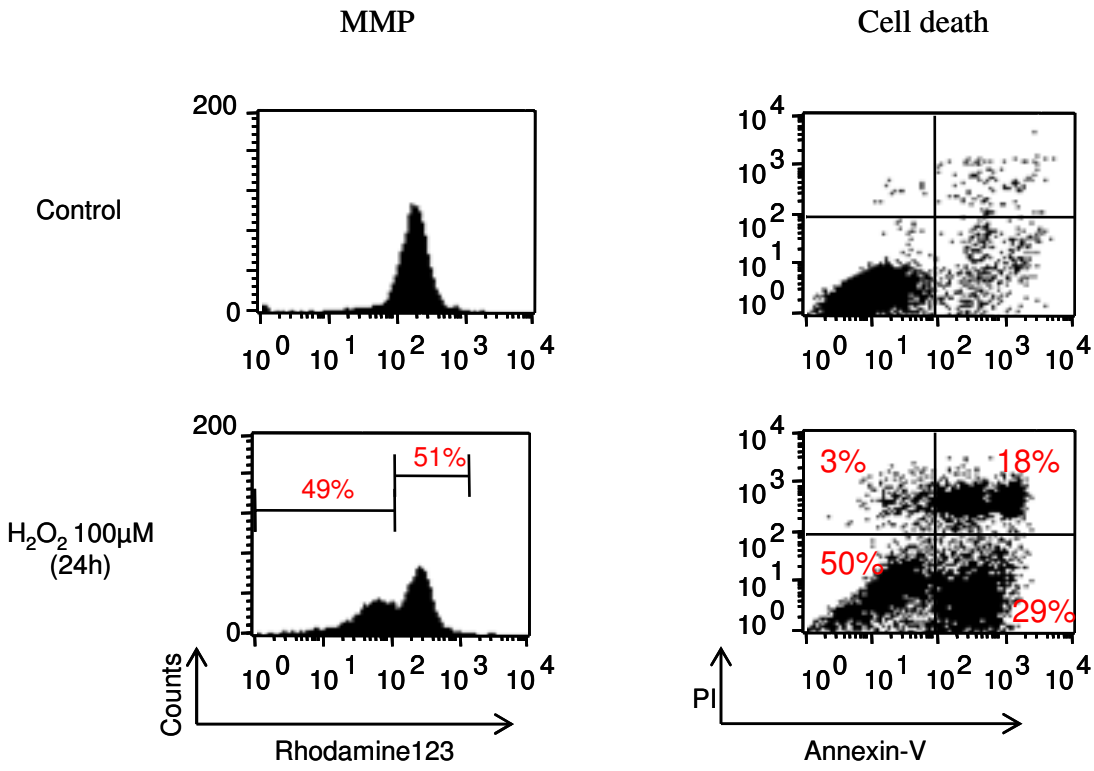
MMP
Cell death
Control
H_2O_2 100μM
(24h)
200
0
10^0 10^1 10^2 10^3 10^4
49%
51%
3%
18%
50%
29%
Counts
Rhodamine123
PI
Annexin-V

Figure 22. K562 is less sensitive to oxidative stress-induced mitochondrial membrane potential (MMP) collapse than KBM5. K562 and KBM5 cells were treated with 50 μM H_2O_2 at different time points. MMP was detected by Rhodamine 123. Decreased Rhodamine 123 fluorescence indicates the MMP collapsed cells. Percentages of MMP collapsed cells are labeled.

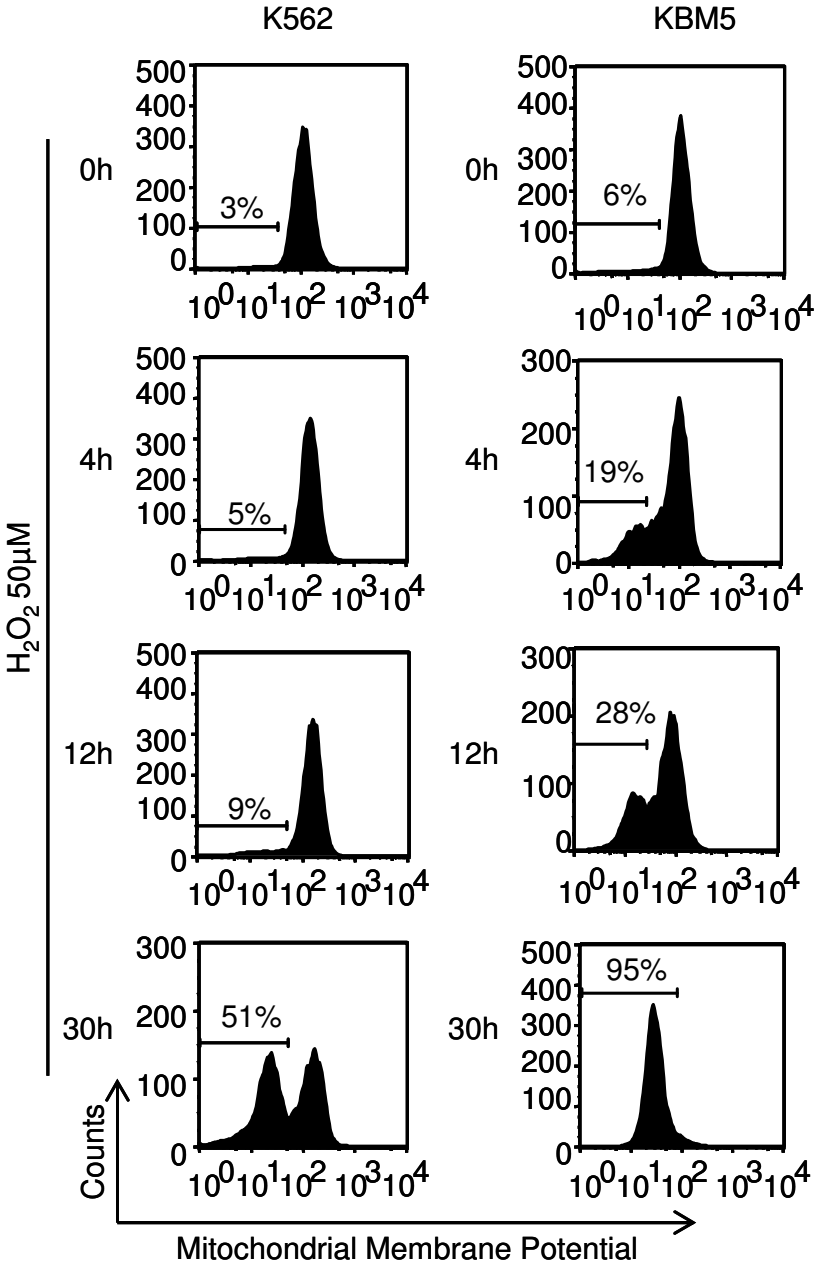
K562
KBM5
0h
4h
12h
30h
3%
6%
5%
19%
9%
28%
51%
95%
H_2O_2 50μM
Counts
Mitochondrial Membrane Potential

Figure 23. Over-expression of BCL-XL but not BCL-2 prevents oxidative stress induced mitochondrial membrane potential (MMP) collapse. K562, K562-BCLXL-HA and K562-BCL2-GFP cells were treated with 50 μM H_2O_2 for 72 hours. MMP was detected by Rhodamine 123. Decreased Rhodamine 123 fluorescence indicates the MMP collapsed cells. Sample contains MMP collapsed cells shown in the divided peak pattern. The peaks are indicated by arrows.

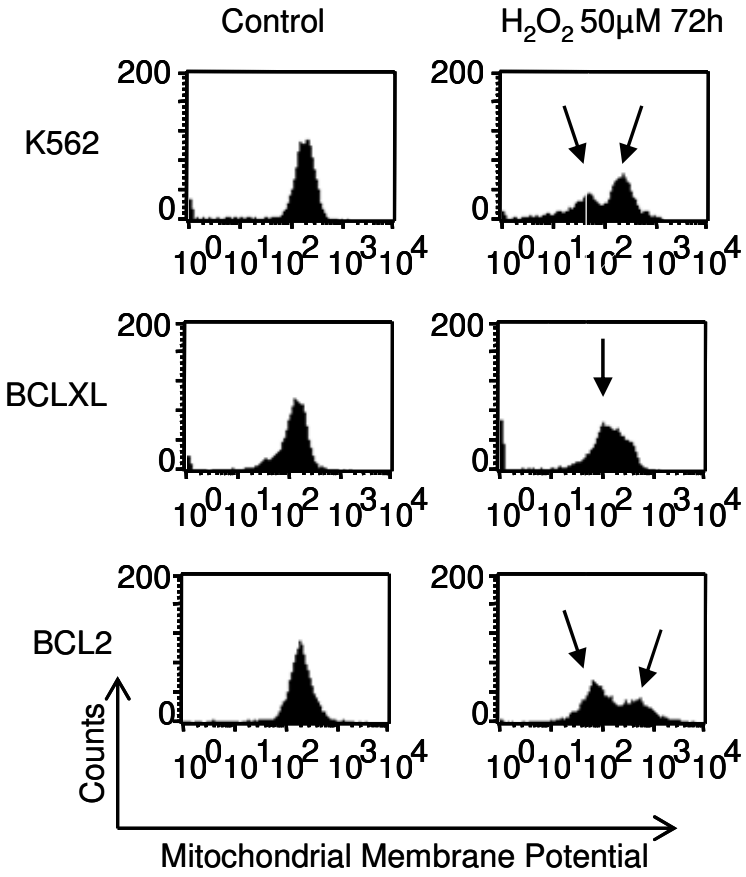
Control
H2O2 50µM 72h
K562
BCLXL
BCL2
200
0
Counts
Mitochondrial Membrane Potential

4.2.3 BCL-XL but not BCL-2 Maintains Cell Mitochondrial Integrity Under Oxidative Stress.

The above results suggested that BCL-XL specifically protects mitochondria against oxidative stress. However, whether BCL-XL protects mitochondria by limiting mitochondrial ROS generation or enhancing cell tolerance of oxidative stress was not answered. Therefore, I further tested the intracellular and mitochondria ROS generation caused by the treatment of H_2O_2. No dramatic difference was observed between BCL-XL over-expressing cells and the parental cells (Figure 24). This result indicated that H_2O_2 is effective in promoting mitochondrial oxidative stress in both cells and BCL-XL mediated protection effects on mitochondria is not through limiting mitochondrial ROS generation. Furthermore, I tested the mitochondrial integrity under oxidative stress. Mitochondrial respiratory complexes are the major functional components and are localized on the mitochondria membrane space. The stability of these proteins can indicate the function and integrity of mitochondrial organelles. I treated K562, k562-BCLXL-HA and K562-BCL2-GFP with H_2O_2 for 48 and 96 hours. Cell lysates were collected and blotted with different mitochondrial complex marker subunits. A dramatic loss of mitochondrial complex II 30KD subunit was observed in K562 and K562-BCL2-GFP but not in K562-BCLXL-HA (Figure 25). Along with this change, endogenous BCL-XL was also found decreased in K562 and K562-BCL2-GFP but not in K562-BCLXL-HA (Figure 25). These results indicated that BCL-XL plays an important role to maintain the stability of mitochondria and mitochondrial membrane bound complexes under

oxidative stress. Additionally, I also blotted these samples with PARP and Capase3 antibodies to evaluate the apoptosis activation. Interestingly, the cleavage of Caspase3 and PARP was only observed in K562 (Figure 25). However, the decrease of PARP was found in K562-BCL2-GFP, but no cleaved Caspase3 was detected (Figure 25). More important, there was no oxidative stress-induced cleavage of either PARP or Capase3 in K562-BCLXL-HA (Figure 25). These results have demonstrated that BCL-XL functions in both protecting mitochondria and preventing apoptotic activation against oxidative stress. On the other hand, BCL-2 can not protect mitochondria against oxidative stress but still plays a role in inhibiting apoptotic activation.

Figure 24. Over-expression of BCL-XL can not prevent oxidative stress induced mitochondrial ROS increase. K562 and K562-BCLXL-HA cells were treated with 50 μM H_2O_2 for 2 hours. Cellular and mitochondrial ROS levels were detected by DCF-DA and MitoSOX Red respectively. Medians of different samples are labeled.

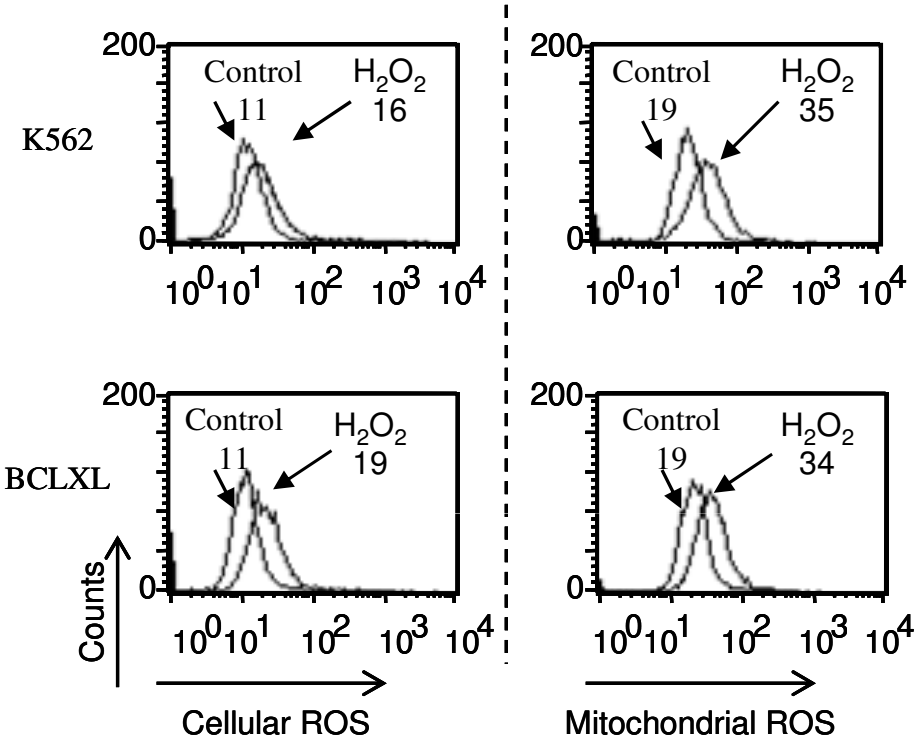
K562
BCLXL
200
0
Control
11
H_2O_2
16
19
35
34
10^0 10^1 10^2 10^3 10^4
Counts
Cellular ROS
Mitochondrial ROS

Figure 25. BCL-XL maintains mitochondria integrity and inhibits apoptosis activation under oxidative stress. K562, K562-BCLXL-HA and K562-BCL2-GFP cells were treated with 50 µM H_2O_2 for 48 or 96 hours. The cell lysates were blotted with antibodies of mitochondrial respiratory complex specific subunits, BCL-2, BCL-XL, HA, PARP and Caspase3. Actin was used as a loading control.

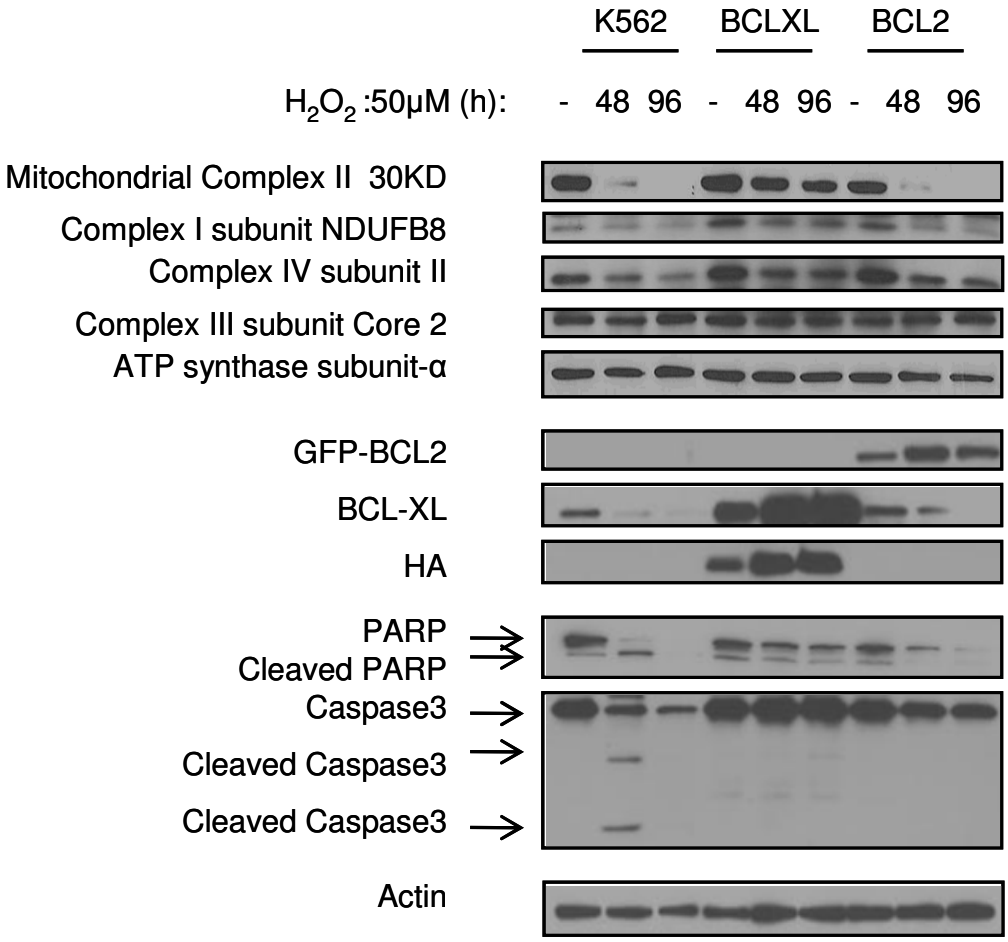
K562
BCLXL
BCL2
H2O2 :50μM (h):
- 48 96 - 48 96 - 48 96
Mitochondrial Complex II 30KD
Complex I subunit NDUFB8
Complex IV subunit II
Complex III subunit Core 2
ATP synthase subunit-α
GFP-BCL2
BCL-XL
HA
PARP
Cleaved PARP
Caspase3
Cleaved Caspase3
Cleaved Caspase3
Actin

4.3 Redox Modulation Reagent PEITC Induces Potent Cell Killing Effects in Imatinib-Resistant CML cells.

The figures and texts in this section have been cited and revised from 'Effective killing of Gleevec-resistant CML cells with T315I mutation by a natural compound PEITC through redox-mediated mechanism. Leukemia. 2008 Jun;22(6):1191-9.' [114]

4.3.1 PEITC Increases Cellular ROS and Depletes Cellular GSH in Imatinib-Resistant Cells.

'Imatinib mesylate (Gleevec) is a BCR-ABL tyrosine kinase inhibitor that is very effective in the clinical treatment of CML. However, a set of BCR-ABL mutants, especially the T315I mutation, leads to alteration in the three-dimension structure of the enzyme active site and exhibits continuously kinase activity and resistance to Imatinib. Such Bcr-Abl mutations impose new challenges in treatment of CML. Based on the previous observations that the BCR-ABL oncogenic signal can promote ROS generation and induce cellular redox imbalance, I postulated that such oxidative stress might serve as a biochemical basis for preferentially triggering ROS-mediated damage to CML cells by further oxidative stress with exogenous ROS-generating agents. My study was design to test this hypothesis using β-phenylethyl isothiocyanates (PEITC) as an agent to modulate cellular redox status in CML cells. PEITC has previously been shown to effectively disable the cellular glutathione system by inducing depletion of cellular glutathione and inhibition of glutathione peroxidase activity, and cause the massive ROS accumulation in cancer cells. [123] It should be noted that the

plasma PEITC concentrations in the μM range were clinically achievable through oral administration. [124,114]

To evaluate the biological basis for my above strategy design, the correlation between BCR-ABL induced cellular ROS generation and intracellular GSH status was tested. BCR-ABL inducible cell line TonB210 was used to detect the level of cellular ROS and GSH along with the over-expression of BCR-ABL. The parellel increase of intracellular GSH and cellular ROS upon BCR-ABL induction (Figure 26) was observed. This data suggested that the cellular GSH is likely served as cellular defense component responsive to BCR-ABL-promoted ROS elevation. Based on this suggestion, the biological effects of PEITC on Imatinib-resistant CML cells were further investigated. 'KBM5-T315I cells were significantly less sensitive to Imatinib (IC_{50} = 5.4 ± 0.07 μM) than the parental KBM5 cells (IC_{50} = 0.28 ± 0.05 μM, $p<0.0001$), and approximate 30% of KBM5-T325I cells remained viable after treatment with even 10 μM of Imatinib (Figure 27). In agreement with my previous prediction, the incubation of KBM5 and KBM5-T315I cells with PEITC led to a significant increase in cellular ROS. KBM5 and KBM5-T315I cells treated with 10 μM of PEITC for 90 minutes showed the dramatic increase of cellular ROS by 129% and 282%, respectively (Figure 28). Additionally, I also confirmed the GSH depletion caused by PEITC in both KBM5 and KBM5-T315I cells. Incubation of cells with 10 μM PEITC caused about 30-40% depletion of glutathione at 5 hour, and a complete depletion at 10 hour in both KBM5 and KBM5-T315I cells (Figure 29). Because N-acetylcysteine (NAC) is a precursor for glutathione synthesis, pre-incubation of

cells with NAC would protect cellular GSH pool. I found that pre-incubation with 2 mM NAC largely restored cellular glutathione, even with 10 hour PEITC treatment (Figure 29). This result has suggested that NAC can be used as negative regulator of PEITC in my experimental system.' [114]

Figure 26. Over-expression of BCR-ABL elevates cellular GSH along with increased ROS. Doxycycline 0.5 μg/ml was used to induce BCR-ABL expression in TonB210 cells. Flow cytometry was used to detect cellular GSH and ROS level by CMFDA and DCF-DA, respectively.

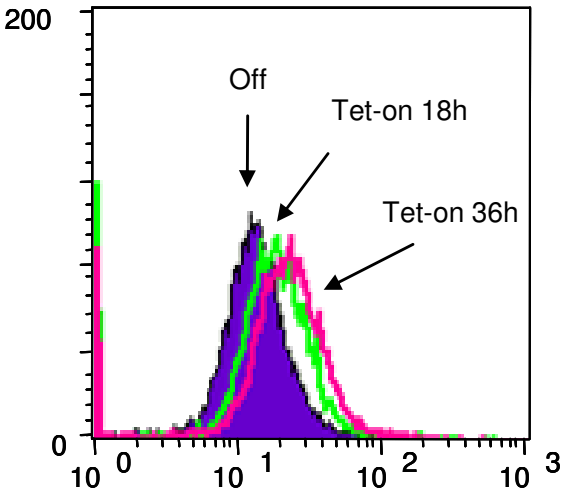

Cellular GSH

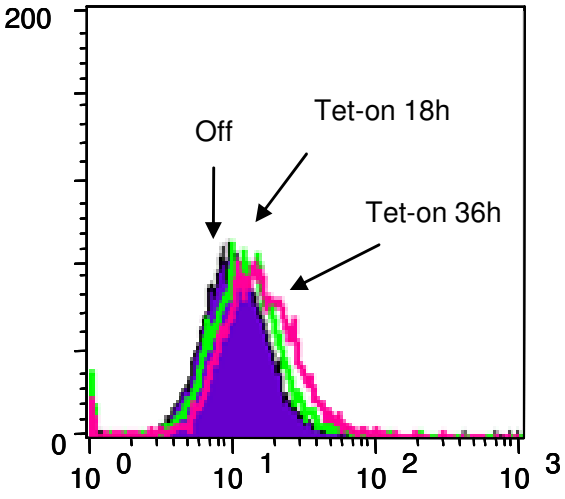

Cellular ROS

Figure 27. KBM5-T315I cells are resistant to Imatinib-induced cell growth inhibition. KBM5 and KBM5-T315I cells are cultured with Imatinib at 0, 1, 3, 6, 10 and 30 μM. Cell growth was analyzed by MTT assay. (Cited from Zhang H. et al. 2008 Leukemia) [114]

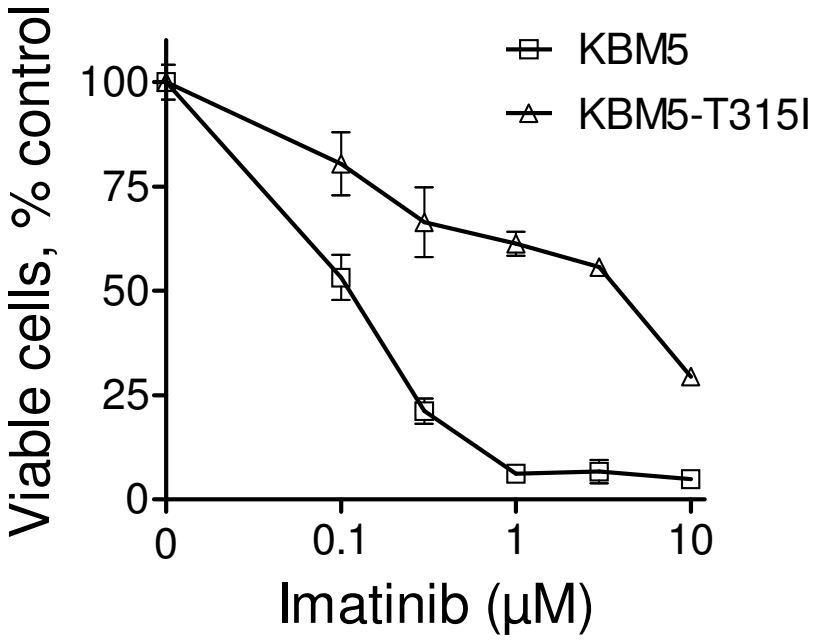
KBM5
KBM5-T315I
Viable cells, % control
100
75
50
25
0
0
0.1
1
10
Imatinib (μM)

Figure 28. PEITC promotes ROS generation in both KBM5 and KBM5-T315I cells. KBM5 and KBM5-T315I cells are cultured with PEITC (10 μM, 1.5 hours). Cellular ROS contents were measured by flow cytometric analysis after the cells were stained with CM-H_2DCF-DA fluorescence dye. (Cited from Zhang H. et al. 2008 Leukemia) [114]

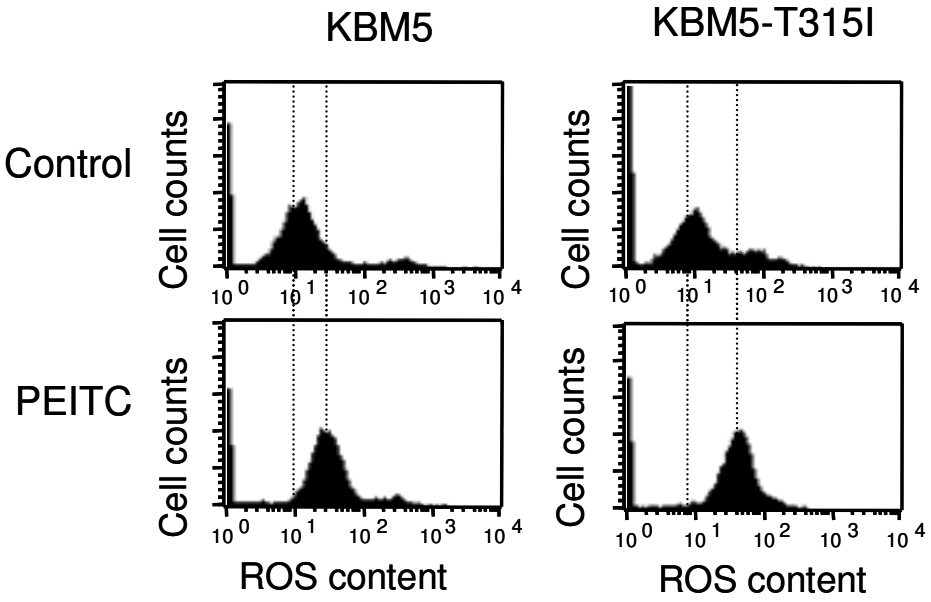
KBM5
KBM5-T315I
Control
PEITC
Cell counts
Cell counts
Cell counts
Cell counts
10^0 10^1 10^2 10^3 10^4
10^0 10^1 10^2 10^3 10^4
10^0 10^1 10^2 10^3 10^4
10^0 10^1 10^2 10^3 10^4
ROS content
ROS content

Figure 29. PEITC depletes cellular GSH in both KBM5 and KBM5-T315I cells. KBM5 (A) and KBM5-T315I (B) cells were incubated with 10 μM PEITC in the presence or absence of 2 mM NAC for 5 or 10 hours as indicated. Total cellular glutathione contents were then measured by using DTNB-enzyme cycling glutathione assay kit. (**): The GSH is undetectable in the sample. (Cited from Zhang H. et al. 2008 Leukemia) [114]

A

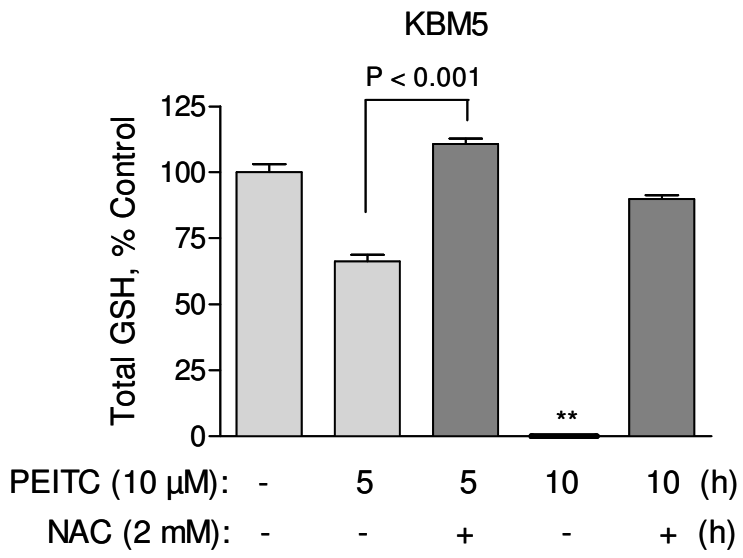
KBM5
P < 0.001
Total GSH, % Control
125
100
75
50
25
0
**
PEITC (10 µM): - 5 5 10 10 (h)
NAC (2 mM): - - + - + (h)

B

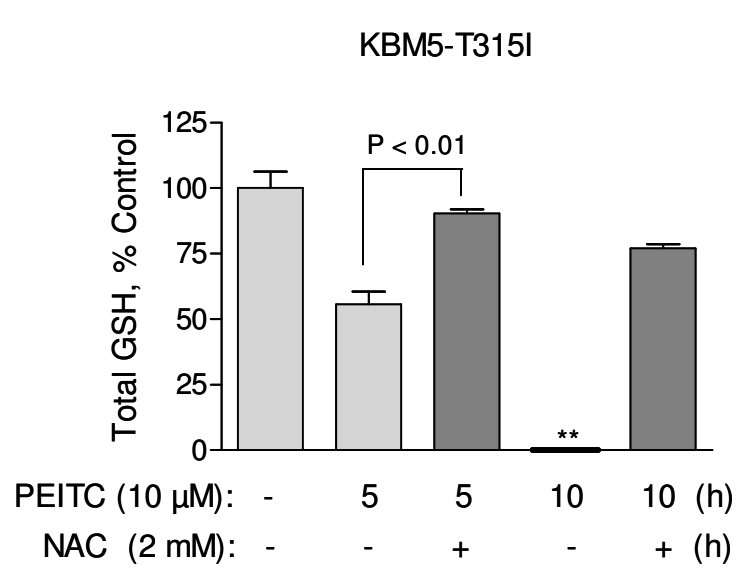
KBM5-T315I
P < 0.01
Total GSH, % Control
125
100
75
50
25
0
**
PEITC (10 µM): - 5 5 10 10 (h)
NAC (2 mM): - - + - + (h)

4.3.2 PEITC Effectively Promotes Apoptosis in Cells Expressing T315I-BCR-ABL Mutant Protein.

'Based on the hypothesis that the increase of ROS generation in CML under the stimulation of BCR-ABL oncogenic signal might render these cells highly dependent on glutathione to maintain redox balance, depletion of glutathione by PEITC would cause severe ROS accumulation and trigger cell death. Since T315I mutation retains the constitutive tyrosine kinase activity, CML cells with this mutation should, like their parental, exhibit increased ROS stress and sensitive to PEITC.

In contrast to the results from Imatinib treatment (Figure 27), both KBM5 and KBM5-T315I cells were equally sensitive to PEITC, with the IC_{50} values of 3.1 ± 0.08 for KBM5 cells and 2.8 ± 0.42 for KBM5-T315I cells (Figure 30A). Especially, at 10 µM, PEITC caused complete inhibition of cell growth in both KBM5 and KBM5-T315I cells (Figure 30A). The potent activity of PEITC in killing both KBM5 and KBM5-T315I cells was further demonstrated by annexin-V/PI assay. Exposure of CML cells to 10 µM PEITC for 24 hours resulted in 66% and 63% acute cell death in KBM5 and KBM5-T315I cells, respectively (Figure 30B). This result was further confirmed in a pair of murine cell lines derived from BaF3 by stably transfecting with either the wild-type or T315I mutant Bcr-Abl. As expected, PEITC was also effective in inducing apoptosis in both murine cell lines, whereas Imatinib caused cell death only in BaF3-BCR-ABL cells but not in BaF3-BCR-ABL-T315I cells (Figure 31). I further tested the ability of PEITC in killing primary CML cells isolated from patients who were clinically resistant to

Imatinib treatment. The primary CML cells from two Imatinib-resistant blast crisis patients also exhibited resistance to Imatinib in vitro. The CML cells from a patient with T315I mutation were particularly resistant to Imatinib, with the IC_{50} value more than 50 μM (Figure 32A). In contrast, the CML cells from both patients were equally sensitive to PEITC in vitro, with the IC_{50} values of 8.3 and 10.5 μM, respectively (Figure 32B). Consistently, flow cytometry analysis revealed that incubation with 10 μM PEITC for 24 hours caused more than 50% cell death in the primary CML cells of both patient samples (Figure 32C). MTT assay of a total of 6 CML patient samples showed that the IC_{50} values of PEITC were 13.6 ± 4.04 μM (Table 1). In contrast to the potent cytotoxicity in primary CML cells, PEITC exhibited relatively low cytotoxic effects on normal lymphocytes isolated from healthy donors. Figure 33 shows the dose-response curves of two representative normal lymphocytes samples. The mean IC_{50} value of PEITC in normal lymphocytes was 31.5 ± 5.3 μM, which was significantly higher than that of the primary CML cells (P=0.002). In summary, the above results has identified that PEITC is effective in killing CML cells harboring T315I mutation, which confers resistance to tyrosine kinase inhibitor Imatinib. [114]

Figure 30. Both KBM5 and KBM5-T315I cells are sensitive to PEITC-induced growth inhibition and cell death. (A) KBM5 and KBM5-T315I cells are cultured with PEITC at 0, 1, 3, 6, 10 and 30 μM. Cell growth was analyzed by MTT assay. (B) Time-dependent induction of cell death by PEITC in KBM5 and KBM5-T315I cells. Cell death was detected by annexin-V/PI assay. The number shown below each panel indicates the percentage of annexin-V and PI double-negative cells (viable). (Cited from Zhang H. et al. 2008 Leukemia) [114]

A

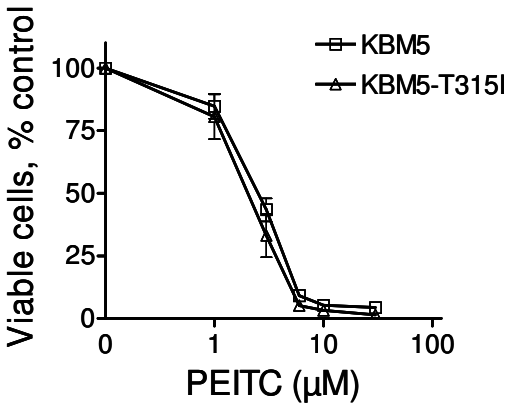
KBM5
KBM5-T315I
Viable cells, % control
100
75
50
25
0
0
1
10
100
PEITC (μM)

B

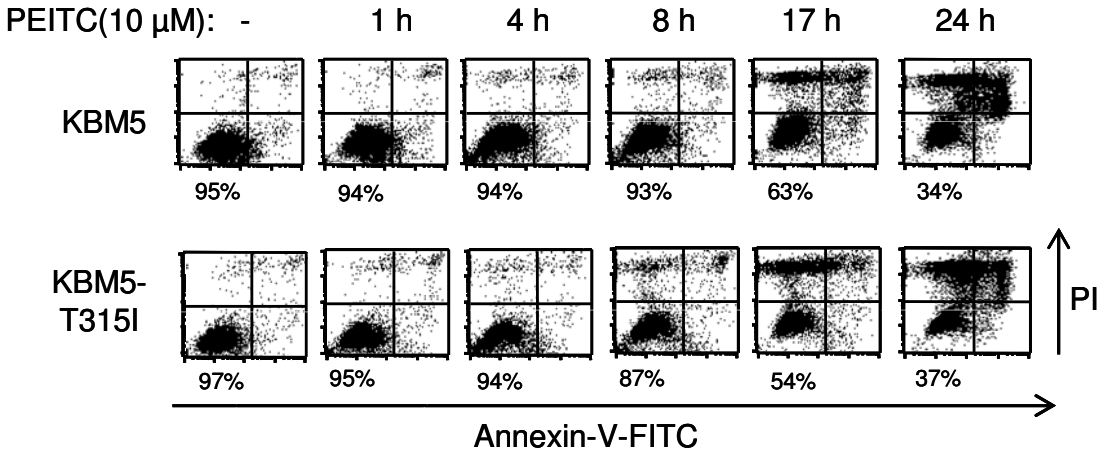
PEITC(10 μM): -
1 h
4 h
8 h
17 h
24 h
KBM5
95%
94%
94%
93%
63%
34%
KBM5-
T315I
97%
95%
94%
87%
54%
37%
PI
Annexin-V-FITC

Figure 31. PEITC induces cell death in BCR-ABL-T315I transformed cells. BaF3-BCR-ABL and BaF3-BCR-ABL-T315I cells were incubated with 10 μM PEITC or 2 μM Imatinib for 24 h, and cell death was measured by the annexin-V/PI assay. The number shown below each panel indicates the percentage of the annexin-V and PI double-negative cells (viable). (Cited from Zhang H. et al. 2008 Leukemia) [114]

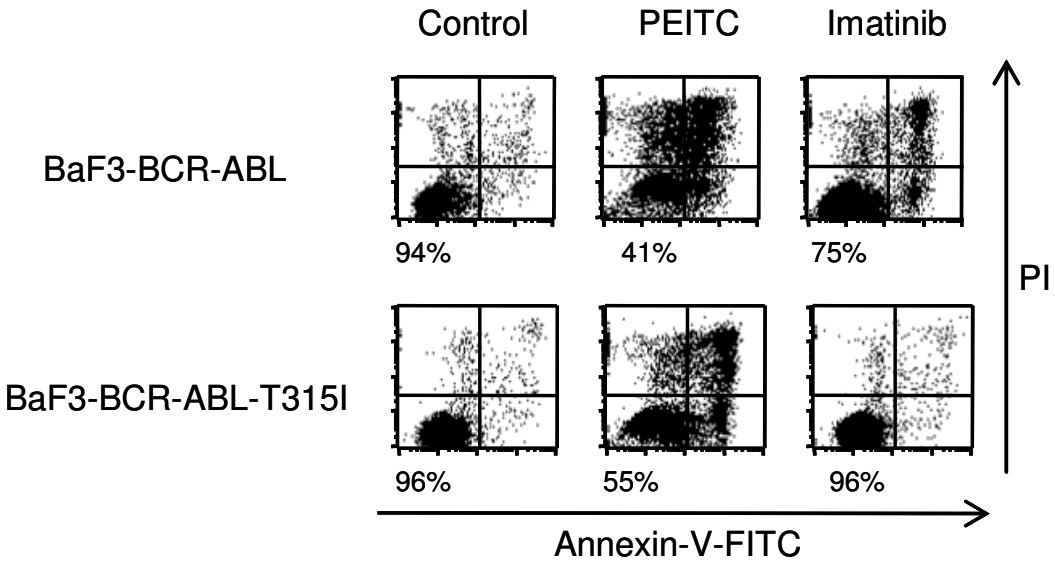
Control
PEITC
Imatinib
BaF3-BCR-ABL
94%
41%
75%
BaF3-BCR-ABL-T315I
96%
55%
96%
PI
Annexin-V-FITC

Figure 32. PEITC induces growth inhibition and cell death in Imatinib-resistant CML patient samples. (A, B) Representative dose-dependent cytotoxic effect of Imatinib (A) and PEITC (B) in primary CML cells with or without T315I mutation. Cells were incubated with the indicated concentrations of Imatinib or PEITC for 72 hours, and cell viability was measured by MTT assay. (C) Induction of cell death by PEITC (10 μM, 24 hours) in primary blast crisis CML cells with or without T315I mutation. Cell viability was measured by annexin-V/PI assay. The number shown below each panel indicates the percentage of viable cells. (Cited from Zhang H. et al. 2008 Leukemia) [114]

A

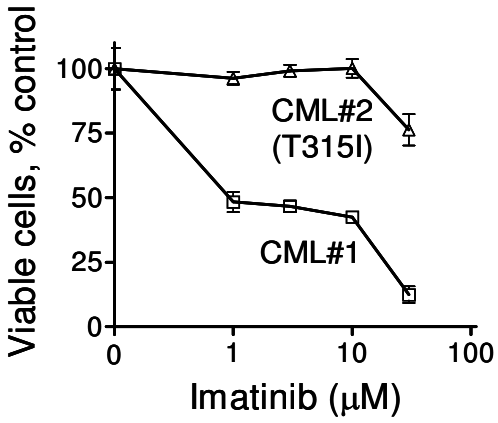
Viable cells, % control
100
75
50
25
0
0
1
10
100
Imatinib (μM)
CML#2
(T315I)
CML#1

B

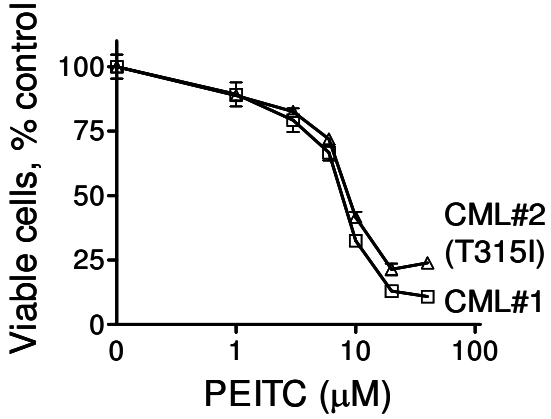
Viable cells, % control
100
75
50
25
0
0
1
10
100
PEITC (μM)
CML#2
(T315I)
CML#1

C

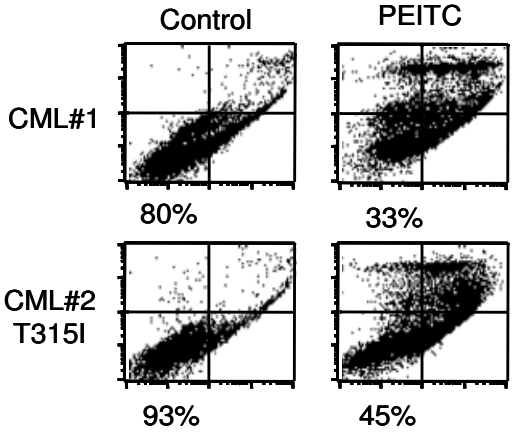
Control
PEITC
CML#1
80%
33%
CML#2
T315I
93%
45%

Table 1. IC_{50} values of PEITC in primary Imatinib-resistant CML cells. The primary Imatinib-resistant CML cells were isolated from 6 patients clinically refractory to Imatinib. Cells were incubated with the gradient concentrations of Imatinib for 72 hours, and cell viability and the IC_{50} values were measured by MTT assay. (Cited from Zhang H. et al. 2008 Leukemia) [114]

Sample#	CML stage	IC_{50} ±SD (μM)
1	Blast crisis	8.3 ± 0.8
2	Blast crisis (T315I)	10.5 ± 0.8
3	Accelerated phase	10.9 ± 1.5
4	Accelerated phase	13.2 ± 0.9
5	Accelerated phase	16.1 ± 1.6
6	Accelerated phase	16.6 ± 1.0
Mean±SD		12.6 ± 3.3

Figure 33. Normal donors are less sensitive to PEITC-induced cell growth inhibition. Cells isolated from normal donors were incubated with the indicated concentrations of PEITC for 72 hours, and cell viability was measured by MTT assay.

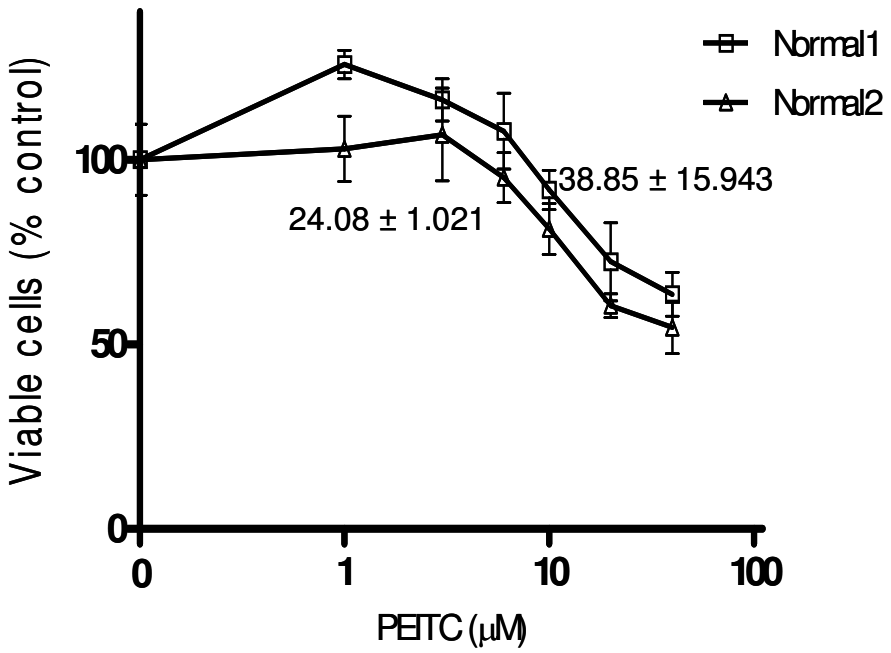
Normal1
Normal2
Viable cells (% control)
100
50
0
38.85 ± 15.943
24.08 ± 1.021
0
1
10
100
PEITC (μM)

4.3.3 PEITC Induces BCR-ABL Cleavage and Degradation.

'Furthermore, since many proteins, include BCR-ABL, contain redox-sensitive cysteine residuals which can be oxidized by ROS and affect protein structure and stability, I speculated that induction of severe ROS stress in CML cells might potentially alter the redox status of BCR-ABL and render it vulnerable to degradation.

Based on the observations that PEITC caused a substantial increase in cellular ROS, I tested the possibility that PEITC might alter the protein stability of wild-type and T315I mutant BCR-ABL. Exposure of KBM5 and KBM5-T315 cells to 10 μM PEITC caused a and time-dependent decrease of the 210 kD BCR-ABL protein. The decrease of total BCR-ABL proteins occurred as early as 4 hour of PEITC incubation, with a concurrent appearance of a 52-kD cleavage product (Figure 34). The ability of PEITC to induce degradation of wild-type and mutant BCR-ABL proteins was further confirmed in BaF3-BCR-ABL and BaF3-BCR-ABL-T315I cells, which express the single isoform of BCR-ABL (Figure 35). Since caspase-3 activation and the cleavage of poly (ADP-ribose) polymerase (PARP) are hallmarks of apoptosis, I analyzed the cleavage of caspase-3 (activation) and PARP at various time points after cells were treated with PEITC, and evaluated the temporal relationship between the protein cleavage, BCR-ABL degradation, and apoptosis activation. It appeared that caspase-3 activation and PARP cleavage occurred before BCR-ABL degradation, and that the cleavage of all these three proteins proceeded well before cell death (Figure 34, Figure 30B).'[114]

Figure 34. PEITC induces cleavage of BCR-ABL and BCR-ABL-T315I mutant correlated with caspase-3 activation. PEITC induced time-dependent cleavage of BCR-ABL, caspase-3 and PARP in KBM5 and KBM5-T315I cells. Cells were incubated with 10 μM PEITC for the indicated times, and protein cleavage was detected by immunoblotting using the respective specific antibodies. (Cited from Zhang H. et al. 2008 Leukemia) [114]

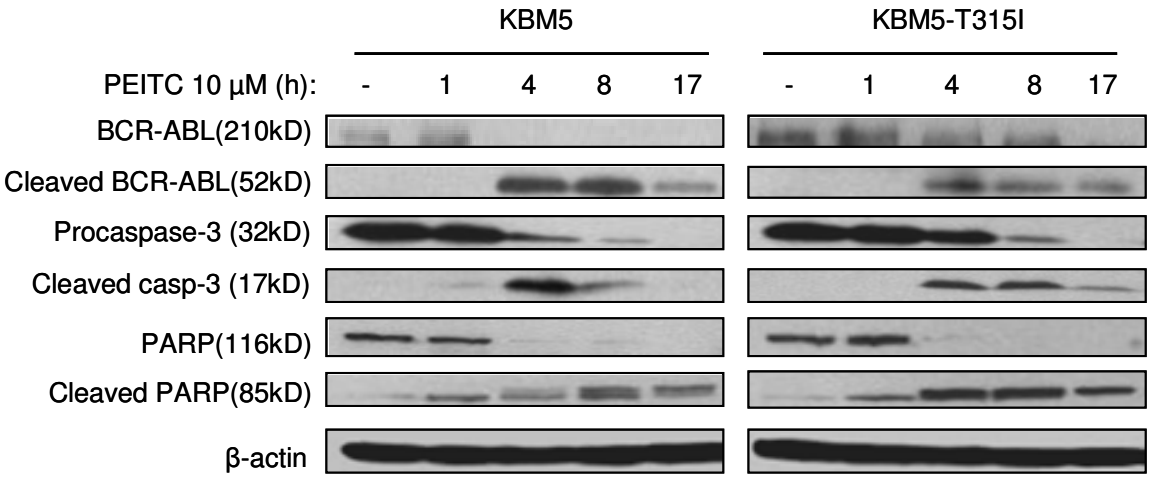
KBM5
KBM5-T315I
PEITC 10 μM (h):
-
1
4
8
17
-
1
4
8
17
BCR-ABL(210kD)
Cleaved BCR-ABL(52kD)
Procaspase-3 (32kD)
Cleaved casp-3 (17kD)
PARP(116kD)
Cleaved PARP(85kD)
β-actin

Figure 35. PEITC induces decreases of BCR-ABL and BCR-ABL-T315I mutant in BCR-ABL over-expressing cells. PEITC treatment induces a time-dependent decrease of BCR-ABL levels in BaF3-BCR-ABL and BaF3-BCR-ABL-T315I cells. Cells were incubated with 10 μM PEITC for the indicated times, and protein cleavage was detected by immunoblotting using the respective specific antibodies. (Cited from Zhang H. et al. 2008 Leukemia) [114]

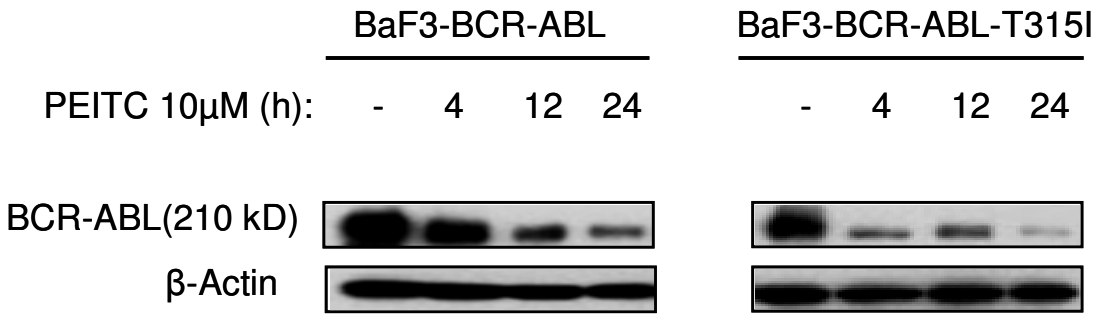
BaF3-BCR-ABL
BaF3-BCR-ABL-T315I
PEITC 10μM (h):
-
4
12
24
-
4
12
24
BCR-ABL(210 kD)
β-Actin

'To further test if caspases or proteasome might be involved in mediating PEITC-induced BCR-ABL degradation, I used chemical inhibitors of caspases or proteasome to evaluate the role of these enzymes. Pre-treatment of cells with 20 μM Z-VAD-FMK, a common inhibitor of multi caspases, effectively prevented the cleavage of the wild-type and T315I-mutant BCR-ABL protein, as evidenced by the preservation of the full-length (210 KD) BCR-ABL and suppression of the generation of the 52kD BCR-ABL (Figure 36, lanes 4-6). Interestingly, the proteasome inhibitor MG132 (5 μM) did not prevent the cleavage of BCR-ABL to 52 KD fragment (Figure 36, lanes 7-9), but only delay the loss of full length protein at the early time point (Figure 36, lane 8). This held true for both the wild-type and T315I-mutant BCR-ABL. Thus, it appeared that the PEITC-induced cleavage of BCR-ABL into 52-kD fragment was largely mediated by a caspase, whereas proteasome might only play a complementary role to accelerate further degradation. This is in agreement with the previous observations that caspase-3 is a redox-sensitive enzyme [125] and that inhibition of proteasome by MG132 may affect caspase activity in a ROS-dependent manner. Furthermore, I demonstrated that Z-VAD-FMK was able to significantly reduce PEITC-induced cell death in both KBM5 and KBM5-T315I cells, whereas MG132 exhibited little effect in preventing apoptosis (Figure 37), consistent with the important role of caspase in mediating degradation of BCR-ABL. Because Z-VAD-FMK is a broad-spectrum caspase inhibitor, these results did not allow the identification of the specific caspase responsive for the cleavage of BCR-ABL. I then tested if Z-DEVD-FMK, a specific inhibitor of caspase-3, could prevent BCR-ABL cleavage

and suppress PEITC-induced cell death. I identified that inhibition of caspase-3 by Z-DEVD-FMK exhibited similar preventive effects on BCR-ABL cleavage and cell death as the pan-caspase inbitor Z-VAD-FMK (Figure 38, Figure 39). This result suggested that caspase-3 is the key effective protease that mediates PEITC-induced degradation of BCR-ABL and apoptosis. This is in line with the previous observations that the normal c-ABL protein is a substrate of capase-3 and that this protein structural feature is preserved in BCR-ABL chimeric protein. [126-129] Taken together, the above results have suggested that the cleavage of BCR-ABL might not be the primary event that triggered apoptosis. The previous identified biochemical changes induced by PEITC, such as glutathione depletion and ROS accumulation, might be the initial factors to cause cell death in CML cells. More likely, the decrease of BCR-ABL may just accelerate the progress of capase-3 mediated apoptosis.' [114]

Figure 36. Pan caspase inhibitor prevents PEITC-induced cleavage of BCR-ABL and BCR-ABL-T315I mutant. KBM5 and KBM5-T315I cells were treated with PEITC with or without a 1-hour pre-treatment with 20 μM Z-VAD-FMK or MG132. BCR-ABL and BCR-ABL cleavage was detected by immunoblotting. (Cited from Zhang H. et al. 2008 Leukemia) [114]

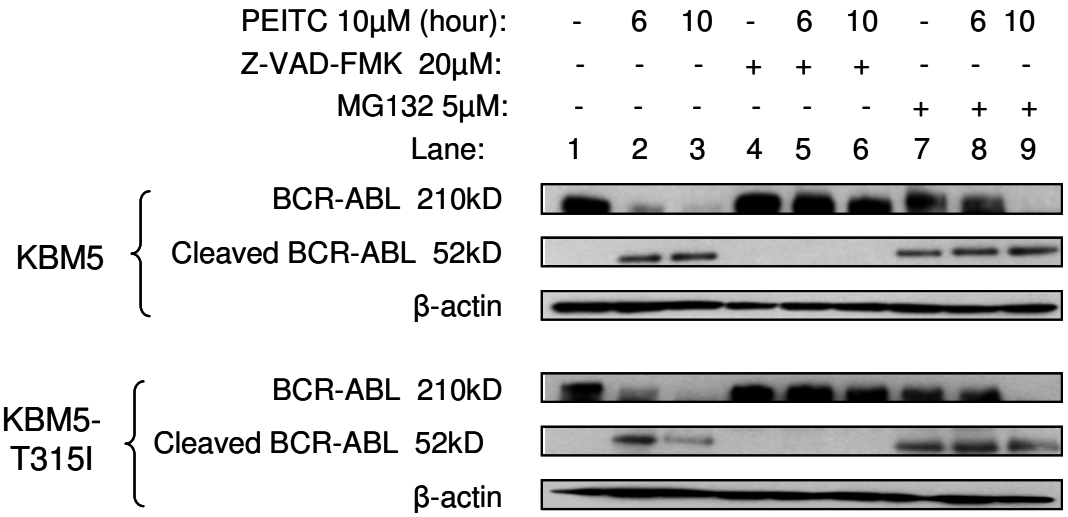
PEITC 10μM (hour): - 6 10 - 6 10 - 6 10
Z-VAD-FMK 20μM: - - - + + + - - -
MG132 5μM: - - - - - - + + +
Lane: 1 2 3 4 5 6 7 8 9
KBM5
BCR-ABL 210kD
Cleaved BCR-ABL 52kD
β-actin
KBM5-T315I
BCR-ABL 210kD
Cleaved BCR-ABL 52kD
β-actin

Figure 37. Pan caspase inhibitor prevents PEITC-induced cell death in KBM5 and KBM5-T315I cells. KBM5 and KBM5-T315I cells were treated with PEITC with or without a 1-hour pre-treatment with 20 μM Z-VAD-FMK or MG132. Cell viability was measured by annexin-V/PI assay. The number shown below each panel indicates the annexin-V/PI double-negative cells (viable). (Cited from Zhang H. et al. 2008 Leukemia) [114]

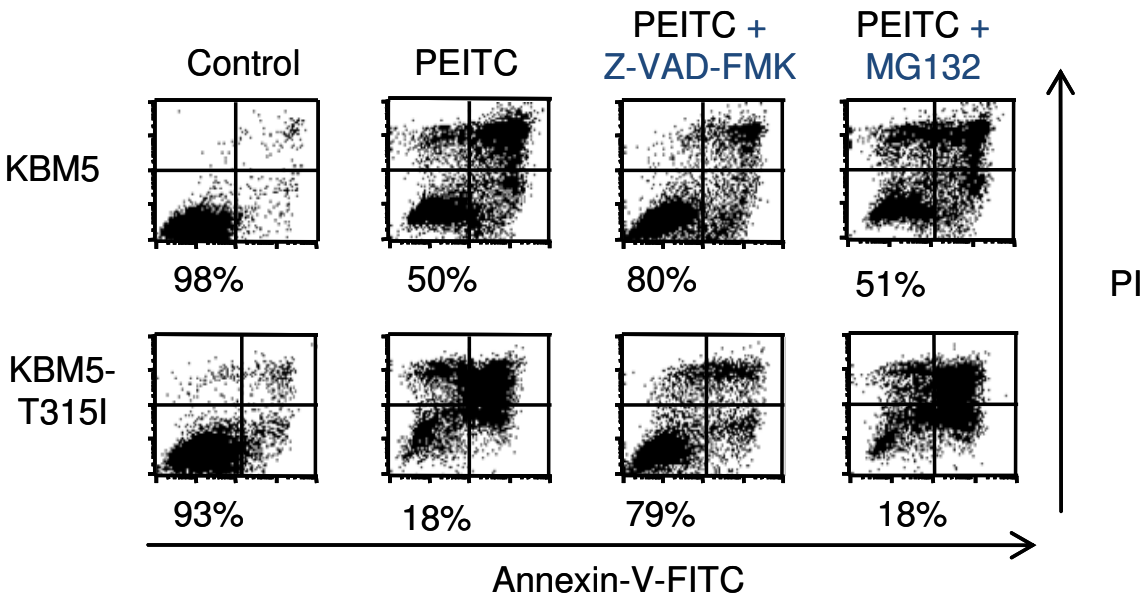
Control
PEITC
PEITC +
Z-VAD-FMK
PEITC +
MG132
KBM5
98%
50%
80%
51%
KBM5-
T315I
93%
18%
79%
18%
PI
Annexin-V-FITC

Figure 38. Caspase-3 inhibitor prevents PEITC-induced cleavage of BCR-ABL and BCR-ABL-T315I mutant. KBM5 and KBM5-T315I cells were treated with PEITC with or without a 1-hour pre-treatment with 20 μM Z-DEVD-FMK. BCR-ABL and BCR-ABL cleavage was detected by immunoblotting. (Cited from Zhang H. et al. 2008 Leukemia) [114]

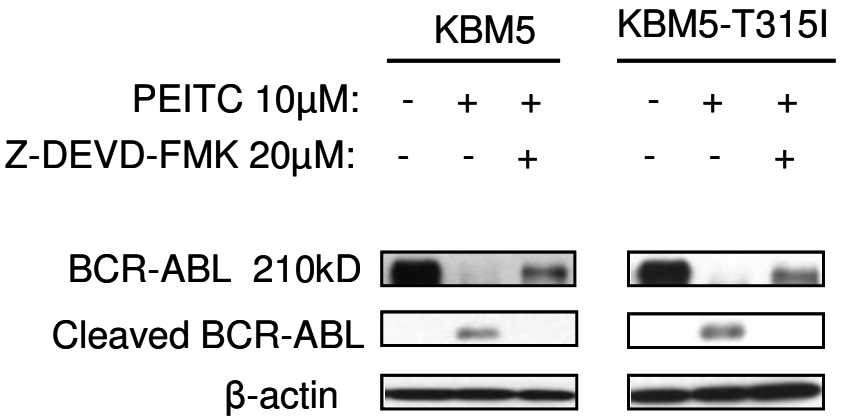
KBM5
KBM5-T315I
PEITC 10μM: - + + - + +
Z-DEVD-FMK 20μM: - - + - - +
BCR-ABL 210kD
Cleaved BCR-ABL
β-actin

Figure 39. Caspase-3 inhibitor prevents PEITC-induced cell death in KBM5 and KBM5-T315I cells. KBM5 and KBM5-T315I cells were treated with PEITC with or without a 1-hour pre-treatment with 20 μM Z-DEVD-FMK. Cell viability was measured by annexin-V/PI assay. The number shown below each panel indicates the annexin-V/PI double-negative cells (viable). (Cited from Zhang H. et al. 2008 Leukemia) [114]

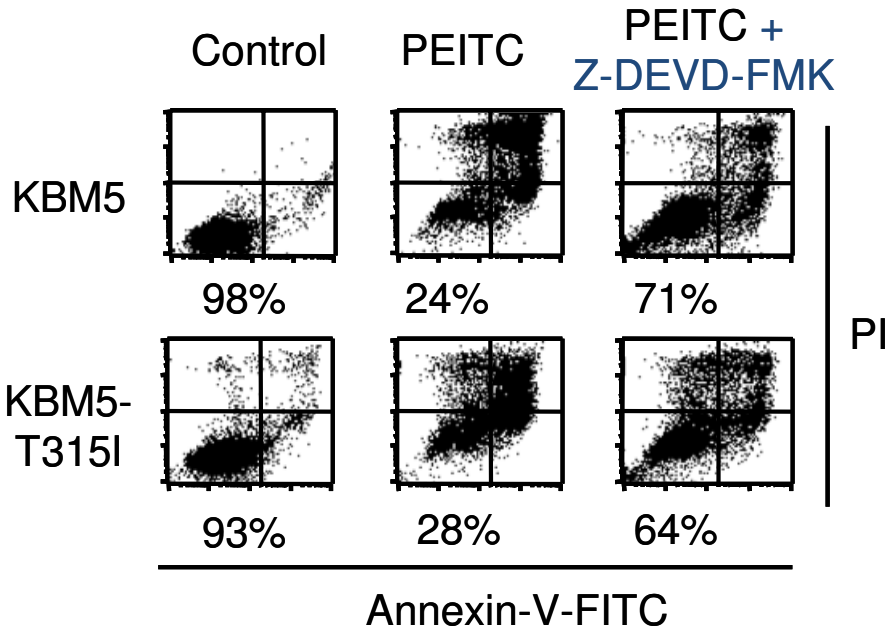
Control
PEITC
PEITC +
Z-DEVD-FMK
KBM5
98%
24%
71%
KBM5-
T315I
93%
28%
64%
PI
Annexin-V-FITC

4.3.4 Elevated Intrinsic Oxidative Stress Mediates PEITC Cellular Effects.

'To further demonstrate the essential role of oxidative stress in mediating PEITC induced cell killing effects in CML cells, I used the antioxidant N-acetyl-cysteine (NAC) and the H_2O_2 scavengering enzyme catalase to evaluate the importance of ROS induced by PEITC. Pre-incubation of cells with 2 mM antioxidant NAC almost completely suppressed PEITC-induced ROS increase (Figure 40A) and prevented cell death (Figure 41) in both KBM5 and KBM5-T315I cells. These results have suggested that intracellular ROS elevation might play an important role in mediating the cytotoxic effect of PEITC. Interestingly, pre-incubation with catalase at 500 units/ml only partially reduced PEITC-induced ROS increase (Figure 40B), and did not decrease cytotoxicity (Figure 41). However, the same concentrations of catalase fully prevented cell death induced by exogenous H_2O_2 (Figure 41). Because catalase is only functional in extra-cellular space, the difference I observed above has suggested that the oxidative stress induced by PEITC is intrinsic, and this intrinsic stress is important to promote apoptosis. Consistent with this observation, Western blotting analysis showed that only NAC prevented the PEITC-induced cleavage of BCR-ABL (Figure 42, Lane 7-9), whereas catalase did not suppress BCR-ABL degradation (Figure 42, Lane 15-16). These data also suggested that the intracellular redox buffer components are important for the stability of BCR-ABL, and the elevated intrinsic oxidative stress might render it vulnerable to degradation.' [114]

Figure 40. NAC prevents PEITC-elevated ROS in KBM5 and KBM5-T315I cells. Changes in ROS content in KBM5 and KBM5-T315I cells were measured following treatment with10 μM PEITC for 1.5 hours with and without a 1-hour pre-treatment with 2 mM NAC or 500 units/ml bovine catalase. Intracellular ROS was detected by CM-H_2DCF-DA fluorescent dye (control, purple; NAC or catalase, green; PEITC, pink; PEITC + NAC or catalase, blue). (Cited from Zhang H. et al. 2008 Leukemia) [114]

A

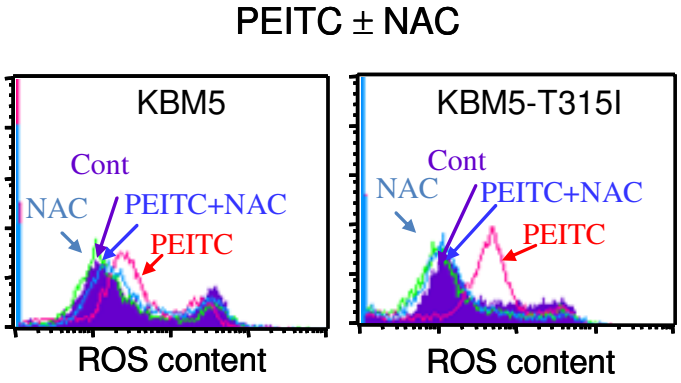
PEITC ± NAC
KBM5
Cont
NAC
PEITC+NAC
PEITC
ROS content
KBM5-T315I
Cont
NAC
PEITC+NAC
PEITC
ROS content

B

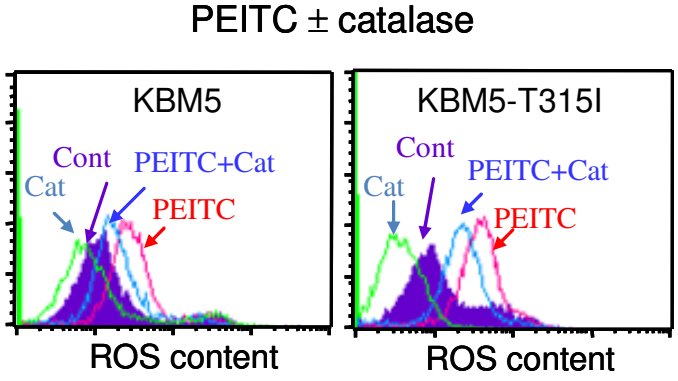
PEITC ± catalase
KBM5
Cont
Cat
PEITC+Cat
PEITC
ROS content
KBM5-T315I
Cont
Cat
PEITC+Cat
PEITC
ROS content

Figure 41. NAC prevents PEITC-induced cell death in KBM5 and KBM5-T315I cells. Cells were treated with 10 μM PEITC for 40 hours with or without a 1-hour pre-treatment with 2 mM NAC or 500 units/ml bovine catalase. For comparison, cells were also treated with 100 μM H_2O_2 in the presence or absence of 500 units/ml catalase as a positive control for catalase activity. Cell death was determined by the annexin-V/PI assay. The number shown below each panel indicates the annexin-V and PI double-negative cells (viable). (Cited from Zhang H. et al. 2008 Leukemia) [114]

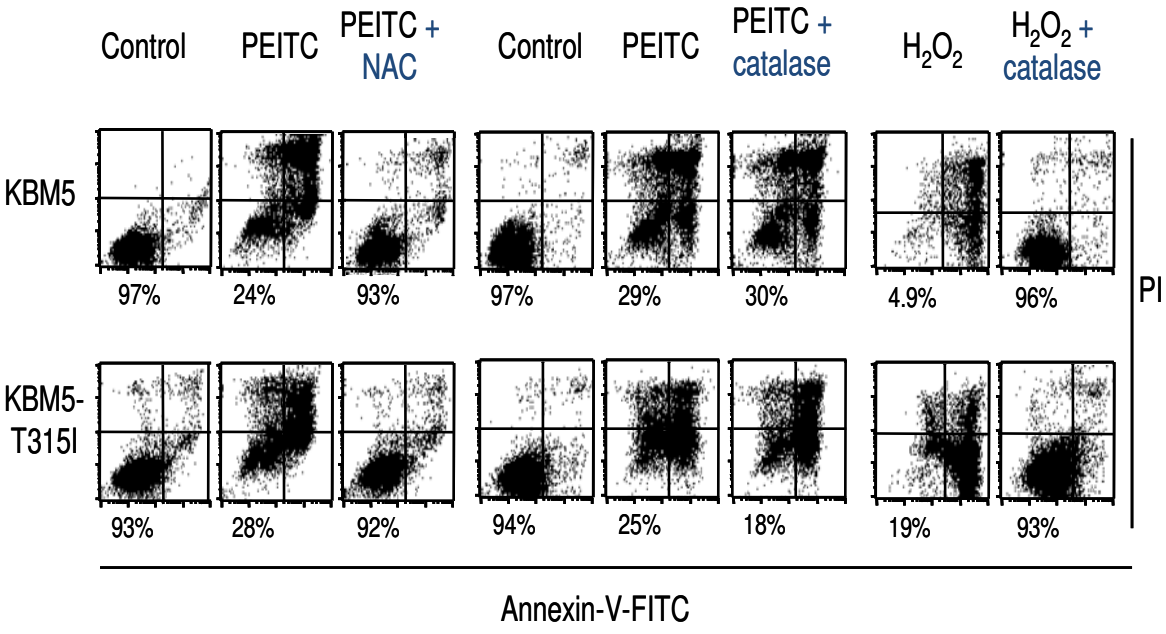
Control
PEITC
PEITC + NAC
Control
PEITC
PEITC + catalase
H_2O_2
H_2O_2 + catalase
KBM5
KBM5-T315I
97%
24%
93%
97%
29%
30%
4.9%
96%
93%
28%
92%
94%
25%
18%
19%
93%
PI
Annexin-V-FITC

Figure 42. NAC prevents PEITC-induced BCR-ABL cleavage in KBM5 and KBM5-T315I cells. Time-dependent cleavage of BCR-ABL following PEITC treatment with or without a 1-hour pre-treatment with 2 mM NAC or 500 units/ml catalase. BCR-ABL protein expression was detected by immunoblotting. (Cited from Zhang H. et al. 2008 Leukemia) [114]

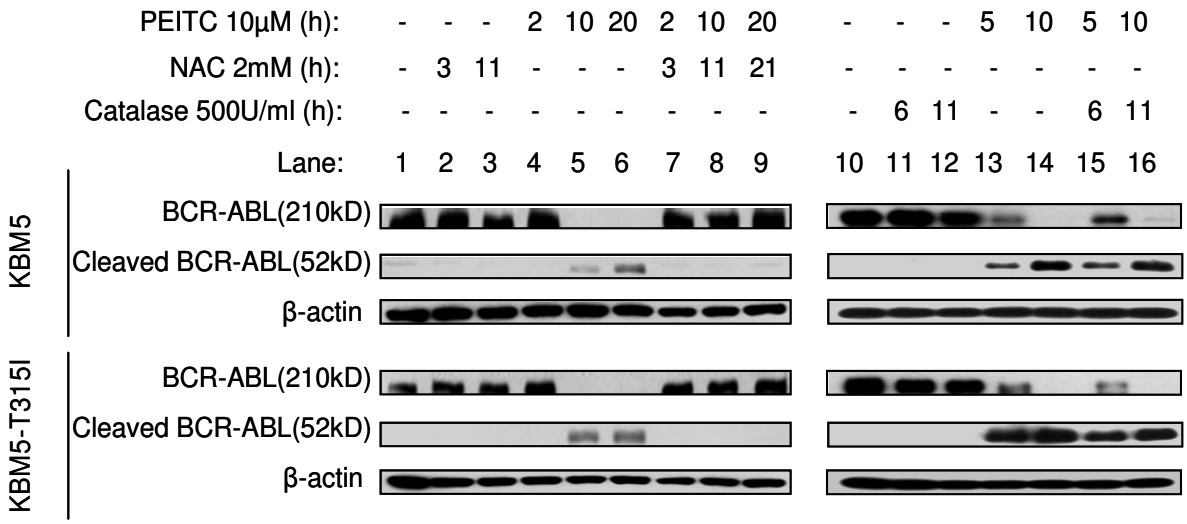
PEITC 10μM (h): - - - 2 10 20 2 10 20 - - - 5 10 5 10
NAC 2mM (h): - 3 11 - - - 3 11 21 - - - - - - -
Catalase 500U/ml (h): - - - - - - - - - - 6 11 - - 6 11
Lane: 1 2 3 4 5 6 7 8 9 10 11 12 13 14 15 16
KBM5
BCR-ABL(210kD)
Cleaved BCR-ABL(52kD)
β-actin
KBM5-T315I
BCR-ABL(210kD)
Cleaved BCR-ABL(52kD)
β-actin

4.4 Imatinib and ABT737 Enhances the Sensitivity of CML Blast Crisis Cells to Oxidative Stress-Induced Apoptosis.

4.4.1 Establishing K562-Mix, an in vitro Model with Heterogenic Expression of BCL-XL and BCL-2.

the single target drug BCR-ABL inhibitor Imatinib has high selectivity and low side effects. However, CML cells may exhibit uneven response to Imatinib resulted from their phenotypic heterogeneity. Especially, in some cases, Imatinib is effective to inhibit BCR-ABL activity in CML cells, but the alternative survival pathway promotes CML cell survival. [130] To solve this problem, the therapeutic strategy to limit the survival role of alternative pathway should be developed. It would be useful to establish an experimental model with the heterogenic expressions of cell survival factors. In this model, the phenotypic genotype of the drug sensitive or resistant population could be identified. Therefore, the experimental model, K562-Mix was established to detect the drug sensitivity of CML cells with different BCL-XL and BCL2 expressions. Besides K562-BCLXL-KD (Figure 17) and K562-BCL2-GFP (Figure 19), another cell pool K562-BCL2-GFP-BCLXL-KD was generated by over-expression of BCL-2 and down-regulation of BCL-XL using GFP fused BCL-2 plasmid and RFP linked tet-on inducible Bcl-XL shRNA plasmid. The BCL-XL and BCL-2 expression levels of the different cell pools were detected by Western blotting (Figure 43). K562-Mix was generated as the mixture of K562, K562-BCLXL-KD, K562-BCL2-GFP and K562-BCL2-GFP-BCLXL-KD cells.

Figure 43. Establishment of K562-Mix. K562 cells were transfected with GFP-fused BCL-2 plasmids. The successful transfected cells were enriched by selector G418 for one month, named as K562-BCL2-GFP. K562 cells and K562-BCL2-GFP were further transfected with RFP-linked tet-on inducible Bcl-XL shRNA plasmids. The successful transfected cells were enriched by selector puromycin for one month, named as K562-BCLXL-KD and K562-BCL2-GFP-BCLXL-KD, respectively. Expression of GFP-fused BCL-2 was identified by BCL-2 antibodies. The BCL-XL level after 7 day shRNA induction was identified by BCL-XL antibody. Actin was used as a loading control. K562-Mix is the mixture of four cell pools including K562 parental, K562-BCLXL-KD, K562-BCL2-GFP and K562-BCL2-GFP-BCLXL-KD.

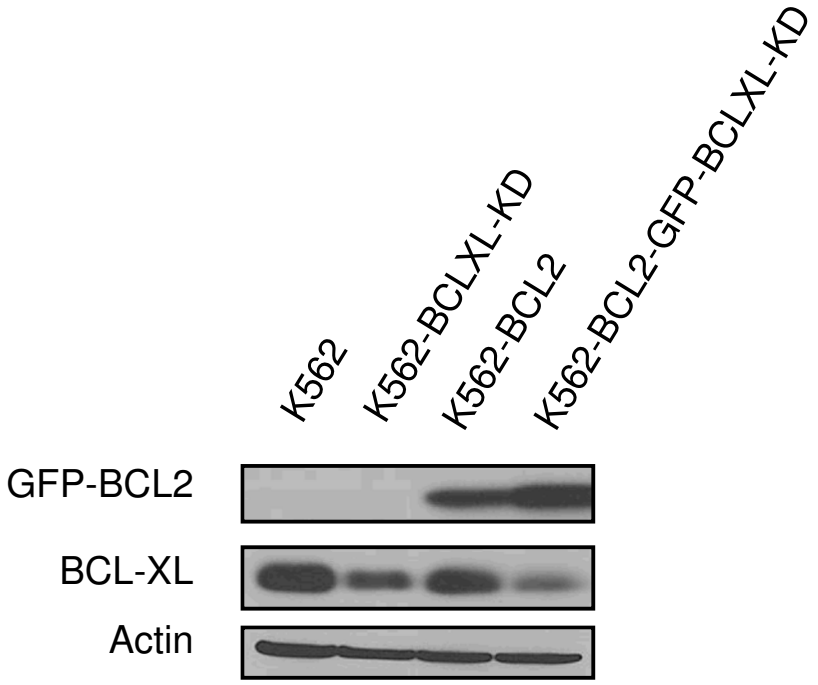
K562
K562-BCLXL-KD
K562-BCL2
K562-BCL2-GFP-BCLXL-KD
GFP-BCL2
BCL-XL
Actin

The different fluorescence patterns of K562-Mix cells were used to represent the different BCL-XL and BCL-2 expressions (Table 2). The percentage change of the different fluorescence pattern in viable K562-Mix cells indicates the survival rate of K562-Mix cells with different BCL-XL and BCL-2 expressions. An increased percentage of a cell pool indicates a higher survival rate or the relative growth advantage of this cell pool in K562-Mix. In contrast, a decreased percentage indicates a lower survival rate or the relative growth disadvantage.

In the K562-Mix experimental model, a non-staining method was used to demonstrate cell viability. Because the dying or dead CML cells often show smaller cell size due to shrinkage, FSC high was used as the parameter to gate the survived cell population by flow cytometry. The correlation between FSC high and cell survival was tested in K562 parental cells by incubation of Imatinib or H_2O_2. The FSC high cells showed both Annexin-V and PI negative (viable cells) in majority (Figure 44). Based on this test, the FSC high cells of K562-Mix were gated after incubation of Imatinib or H_2O_2 (Figure 45). The change of percentage was evaluated by the fold numbers calculated based on the data from 24 hour cultured original seed sample (Figure 46, Table 3). K562-BCLXL-KD cells, expressing low BCL-XL and low BCL-2 and shown as only RFP positive in the upper left of each panel, were dramatically suppressed by either Imatinib or H_2O_2. This data suggested that CML cells with both low BCL-XL and BCL-2 expressions are hyposensitive to both Imatinib and oxidative stress-induced cell death. K562-BCL2-GFP cells, expressing high BCL-XL and high BCL-2 and

shown as only GFP positive in the lower right of each panel, are the largest survived population followed with the incubation of either Imatinib or H_2O_2. Because I previously identified that over-expression of BCL-2 did not dramatically enhance K562 cell survival ratio with the 72 hour treatment of H_2O_2 (Figure 20), the increased percentage of K562-BCL2-GFP may be caused by the relative cell growth advantage under oxidative stress. This data indicated that both BCL-XL and BCL-2 contributes to form the treatment-resistant sub-population from heterogeneous CML cells. K562-BCL2-GFP-BCLXL-KD cells, expressing low BCL-XL and high BCL-2 and shown as GFP RFP double positive in the upper right of each panel, have increased percentage followed with the incubation of Imatinib, but not H_2O_2. This data suggested that oxidative stress may limit the development of BCL-2-over-expressed Imatinib-resistant cell population when BCL-XL is down-regulated. K562 cells, expressing high BCL-XL and low BCL-2 and shown as GFP RFP double negative in the lower left of each panel, are dramatically suppressed by Imatinib, but not that striking by H_2O_2.

Table 2. Correlation between BCL-XL and BCL-2 expression pattern and the cellular fluorescence in K562-Mix. K562-Mix is the mixture of four cell pools, including K562 parental, K562-BCLXL-KD, K562-BCL2-GFP and K562-BCL2-GFP-BCLXL-KD. Cell pool name, BCL-XL level, BCL-2 level and fluorescence status of each cell pool are indicated.

K562-Mix	BCL-XL	BCL2	fluorescence
K562	High	Low	None
K562-BCLXL-KD	Low	Low	Red
K562-BCL2-GFP	High	High	Green
K562-BCL2-GFP-BCLXL-KD	Low	High	Red and Green

Figure 44. Gating viable and apoptotic cells by FSC in K562. K562 cells were incubated with PEITC or Imatinib. Cell death of gated FSC High or FSC Low cells was measured by the annexin-V/PI assay. The number shown below each panel indicates the percentage of the annexin-V and PI double-negative cells (viable).

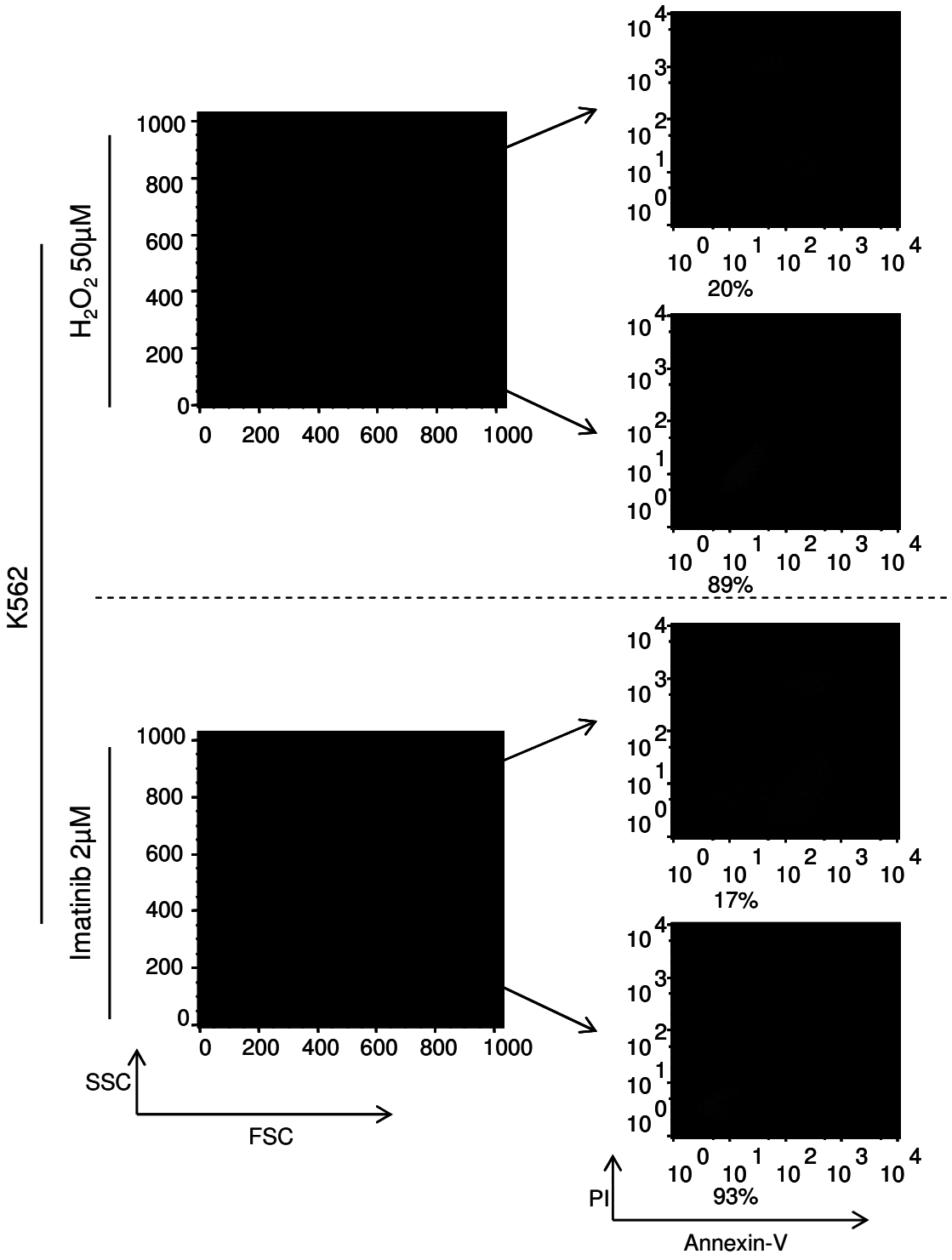
K562
H2O2 50µM
Imatinib 2µM
1000
800
600
400
200
0
0 200 400 600 800 1000
SSC
FSC
10 4
10 3
10 2
10 1
10 0
10 0 10 1 10 2 10 3 10 4
20%
89%
17%
93%
PI
Annexin-V

Figure 45. Gating viable cells by FSC in K562-Mix. K562-Mix cells were incubated with 2 μM Imatinib or 50 μM H_2O_2 for 72 hours. FSC High cell population was gated in each sample. The percentage of gated cells is labeled.

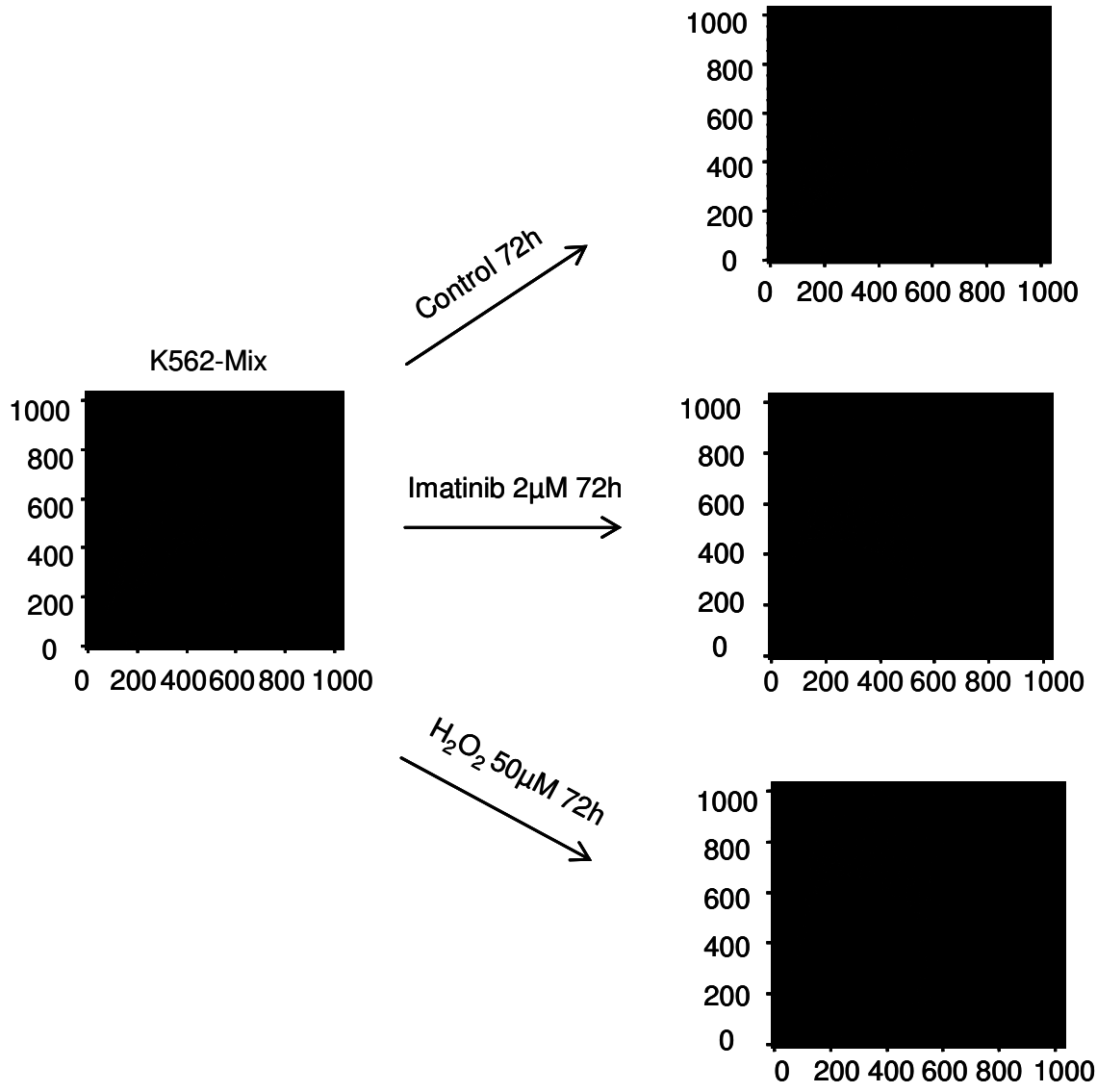
K562-Mix
1000
800
600
400
200
0
0 200 400 600 800 1000
Control 72h
Imatinib 2µM 72h
H2O2 50µM 72h

Figure 46. Differential cell survival of the different cell pools with the treatment of Imatinib or H_2O_2 in K562-Mix. K562-Mix cells were incubated with 2 μM Imatinib or 50 μM H_2O_2 for 72 hours. FSC High cell population was further analyzed according to the expressions of GFP and RFP. The position of each cell pool is representing as follows: K562 (Lower Left, GFP-/RFP-, BCL-XL High/BCL-2 Low), K562-BCLXL-KD (Upper Left, GFP-/RFP+, BCL-XL Low/BCL-2 Low), K562-BCL2-GFP (Lower Right, GFP+/RFP-, BCL-XL High/BCL-2 High), and K562-BCL2-GFP-BCLXL-KD (Upper Right, GFP+/RFP+, BCL-XL Low/BCL-2 Low). The percentage of each cell pool in K562-Mix is labeled. The uneven distribution in the control sample is due to the different cell growth of each cell pool in K562-Mix.

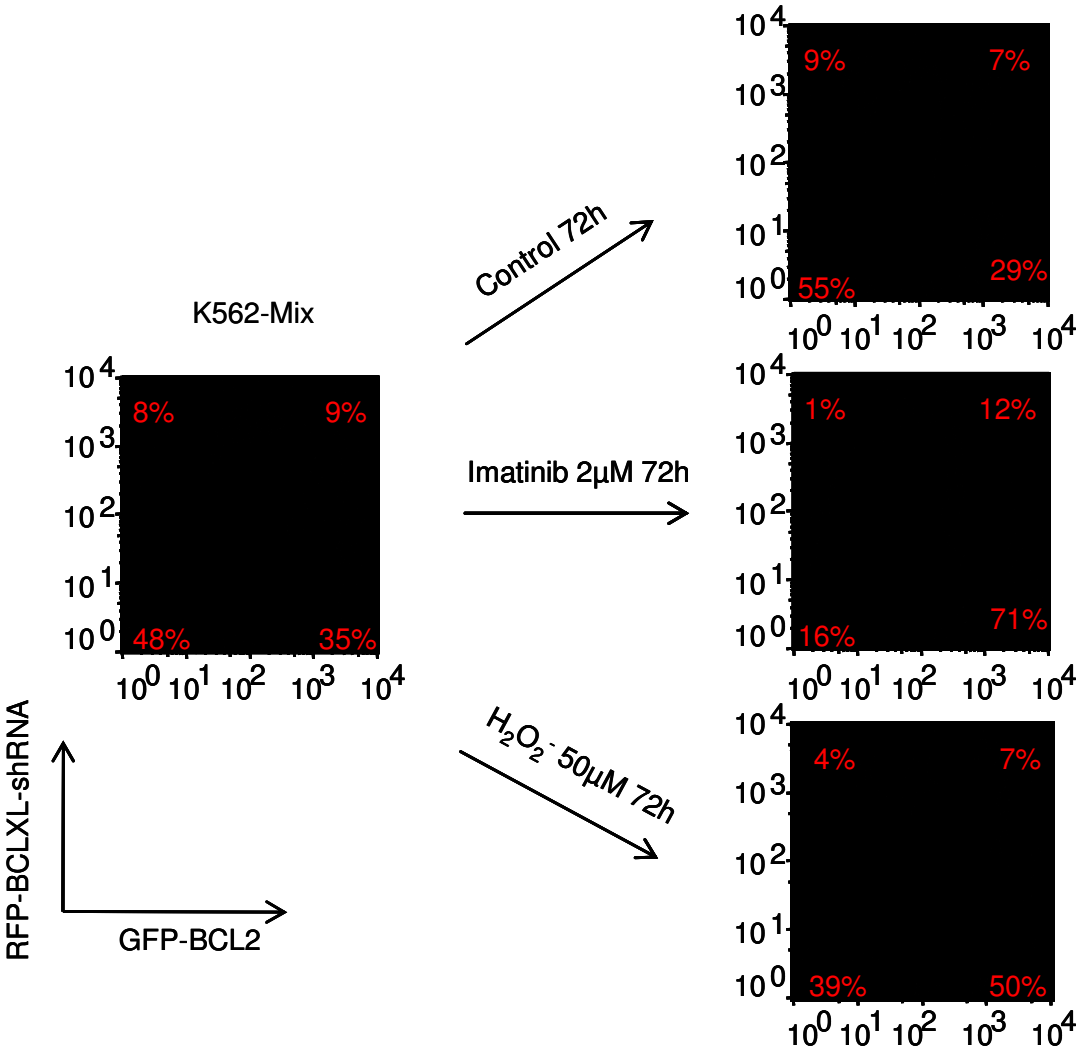
K562-Mix
8%
9%
48%
35%
Control 72h
9%
7%
55%
29%
Imatinib 2µM 72h
1%
12%
16%
71%
H2O2 - 50µM 72h
4%
7%
39%
50%
RFP-BCLXL-shRNA
GFP-BCL2

Table 3. Fold changes of the original seeding population under different treatments. From the percentage data in Figure 46, the fold changes of the different cell population in K562-Mix were calculated between its statistical percentage results from the original seeds (Left) and the experimental sample (Right). The number shown in different color indicates increase (Red), no dramatic change (Blue) and decrease (Green).

K562-Mix	Control	Imatinib	H_2O_2
K562	1.17 ± 0.06	0.32 ± 0.02	0.79 ± 0.03
K562-BCLXL-KD	1.12 ± 0.04	0.14 ± 0.03	0.55 ± 0.07
K562-BCL2-GFP	0.84 ± 0.02	2.02 ± 0.01	1.43 ± 0.01
K562-BCL2-GFP-BCLXL-KD	0.83 ± 0.08	1.43 ± 0.13	0.81 ± 0.05

Red: > 1.25, increase

Blue: 0.75 - 1.25

Green: < 0.75, decrease

4.4.2 Imatinib and ABT737 Enhances Oxidative Stress-induced Apoptosis in BCR-ABL Cells.

The results from the above experiments have suggested that CML cells with both high BCL-XL and high BCL-2 expression may have higher chance to develop into a drug resistant population, and down-regulation or inhibition of them would enhance cell drug sensitivity. Based on these suggestions, I postulated that Imatinib may enhance the sensitivity of oxidative stress-induced cell apoptosis in its targeting cells through suppression of BCL-XL. In addition, BCL-XL and BCL-2 inhibitors would be another approach to enhance CML cell sensitivity to oxidative stress, especially in the cells with BCR-ABL-independent over-expression of BCL-2. In this study, ABT737, the Bcl-2 homology domain 3 (BH3) mimetic, was used as the pan-BCL-2/BCL-XL inhibitor. ABT737 is the predecessor of Navitoclax (ABT263) using as a single agent against lymphoblastic leukemia in clinic trial. ABT737 mediates the functional inhibition of BCL-XL and BCL-2 as antagonist with no suppression of their expression.

BCR-ABL transformed cell line 32D-p210, derived from the murine myeloid cell 32D, was used to investigate the effects of Imatinib or ABT737 on oxidative stress induced apoptosis. Imatinib was identified to induce a dramatic decrease of BCL-XL in 32D-p210 cells (Figure 47). Pre-treatment of Imatinib or ABT737 enhanced H_2O_2-induced cell death in 32D-p210. The percentage of viable cell was decreased from 89% to 34% or 65% in the combination of H_2O_2 and Imatinib or ABT737 (Figure 48).

Figure 47. Imatinib induces BCL-XL decrease in BCR-ABL-transformed cells. 32D-p210 cells were incubated with 0.25 μM Imatinib for 12 hours. The change of BCL-XL was identified by Western blotting using BCL-XL antibody. Actin was used as a loading control.

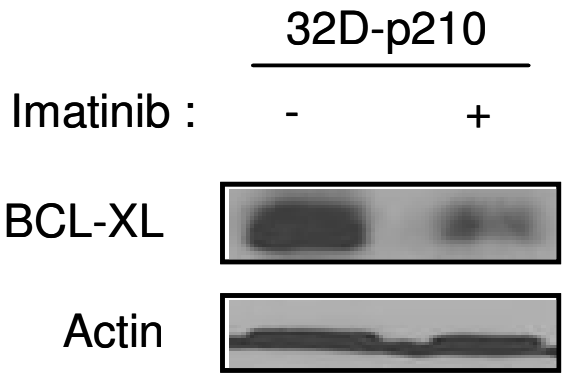
32D-p210
Imatinib :
-
+
BCL-XL
Actin

Figure 48. Imatinib and ABT737 enhance oxidative stress-induced apoptosis in BCR-ABL-transformed cells. 32D-p210 cells were treated with 50 μM H_2O_2 for 12 hours following the 12 hour pre-incubation of 0.25 μM Imatinib or 2 μM ABT737. Cell apoptosis was detected by Annexin-V/PI assay. Percentages of survival cells are labeled.

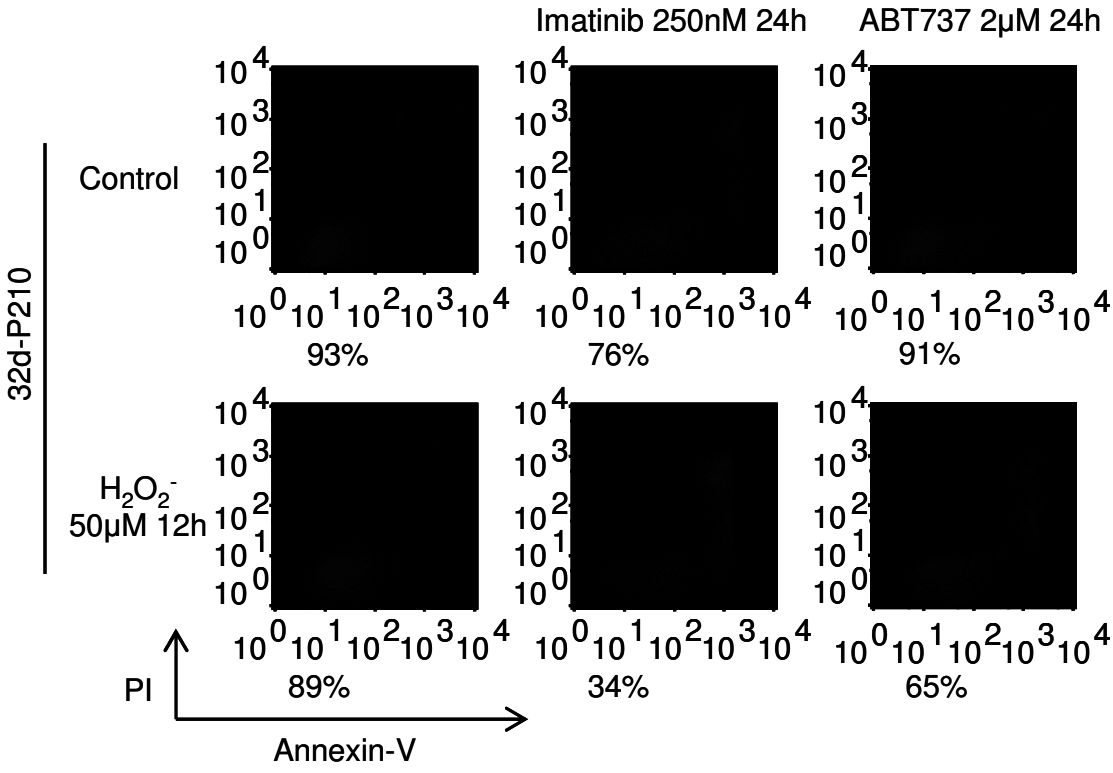
Imatinib 250nM 24h
ABT737 2μM 24h
32d-P210
Control
H_2O_2-
50μM 12h
93%
76%
91%
89%
34%
65%
PI
Annexin-V

Based on the results from 32D-p210 study, the effects of Imatinib and ABT737 on oxidative stress-induced apoptosis were further tested in K562 cells. Because K562 cells have relative high BCL-XL expression but low BCL-2 expression. The results from K562 would be more representing the effects of suppression or inhibition of BCL-XL in CML cells. Consistent with the 32D-p210 results, Imatinb caused a decrease of BCL-XL in K562 (Figure 49). Pre-treatment of Imatinib or ABT737 enhanced H_2O_2 induced cell death in K562. The percentage of viable cell was decreased from 87% to 25% or 79% to 47% in the combination of H_2O_2 and Imatinib or ABT737, respectively (Figure 50, Figure 51). Since the previous observation showed BCL-XL prevents oxidative stress induced mitochondrial membrane potential collapse (Figure 23), the change of mitochondrial membrane potential was further measured in the combination of H_2O_2 and Imatinib or ABT737. Pre-treatment of Imatinib or ABT737 sensitized K562 cells to H_2O_2 induced mitochondrial membrane potential collapse. The percentage of cells with collapsed mitochondrial membrane potential was increased from 5% to 37% or 11% to 33% by the combination of H_2O_2 and Imatinib or ABT737, respectively (Figure 52, Figure 53). Because BCL-XL is heavily localized to mitochondria, the change of mitochondria-bound BCL-XL was investigated in the isolated mitochondria fragments. A large decrease of mitochondria-bound BCL-XL was observed in the cells pre-treated with Imatinib or ABT737 (Figure 54). This data indicated that Imatinib and ABT737 enhance oxidative stress-induced cell damage through decrease the amount of mitochondrial BCL-XL.

Figure 49. Imatinib induces BCL-XL decrease in K562 cells. K562 cells were incubated with 1 μM Imatinib for 12 hours. The change of BCL-XL was identified by Western blotting using BCL-XL antibody. Actin was used as a loading control.

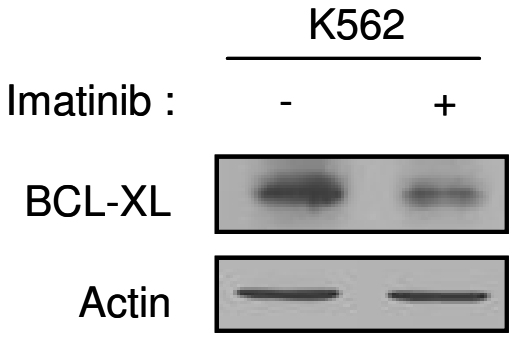
K562
Imatinib :
-
+
BCL-XL
Actin

Figure 50. Imatinib enhances oxidative stress-induced apoptosis in K562 cells. K562 cells were treated with 50 μM H_2O_2 for 24 hours following the 12 hour pre-incubation of 1 μM Imatinib. Cell apoptosis was detected by Annexin-V/PI assay. Percentages of survival cells are labeled.

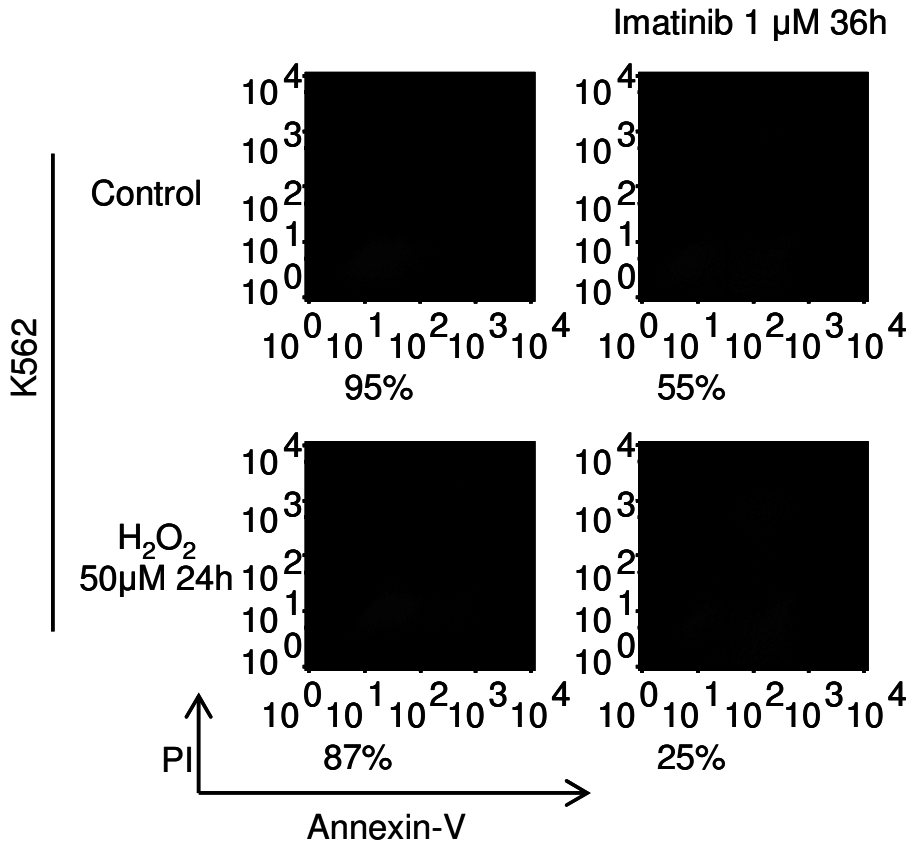
Imatinib 1 µM 36h
Control
K562
H2O2
50µM 24h
95%
55%
87%
25%
PI
Annexin-V

Figure 51. ABT737 enhances oxidative stress-induced apoptosis in K562 cells. K562 cells were treated with 50 μM H_2O_2 for 24 hours following the 12 hour pre-incubation of 2 μM ABT737. Cell apoptosis was detected by Annexin-V/PI assay. Percentages of survival cells are labeled.

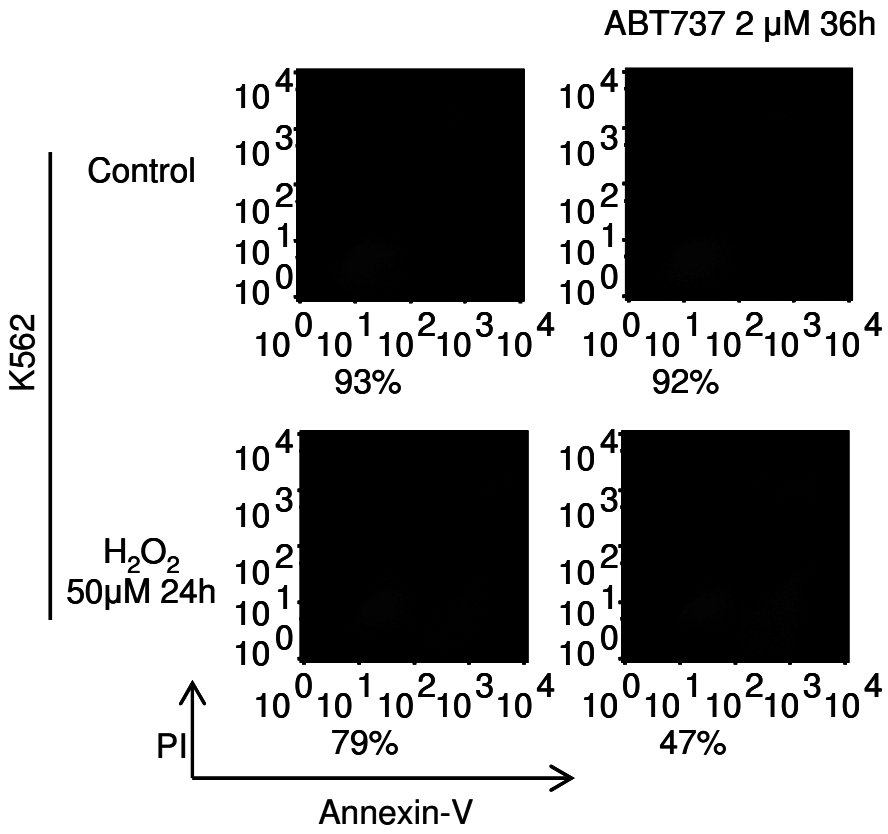
ABT737 2 μM 36h
Control
K562
H_2O_2
50μM 24h
93%
92%
79%
47%
PI
Annexin-V

Figure 52. Imatinib sensitizes K562 cells to oxidative stress-induced mitochondrial membrane potential collapse. K562 cells were treated with 50 μM H_2O_2 for 12 hours following the 12 hour pre-incubation of 1 μM Imatinib. Changes of Mitochondrial membrane potential were measured by Rhodamine 123 staining assay. Percentages of the mitochondrial membrane collapsed cells are labeled.

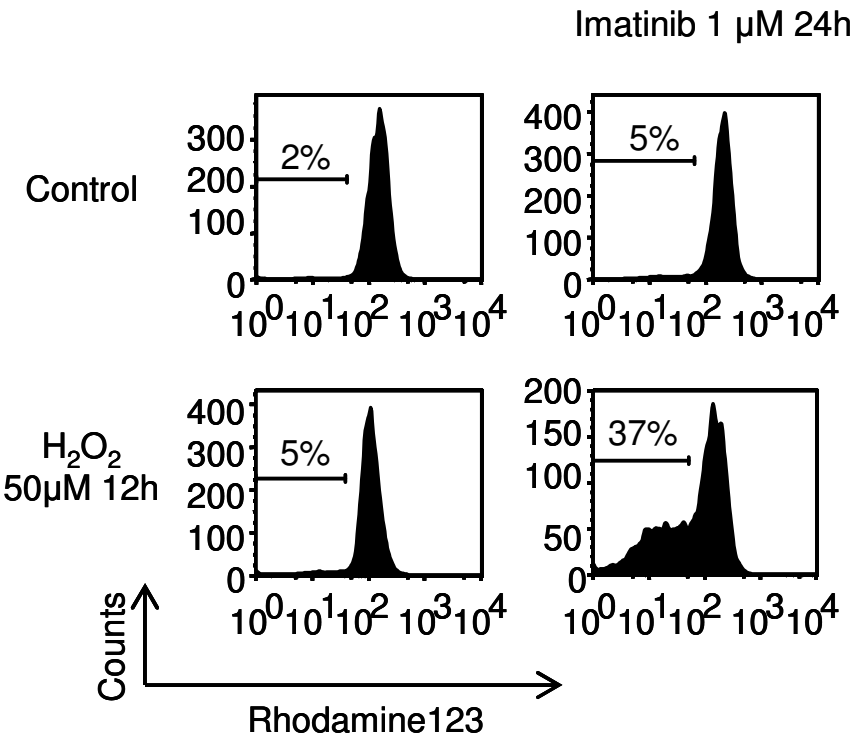
Imatinib 1 μM 24h
Control
H_2O_2
50μM 12h
2%
5%
5%
37%
Counts
Rhodamine123

Figure 53. ABT737 sensitizes K562 cells to oxidative stress-induced mitochondrial membrane potential collapse. K562 cells were treated with 50 μM H_2O_2 for 12 hours following the 12 hour pre-incubation of 2 μM ABT737. Changes of Mitochondrial membrane potential were measured by Rhodamine 123 staining assay. Percentages of the mitochondrial membrane collapsed cells are labeled.

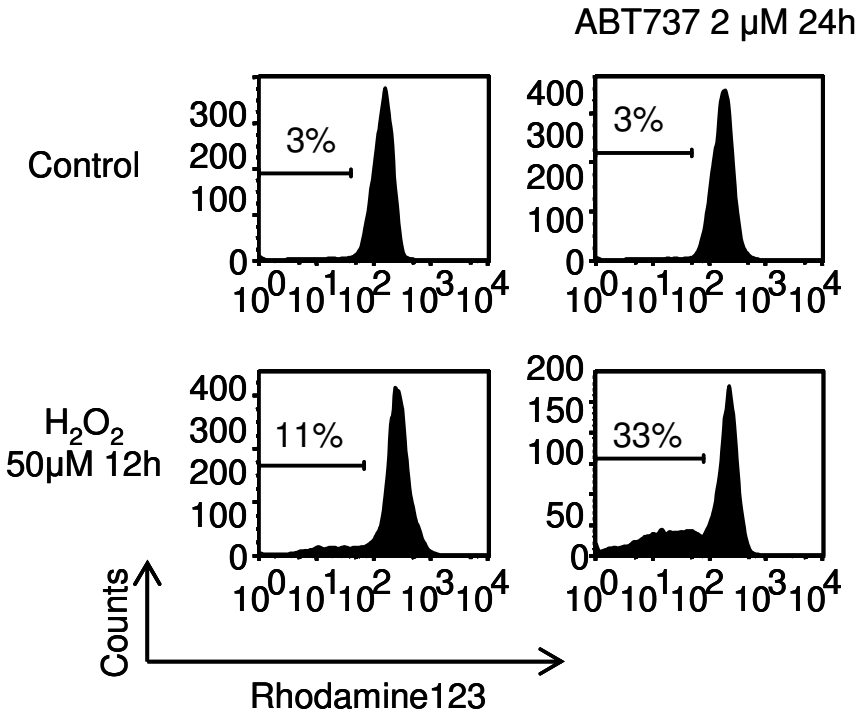
ABT737 2 μM 24h
Control
3%
3%
H_2O_2
50μM 12h
11%
33%
Counts
Rhodamine123

Figure 54. Imatinib and ABT737 cause mitochondrial BCL-XL decrease in K562 cells. K562 cells were treated or non-treated with 50 μM H_2O_2 for 6 hours following the 12 hour pre-incubation of 1 μM Imatinib or 2 μM ABT737. Mitochondria fragments were isolated. BCL-XL was identified by Western blotting using BCL-XL antibody. BAX, HSP60 and ATP synthase subunit-α were used as the internal controls.

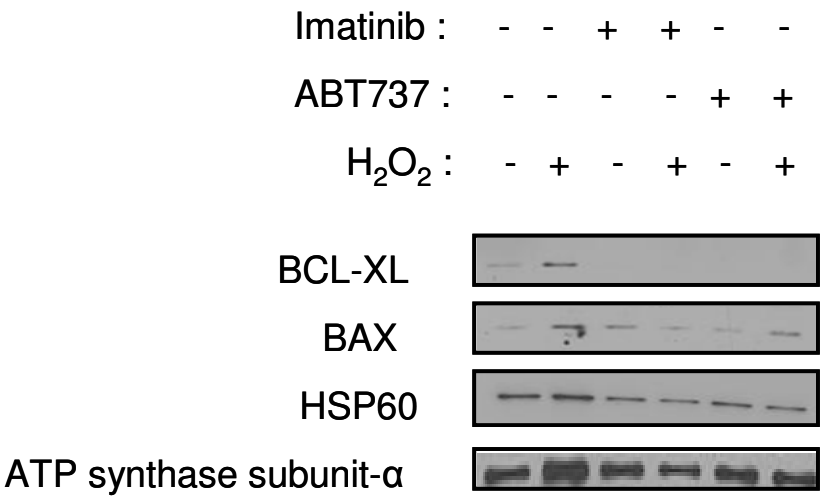
Imatinib : - - + + - -
ABT737 : - - - - + +
H_2O_2 : - + - + - +
BCL-XL
BAX
HSP60
ATP synthase subunit-α

4.4.3 Combination of PEITC with Imatinib or ABT737 Promotes Potent Cell Killing Effects in CML Cells.

PEITC can induce intrinsic oxidative stress and promote massive cell death in CML cells; however, the major concern of PEITC is its non-specific oxidative stress effects on normal cells. A proper drug combination to decrease the minimum effective dose of PEITC will limit its side effects and enhance its therapeutic selectivity. The designs of Imatinib and ABT737 were derived from the concept of targeted therapy. Imatinib and ABT737 specifically suppress their cellular targeting molecules and only disrupt their targeting cells. Therefore, the combination of targeted therapeutic agents with PEITC would only drive the targeted cells hyposensitive to oxidative stress. Ideally, the lower minimum effective dose of PEITC and the higher selectivity could be achieved.

PEITC dramatically promoted ROS generation in CML cell lines K562 and KBM5 (Figure 55). PEITC was used in this experiment at dose of 5 μM, which has no growth inhibition effect on normal peripheral blood mononuclear cells (Figure 33). Pre-treatment of Imatinib sensitized K562 cells to PEITC induced mitochondrial membrane potential collapse. The percentage of cells with collapsed mitochondrial membrane potential was increased from 11% to 35% in the combination of PEITC and Imatinib (Figure 56). Consistently, pre-treatment of Imatinib enhanced PEITC induced cell death in K562. The percentage of viable cell was decreased from 70% to 36% in the combination of PEITC and Imatinib (Figure 57). These results indicated that combination of Imatinib and PEITC is very potent to promote cell killing effects in CML cells. In addition, pre-

treatment ABT737 also enhanced PEITC induced cell death in K562. The percentage of viable cell was decreased from 67% to 30% in the combination of PEITC and ABT737 (Figure 58). Because KBM5 cells showed relatively higher expression of BCL-2, which may delay cell death (Figure 20), inhibition of BCL-2 and BCL-XL by ABT737 would enhance or accelerate oxidative stress-induced apoptosis in KBM5. As expected, pre-treatment of ABT737 enhanced PEITC-induced cell death in KBM5. The percentage of viable cell was decreased from 63% to 42% in the combination of PEITC and ABT737 (Figure 59).

Based on the above results, the combination of redox modulation with suppression of BCL-2 family survival factor function would be an effective strategy to eliminate CML cells. Especially, the combination of PEITC with Imatinib or ABT737 is worthy of further pre-clinical and clinical investigation. Additionally, my study also suggested that the targeted therapy agents could be used as the specific sensitizers to decrease the tolerance of malignant cells to a certain stress.

Figure 55. PEITC promotes cellular ROS generation in CML cells. K562 and KBM5 cells were treated with 10 μM PEITC for 2 hours. Cellular ROS contents were measured by flow cytometric using CM-H_2DCF-DA fluorescence dye. Medians are labeled.

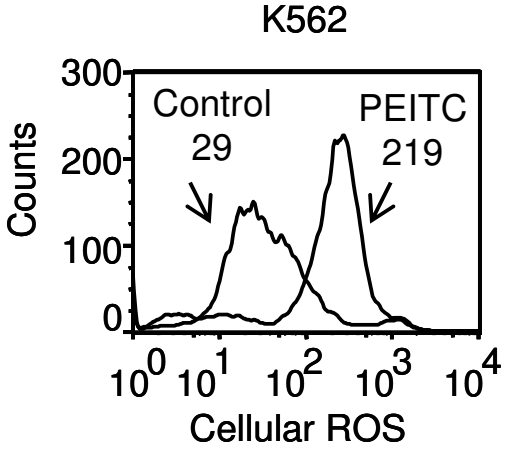
K562
300
200
100
0
Counts
Control
29
PEITC
219
10^0 10^1 10^2 10^3 10^4
Cellular ROS

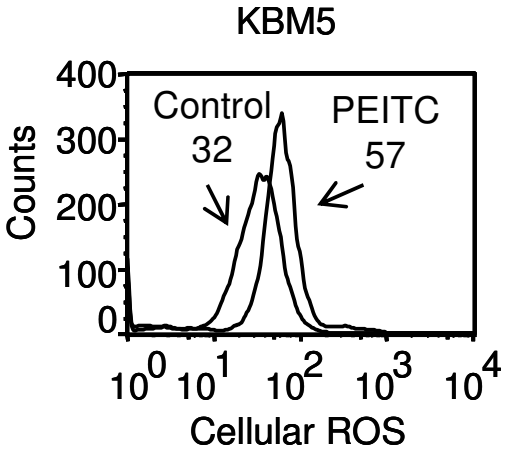
KBM5
400
300
200
100
0
Counts
Control
32
PEITC
57
10^0 10^1 10^2 10^3 10^4
Cellular ROS

Figure 56. Imatinib sensitizes K562 cells to PEITC-induced mitochondrial membrane potential collapse. K562 cells were treated with 5 μM PEITC for 12 hours following the 12 hour pre-incubation of 1 μM Imatinib. Changes of Mitochondrial membrane potential were measured by Rhodamine 123 staining assay. Percentages of the mitochondrial membrane collapsed cells are labeled.

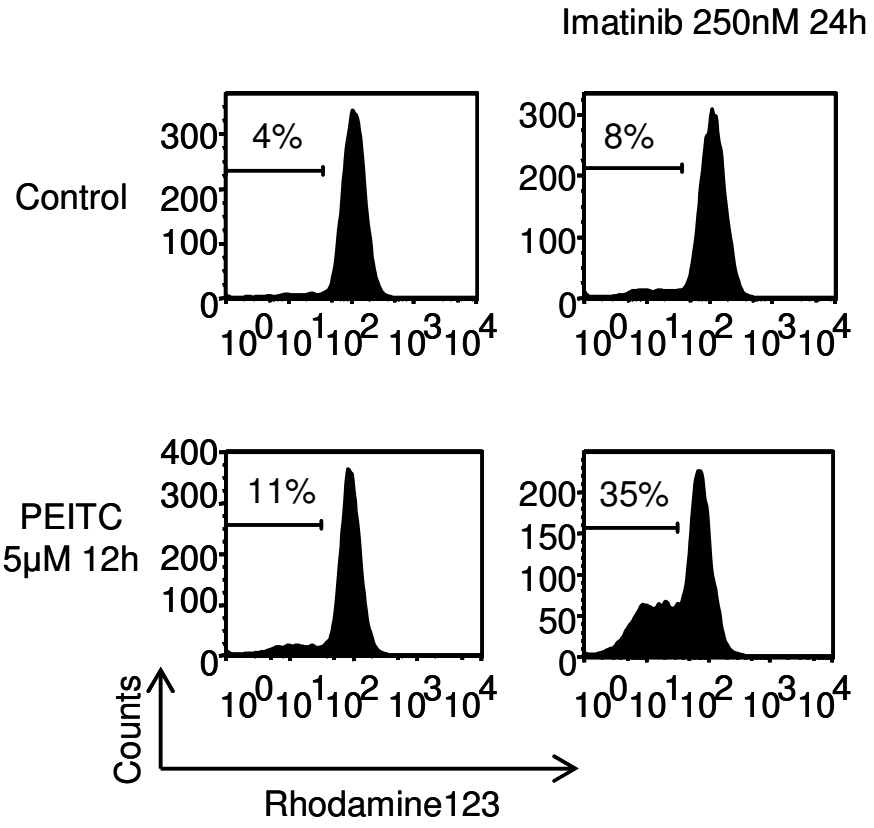
Imatinib 250nM 24h
Control
PEITC
5μM 12h
4%
8%
11%
35%
Counts
Rhodamine123

Figure 57. Imatinib enhances PEITC-induced apoptosis in K562 cells. K562 cells were treated with 5 μM PEITC for 24 hours following the 12 hour pre-incubation of 1 μM Imatinib. Cell apoptosis was detected by Annexin-V/PI assay. Percentages of survival cells are labeled.

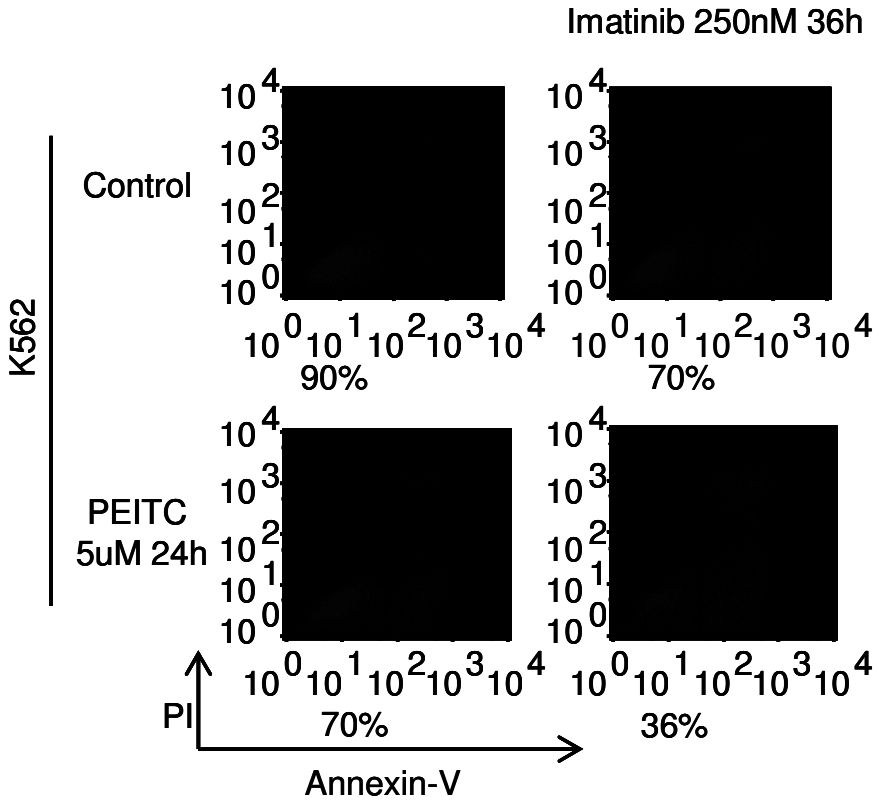
Imatinib 250nM 36h
K562
Control
PEITC
5uM 24h
90%
70%
70%
36%
PI
Annexin-V

Figure 58. ABT737 enhances PEITC-induced apoptosis in K562 cells. K562 cells were treated with 5 μM PEITC for 24 hours following the 12 hour pre-incubation of 2 μM ABT737. Cell apoptosis was detected by Annexin-V/PI assay. Percentages of survival cells are labeled.

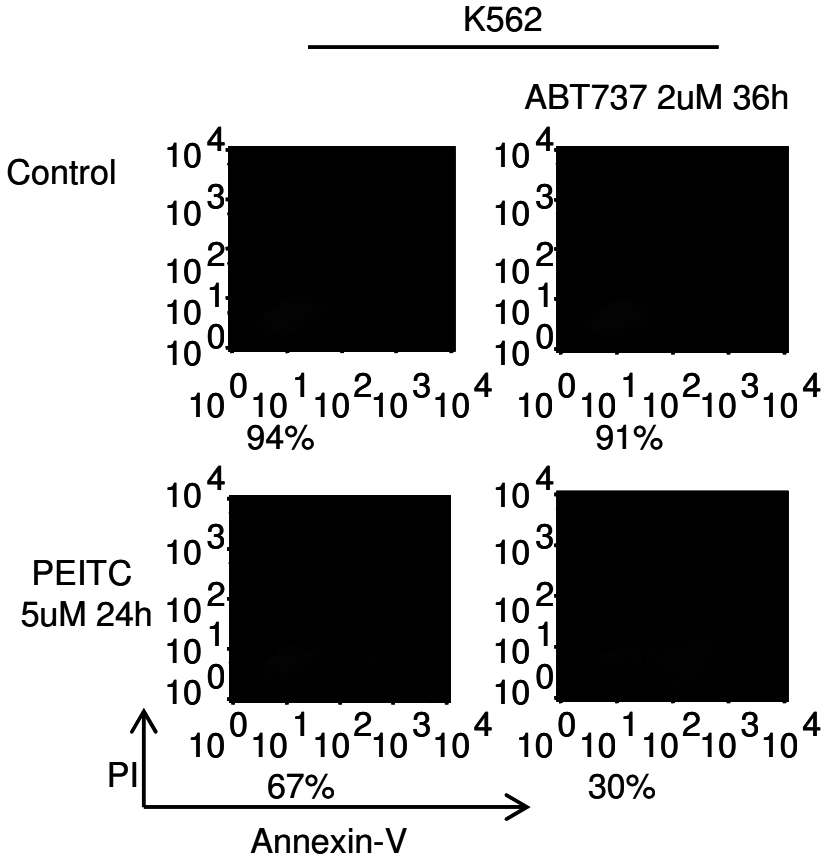
K562
ABT737 2uM 36h
Control
PEITC
5uM 24h
94%
91%
67%
30%
PI
Annexin-V

Figure 59. ABT737 enhances PEITC-induced apoptosis in KBM5 cells. KBM5 cells were treated with 5 μM PEITC for 24 hours following the 12 hour pre-incubation of 2 μM ABT737. Cell apoptosis was detected by Annexin-V/PI assay. Percentages of survival cells are labeled.

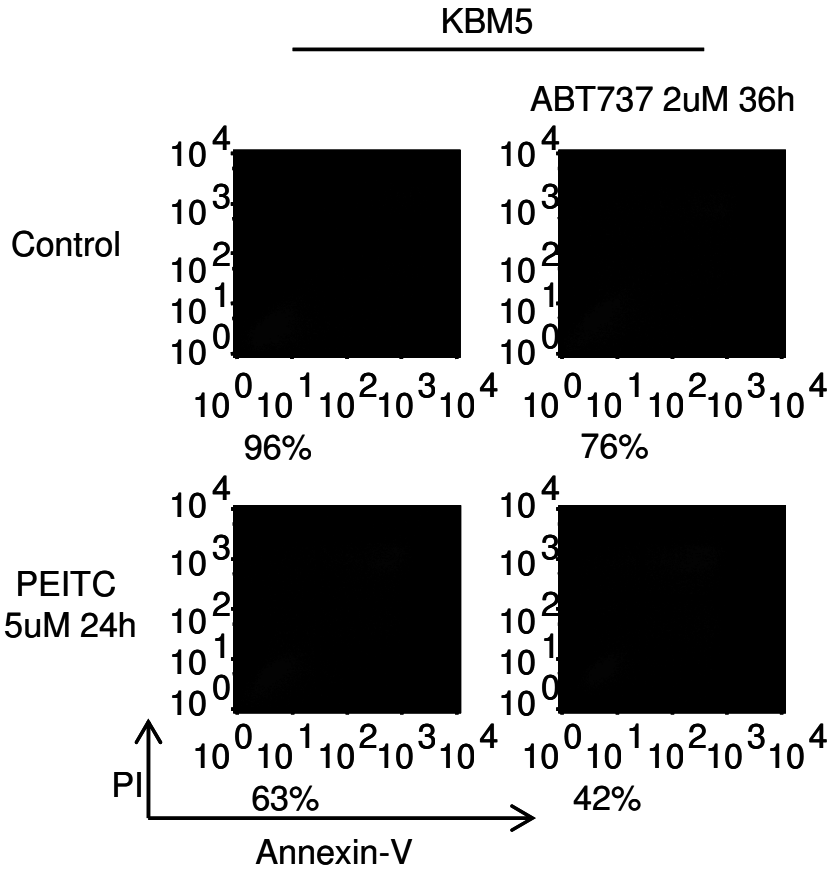
KBM5
ABT737 2uM 36h
Control
PEITC
5uM 24h
96%
76%
63%
42%
PI
Annexin-V

5. Discussion

5.1 BCR-ABL-Induced Cellular Oxidative Stress.

An increase of ROS has been observed in human CML primary cells by comparing with the bone marrow cells isolated from healthy donors. [58,59,61] ROS is believed to mediate multiple biological alterations involved in CML development. [63] Consistent with previous studies, I have also identified that higher ROS levels present in BCR-ABL over-expressing cells. [58-60] Additionally, my study emphasized the supplement of glucose in cell culture is essential to mediate BCR-ABL-induced the increase of cellular and mitochondrial ROS. These results suggested that patient's glucose nutrition conditions and the blood glucose levels should be considered for CML disease management, especially for CML prevention purpose. Since the activation of mitochondria by glucose metabolism is a process involved multiple enzymes involving in glycolysis, pyruvate consumption and TCA cycle, the related genetic alterations of these enzymes may be detectable. I compared the expressions of metabolic enzymes between K562 and normal bone marrow CD34+ cells, based on the profile from NCBI GEO database. In GEO profile GDS596, most enzymes of glycolysis and TCA cycle are more expressed in K562 cells than normal bone marrow CD34+ cells (Figure 60, Figure 61). In addition, pyruvate carboxylase, the enzyme catalyzing irreversible carboxylation of pyruvate to form the critical TCA cycle intermediate oxaloacetate, is also more expressed in K562 (Figure 62). This analysis provided the hint of using metabolic enzymes as the biomarker to evaluate the development of CML.

Figure 60. Expression profiles of glycolytic enzymes in K562 cells. GDS596 data profile was downloaded from Gene Expression Omnibus (GEO) (NCBI). The expressions of glycolysis pathway enzymes in K562 cells (GSM18897 and GSM18898) were analyzed. CD34+ bone marrow cells (GSM18885 and GSM18886) were used as controls. The fold changes of gene expression were listed with gene name and probe codes. Red indicates increase, and green indicates decrease.

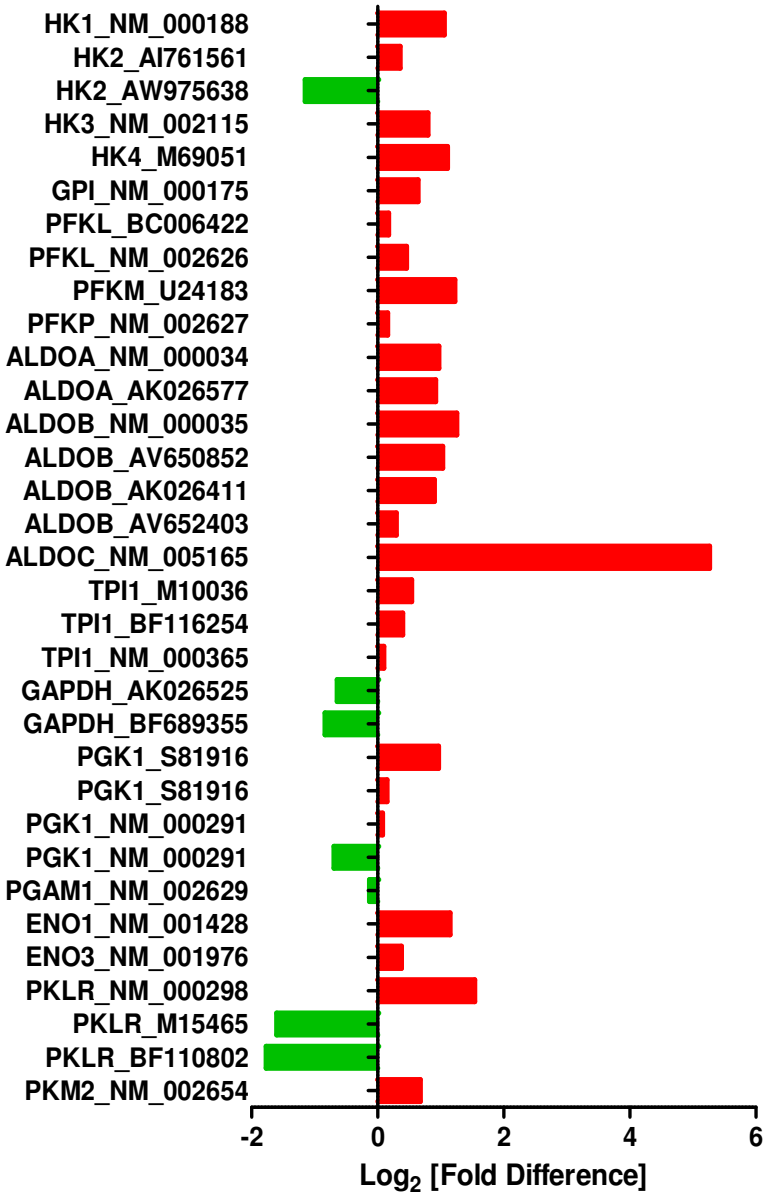
HK1_NM_000188
HK2_AI761561
HK2_AW975638
HK3_NM_002115
HK4_M69051
GPI_NM_000175
PFKL_BC006422
PFKL_NM_002626
PFKM_U24183
PFKP_NM_002627
ALDOA_NM_000034
ALDOA_AK026577
ALDOB_NM_000035
ALDOB_AV650852
ALDOB_AK026411
ALDOB_AV652403
ALDOC_NM_005165
TPI1_M10036
TPI1_BF116254
TPI1_NM_000365
GAPDH_AK026525
GAPDH_BF689355
PGK1_S81916
PGK1_S81916
PGK1_NM_000291
PGK1_NM_000291
PGAM1_NM_002629
ENO1_NM_001428
ENO3_NM_001976
PKLR_NM_000298
PKLR_M15465
PKLR_BF110802
PKM2_NM_002654
-2
0
2
4
6
Log2 [Fold Difference]

Figure 61. Expression profiles of TCA cycle enzymes in K562 cells. GDS596 data profile was downloaded from Gene Expression Omnibus (GEO) (NCBI). The expressions of TCA cycle enzymes in K562 cells (GSM18897 and GSM18898) were analyzed. CD34+ bone marrow cells (GSM18885 and GSM18886) were used as controls. The fold changes of gene expression were listed with gene name and probe codes. Red indicates increase, and green indicates decrease.

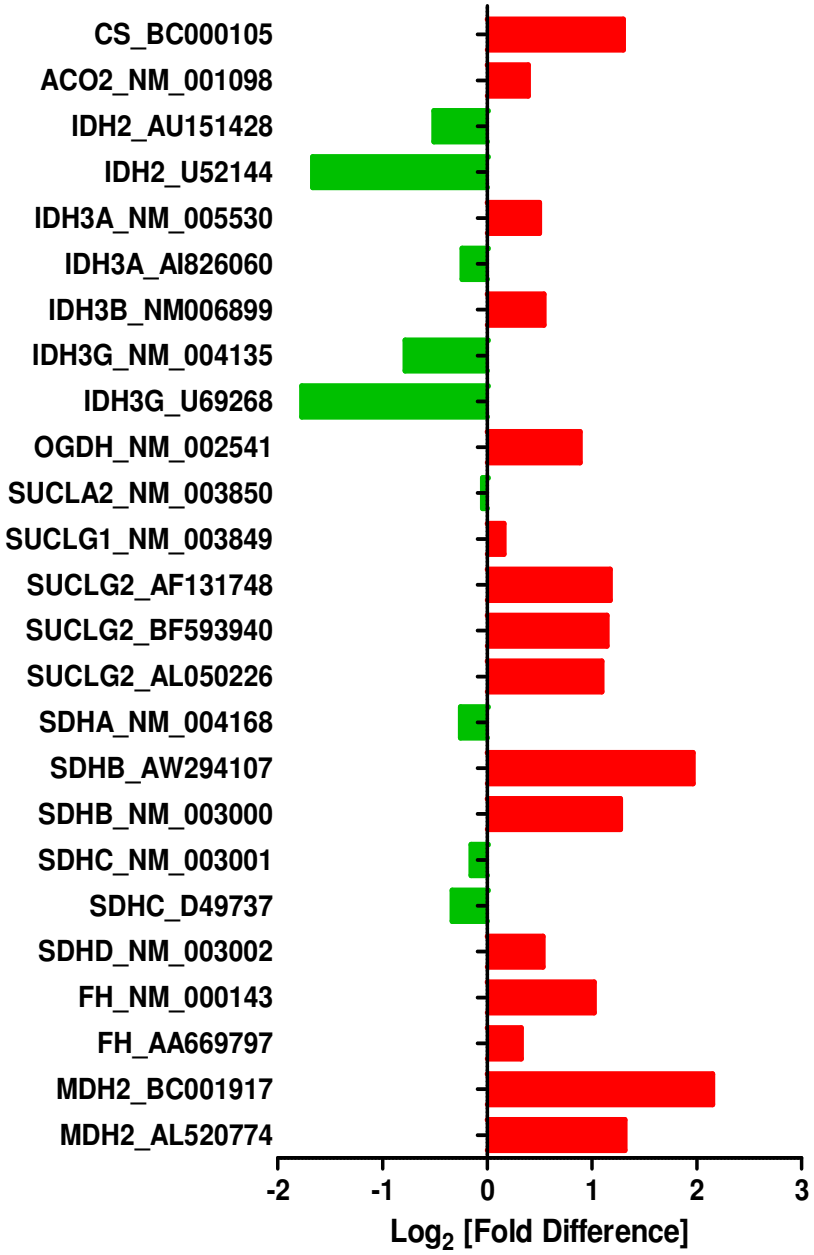
CS_BC000105
ACO2_NM_001098
IDH2_AU151428
IDH2_U52144
IDH3A_NM_005530
IDH3A_AI826060
IDH3B_NM006899
IDH3G_NM_004135
IDH3G_U69268
OGDH_NM_002541
SUCLA2_NM_003850
SUCLG1_NM_003849
SUCLG2_AF131748
SUCLG2_BF593940
SUCLG2_AL050226
SDHA_NM_004168
SDHB_AW294107
SDHB_NM_003000
SDHC_NM_003001
SDHC_D49737
SDHD_NM_003002
FH_NM_000143
FH_AA669797
MDH2_BC001917
MDH2_AL520774
-2
-1
0
1
2
3
Log2 [Fold Difference]

Figure 62. Expression profiles of Pyruvate carboxylase (PC), pyruvate dehydrogenases (PDHA1 and PDHB) and lactate dehydrogenases (LDHA and LDHB) in K562 cells. GDS596 data profile was downloaded from Gene Expression Omnibus (GEO) (NCBI). Pyruvate carboxylase (PC), pyruvate dehydrogenases (PDHA1 and PDHB) and lactate dehydrogenases (LDHA and LDHB) expressions of K562 cells (GSM18897 and GSM18898) were analyzed. CD34+ bone marrow cells (GSM18885 and GSM18886) were used as control. The fold changes of gene expression were listed with gene name and probe codes. Red indicates increase, and green indicates decrease.

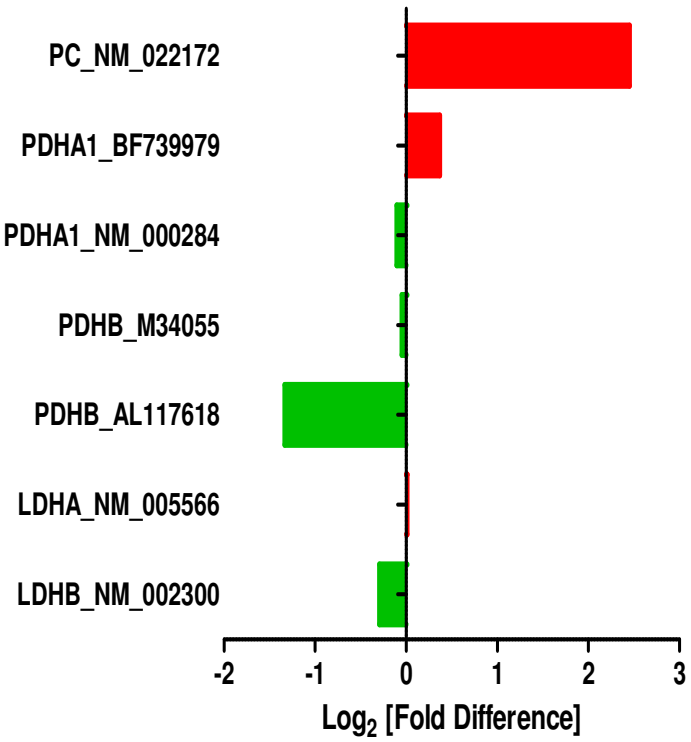
PC_NM_022172
PDHA1_BF739979
PDHA1_NM_000284
PDHB_M34055
PDHB_AL117618
LDHA_NM_005566
LDHB_NM_002300
-2
-1
0
1
2
3
Log2 [Fold Difference]

5.2 Differential Roles of BCL-XL and BCL-2 in Protecting Mitochondria Under Oxidative Stress.

BCL-XL and BCL-2 play important roles in negatively regulating mitochondria dependent apoptosis through inhibiting Apaf-1 mediated Caspase-9 activation. [131-133] BCL-2 family survival factors maintain mitochondrial integrity by preventing cytochrome c release. [134] However, there is no clear evidence to demonstrate the distinct roles of BCL-XL and BCL-2 in response to different apoptosis stimuli. Therefore, one goal of my study was to investigate the efficiency of BCL-XL and BCL-2 in preventing oxidative stress induced cell damage in CML. According to my results, BCL-XL actually is more essential than BCL-2 to protect mitochondria against oxidative stress in CML cells. It is worthy of noting that unlike BCL-XL, the higher expression of BCL-2 has been mainly observed in blast crisis patients but not chronic phase CML patients. [135,136] These studies have suggested that BCL-2 is most likely functional as the secondary survival factor during the development of malignancy in CML. In addition, CML malignancy is driven by the myeloid progenitors. The promotion of cell proliferation in the early stage progenitors is often linked with ROS increase and differentiation. [137,138] Intriguingly, one recent study has shown that the expression of BCL-XL and BCL-2 is completely opposite during the differentiation of human bone marrow mesenchymal stem cells. [139] In this study, researchers have identified that the expression of BCL-XL is at the similar level in undifferentiated and differentiated cells, however, BCL-2 only expresses in differentiated cells. Additionally, they have demonstrated that BCL-XL but not

BCL-2 plays the dominant survival role in undifferentiated cells. So the differential roles of BCL-XL and BCL-2 in response to oxidative stress in CML cells may involve a cell stage impact.

Previous studies have shown that BCL-XL and BCL-2 also regulate cellular redox capacity. BCL-XL regulates mitochondrial membrane potential and protects oxidative stress-caused GSH pool decrease. [69,70] BCL-2 incorporates with antioxidants and regulates cellular GSH distribution. [140,141] Surprisingly, BCL-2 has also been viewed as a pro-oxidant to promote mitochondrial ROS generation. [142] To address such a controversy, the effects of BCL-XL and BCL-2 on BCR-ABL promoted mitochondrial ROS generation were investigated. The mitochondrial ROS levels of BCL-XL or BCL-2 over-expressing K562 cells were detected with or without glucose in culture media. The 5 hour shortage of glucose caused a decrease of mitochondrial ROS in both BCL-XL over-expressing cells and parental cells, but not in BCL-2 over-expressing cells (Figure 63). The similar phenomenon also observed through the comparison between K562 and KBM5. KBM5 cells, with relatively high BCL-2 expression, were less sensitive to 5 hour glucose shortage-induced mitochondrial ROS drop than K562 (Figure 64). These results suggested that BCL-2 seems play a role in maintaining mitochondrial ROS generation in CML, and implied a disadvantage of BCL-2 in protecting mitochondria under oxidative stress.

Figure 63. BCL-2 over-expressing cells are less sensitive to short term glucose shortage-induced mitochondrial ROS decrease. Mitochondrial ROS levels were detected by MitoSOX Red. K562, K562-BCLXL-HA and K562-BCL2-GFP cells were cultured in regular or glucose free media for 5 hours.

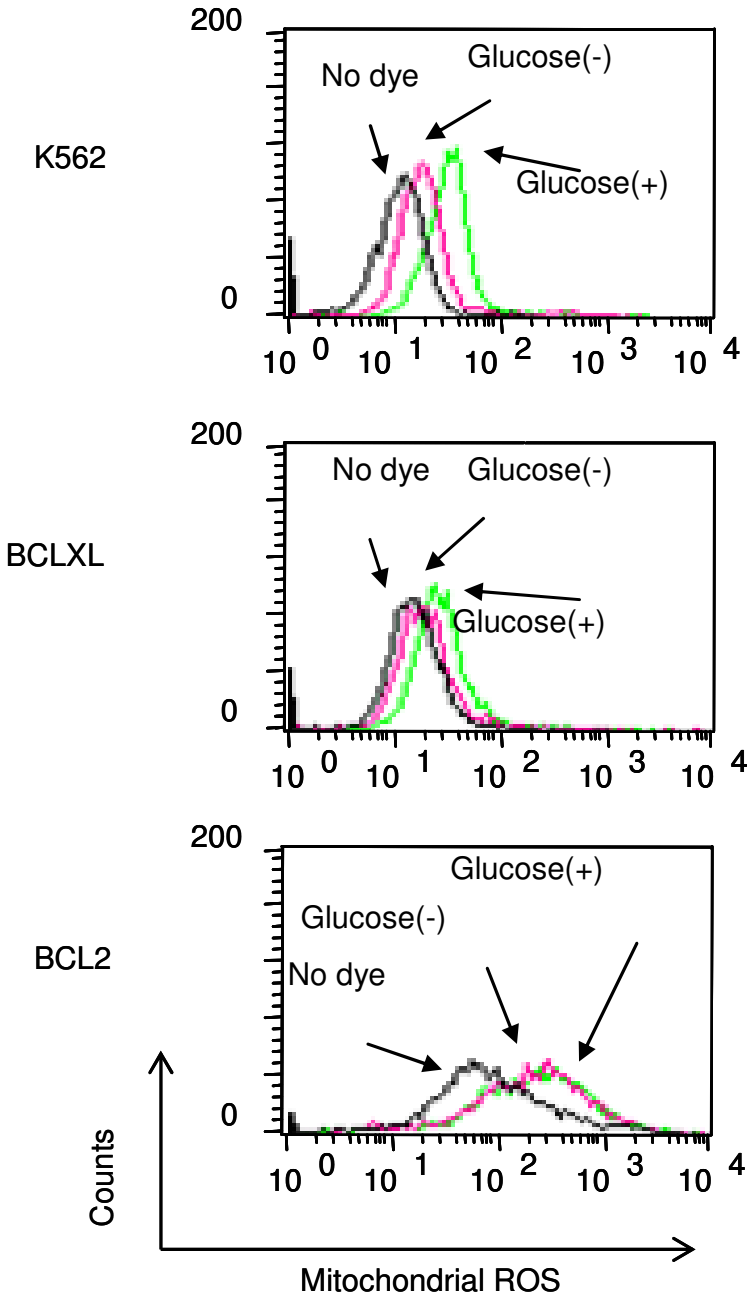
K562
200
0
No dye
Glucose(-)
Glucose(+)
10 0 10 1 10 2 10 3 10 4
BCLXL
200
0
No dye
Glucose(-)
Glucose(+)
10 0 10 1 10 2 10 3 10 4
BCL2
200
0
Glucose(+)
Glucose(-)
No dye
10 0 10 1 10 2 10 3 10 4
Counts
Mitochondrial ROS

Figure 64. BCL-2 high cells are less sensitive to short term glucose shortage-induced mitochondrial ROS decrease. Mitochondrial ROS levels were detected by MitoSOX Red. K562 and KBM5 cells were cultured in regular or glucose free media for 5 hours. The medians are labeled.

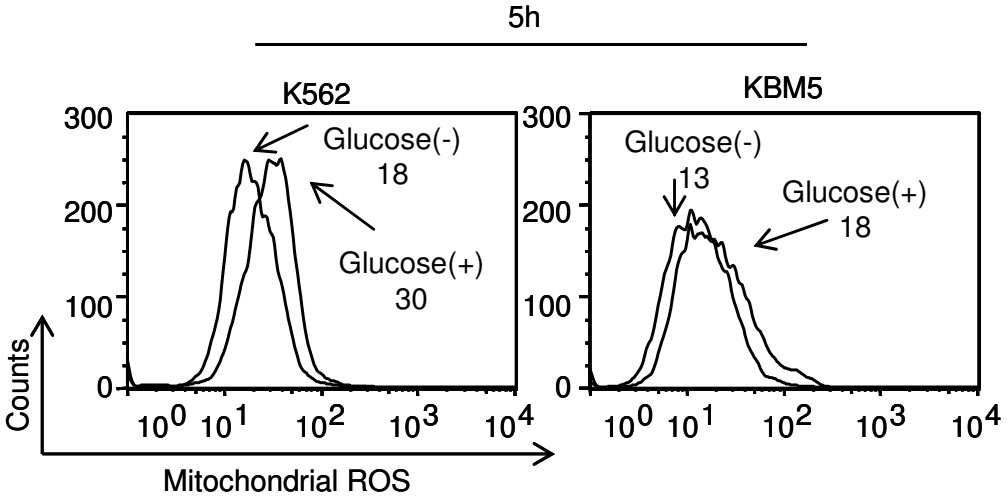
5h
K562
KBM5
300
200
100
0
Glucose(-)
18
Glucose(+)
30
Glucose(-)
13
Glucose(+)
18
Counts
10^0 10^1 10^2 10^3 10^4
Mitochondrial ROS

5.3 Role of Intracellular GSH Pool for Survival.

My results indicated that the depletion of cellular glutathione appeared to be an important biochemical event mediating the cytotoxic effects of PEITC. GSH is viewed as a critical survival antioxidant. A previous study has identified that the levels of GSH determine cell sensitivity to apoptosis in leukemia cells. [143] Consistently, a severe depletion of GSH before cell apoptosis was found in my experiments (Figure 29, Figure 30B). Intriguingly, my colleague has identified that PEITC results in a rapid depletion of mitochondrial GSH and disruption of mitochondrial metabolism function before inducing an entire cellular GSH pool loss in leukemia cells. [144] These results suggested that the non-mitochondria GSH seemed to function as the barrier to prevent the activation of the downstream steps in apoptosis. Since caspase-3 activation and PARP cleavage matched the decrease of total GSH in my experiments (Figure 34, Figure 29), I did an in vitro test to evaluate the effects of GSH levels on caspase-3 mediated PARP cleavage. I observed that 3 mM GSH prevented the spontaneous PARP cleavage in CML cell lysates (Figure 65). I further found that 3 mM GSH also inhibited caspase-3 mediated PARP cleavage in cell lysates (Figure 66). These results suggested that GSH may play a role in the direct regulation of apoptotic activation. The potency of PEITC in inducing cell death may be also due to enhancing cell apoptotic sensitivity by depleting GSH.

Figure 65. GSH prevents spontaneous PARP cleavage in vitro. KBM5 cell pellets were collected. Cell lysate samples were transferred into 100 µl aliquots. The aliquots were incubated in the presence or absence of 3 mM GSH at 37 ℃ for 3, 10 or 60 minutes, and then collected for Western blotting to detect PARP cleavage. The GSH incubation-caused precipitated proteins were also collected and blotted with PARP antibody to exclude the precipitation-caused decrease of cleaved PARP.

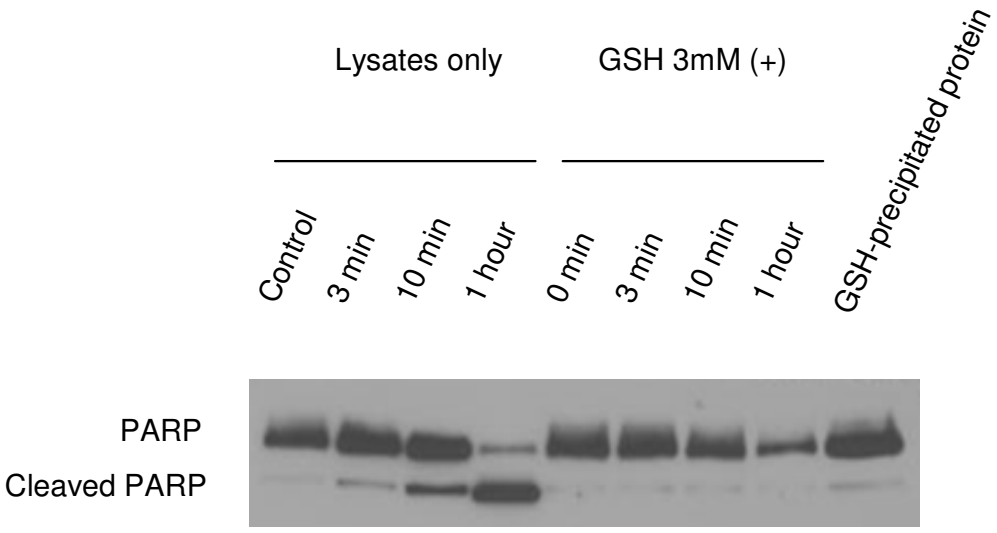
Lysates only
GSH 3mM (+)
Control
3 min
10 min
1 hour
0 min
3 min
10 min
1 hour
GSH-precipitated protein
PARP
Cleaved PARP

Figure 66. GSH prevents caspase-3 induced PARP cleavage in vitro. KBM5 cell pellets were collected. Cell lysate samples were transferred into 100 µl aliquots. The aliquots were incubated in the presence or absence of active caspase-3 enzymes or 3 mM GSH at 37 ℃ for 60 minutes, and then collected for Western blotting to detect PARP cleavage.

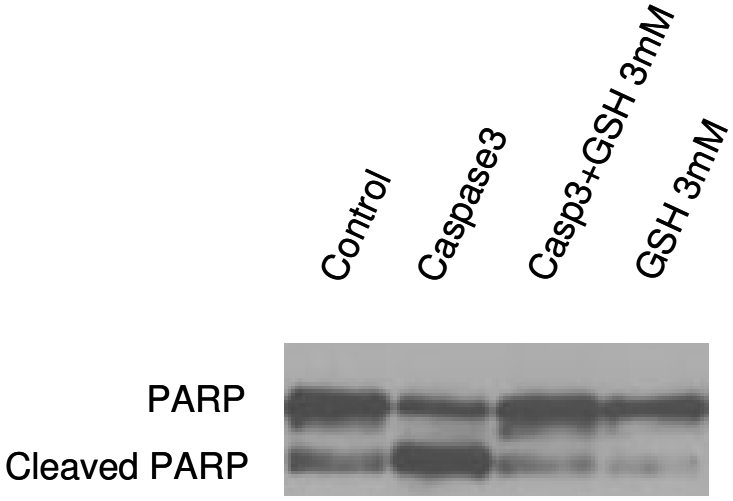
Control
Caspase3
Casp3+GSH 3mM
GSH 3mM
PARP
Cleaved PARP

5.4 Potential Advantage of PEITC in Redox-Directed Therapy in CML.

'The increase of ROS stress in CML cells expressing either wild-type or mutant BCR-ABL can be exploited for therapeutic purpose. Recently, the redox-directed therapeutic strategy has drawn researchers' attention. [145] My present study has suggested that the severe ROS stress induced by PEITC might alter the redox state of BCR-ABL proteins, including the T315I mutant, and render it vulnerable to degradation by caspase-3. This notion is supported by the observation that either NAC or specific inhibitor of caspase-3 could significantly suppress the cleavage of BCR-ABL. It should be pointed out that the degradation of BCR-ABL may not be the primary cause of PEITC-induced cell death, which is likely triggered by direct oxidative damage to mitochondria and other critical cellular molecules. However, the ability of PEITC to induced rapid degradation BCR-ABL may effectively abolish the pro-survival signal of this oncoprotein, thus add to the potency of this compound in killing CML cells. Furthermore, normal lymphocytes have a lower basal ROS output and possess intact redox-regulatory machinery, which make them less vulnerable to ROS stress imposed by PEITC. Based on the promising activity of PEITC against Imatinib-resistant CML cells, its therapeutic selectivity, and its unique mechanism of action, I conclude that this compound may be useful to overcome CML resistance to kinase inhibitors.'[114]

5.5 Potential Advantage of Imatinib in Redox-Directed Therapy in CML.

One of the major concerns of redox-directed therapeutics is the off-targeting effects on the normal cells. Therefore, the improvement of the

therapeutic selectivity would make this strategy more beneficial. Oncoprotein BCR-ABL, encoded by CML specific Bcr-Abl fusion gene, has been identified in more than 95% CML cases. [45-47] In the past few years, molecular targeting BCR-ABL functional inhibitors were derived from the concept of targeted therapy and developed for the chemotherapy of CML. [90] Imatinib specifically suppresses its cellular targeting molecules and only disrupts the targeted cells. The combination of Imatinb with redox modulation agents would only drive the Imatinib targeting cells hyposensitive to oxidative stress. Therefore, the lower minimum effective dose of redox modulation agents and the higher therapeutic selectivity could be achieved.

5.6 Antioxidant Defects in CML.

My results suggested that anti-apoptotic factors play essential roles in preventing oxidative stress-induced cell damage in BCR-ABL expressing cells. However, there are other genes, antioxidant enzymes, constantly scavenging ROS in normal physiological conditions. Why do CML cells highly rely on the anti-apoptotic factors? Are the antioxidant enzymes deregulated in CML cells? These are the questions left for future studies.

One of the major antioxidant enzymes, GPX1, has been reported to dysfunction or lost in some BCR-ABL positive patients or cultured human CML cell lines. [92,108] However, no study has yet demonstrated the link between the regulation of GPX1 and the induction of BCR-ABL. GPX1 is the selenium (Se)-dependent antioxidant enzyme, mainly catalyzing the reduction of the cytosolic H_2O_2 using GSH as the substrates. The regulation of cellular GPX1 expression

is through multiple optional signaling pathways and largely remains unknown. The binding sequences of PU.1 and p53 have been identified in GPX1 promoter region. [146,147] It is worth noting that p53 has been reported to be mutated or deleted in many CML cases. [148] In addition, a previous study suggested that FOXO3a also plays an important role in regulating GPX1 gene expression. [149] Furthermore, the inhibition of FOXO3a activity has been observed in v-Abl transformed cells.[150] These studies suggest that BCR-ABL might interrupt the expression of GPX1 through inhibiting its upstream transcription factors. BCR-ABL-transformed cell 32D-p210 showed increased phosphorylation at FOXO3a Thr32, which inhibits FOXO3a activation (Figure 67A). In addition, a decreased gene expression of GPX1 was also observed in 32d-P210 (Figure 67A, B, P=0.0017). These data implied that over-expression of oncogene BCR-ABL may cause some crucial antioxidant defects and render the transformed cells more dependent on anti-apoptotic factors to respond oxidative stress.

Figure 67. Over-expression of BCR-ABL results in FOXO3a inhibition and GPX1 decrease. (A) Phosphorylation of FOXO3a Thr32 and GPX1 were detected in samples from 32D-p210 and 32D parental by Western blotting. (B) GPX1 mRNA expression was measured by quantitative real-time PCR as described in previous Materials and Methods 3.13.

A

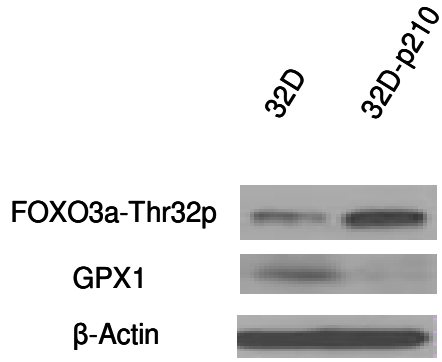
32D
32D-p210
FOXO3a-Thr32p
GPX1
β-Actin

B

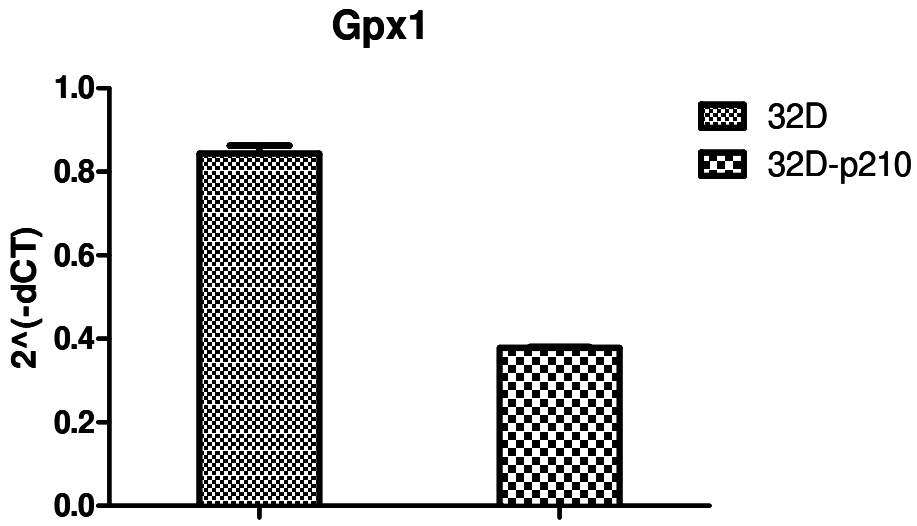
Gpx1
1.0
0.8
0.6
0.4
0.2
0.0
2^(-dCT)
32D
32D-p210

6. Summary and Conclusion

In conclusion, the present studies have demonstrated that BCR-ABL promotes cellular and mitochondrial ROS generation, while elevating the cell survival factors GSH and BCL-XL to prevent oxidative stress-induced apoptosis. Enhancement of glucose metabolism by BCR-ABL contributes to the increase of mitochondrial ROS in CML cells. These findings have provided insight into the persistent oxidative stress observed in CML cells. In addition, the current research has identified the distinct roles of BCL-XL and BCL-2 in preventing excessive ROS induced apoptosis, which are due to their differential function in protecting mitochondria against oxidative stress. Based on the biological mechanism studies, novel therapeutic strategies were investigated. PEITC effectively promotes massive cell death in Imatinib-resistant CML cells through targeting cellular GSH system. The combination of either Imatinib or ABT737 with PEITC diminishes the protecting effects of BCL-2 family survival factors and promotes excessive intrinsic oxidative stress; thus showing cell killing effects in CML cells. This therapeutic strategy could ultimately improve the selectivity and potency of redox-directed therapy in CML and other hematological malignancies (Figure 68).

Figure 68. Model summarizing the biological basis and clinical implications of BCR-ABL-induced mitochondrial oxidative stress and cell survival. Tyrosine kinase onco-protein BCR-ABL promotes mitochondrial ROS increase through the enhancement of glycolysis. BCR-ABL down-stream survival factor BCL-XL plays an essential role in preventing oxidative stress-caused mitochondria damage and cell apoptosis. Redox modulating reagent PEITC induces potent cell death in CML cells by depleting GSH and promoting intrinsic oxidative stress. Combination of PEITC with BCR-ABL inhibitor Imatinib or BCL-XL/BCL-2 inhibitor ABT737 strengthens redox modulation-induced cell death in CML. Glut: Glucose transporter; HK: Hexokinase; LDH: Lactate dehydrogenase; P: phosphorylation; TCA: TCA cycle; I,II,III and IV: Mitochondrial respiratory chain complex I to IV; C: Cytochrome c.

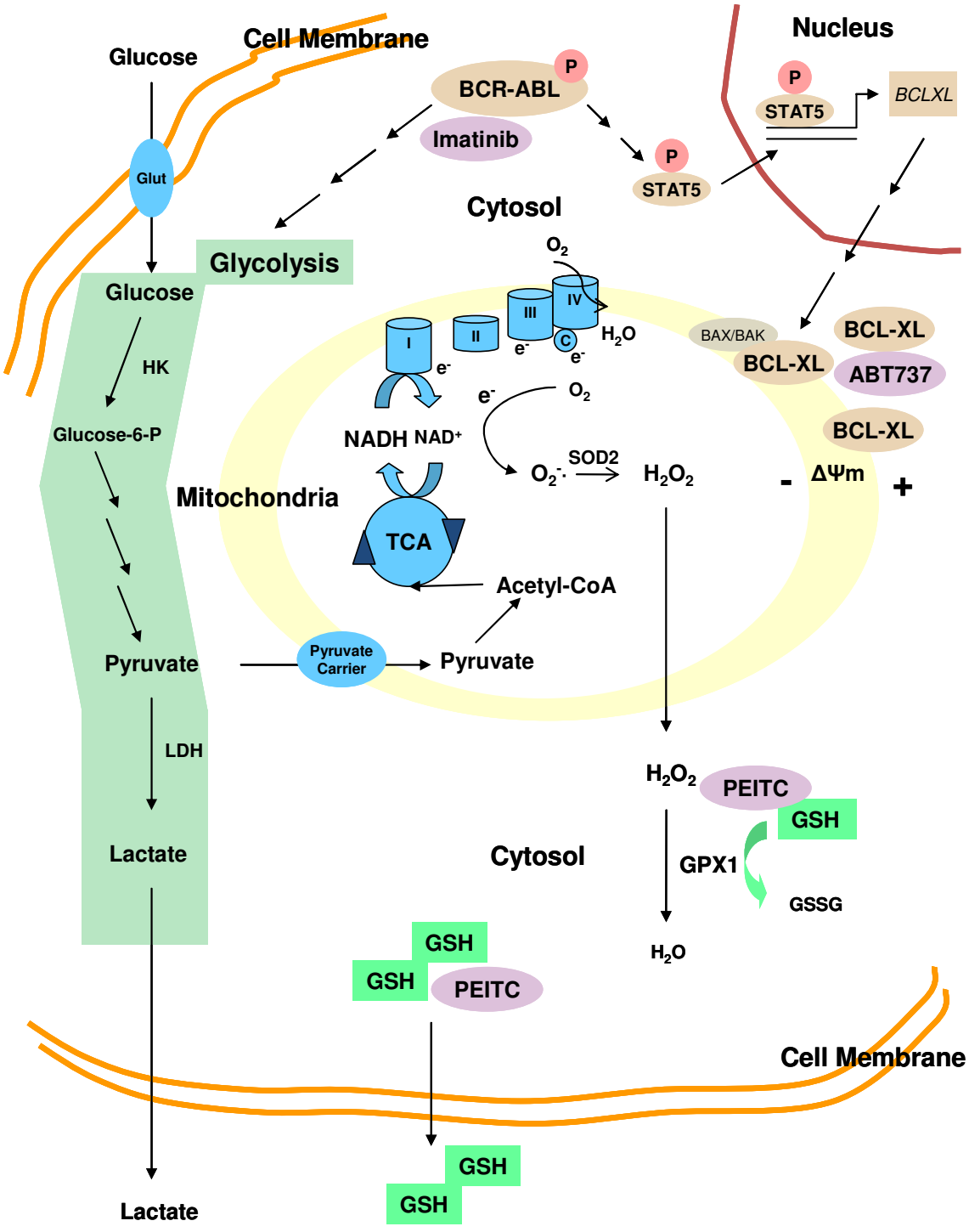
Glucose
Cell Membrane
Nucleus
BCR-ABL
P
Imatinib
STAT5
BCLXL
Glut
Cytosol
Glycolysis
Glucose
HK
Glucose-6-P
Mitochondria
NADH
NAD+
TCA
Acetyl-CoA
Pyruvate
Pyruvate Carrier
LDH
Lactate
BAX/BAK
BCL-XL
ABT737
ΔΨm
SOD2
PEITC
GSH
GPX1
GSSG
Cell Membrane
Lactate

Bibliography

1. Hanahan, D. & Weinberg, R.A. The hallmarks of cancer. *Cell* **100**, 57-70 (2000).
2. Hanahan, D. & Weinberg, R.A. Hallmarks of cancer: the next generation. *Cell* **144**, 646-674 (2011).
3. Ogasawara, M.A. & Zhang, H. Redox Regulation and its Emerging Roles in Stem Cells and Stem-Like Cancer Cells. *Antioxid Redox Signal* (2008).
4. Storz, P. Reactive oxygen species in tumor progression. *Front Biosci* **10**, 1881-1896 (2005).
5. Halliwell, B. Oxidative stress and cancer: have we moved forward? *Biochem J* **401**, 1-11 (2007).
6. Cooke, M.S., Evans, M.D., Dizdaroglu, M. & Lunec, J. Oxidative DNA damage: mechanisms, mutation, and disease. *Faseb J* **17**, 1195-1214 (2003).
7. Evans, M.D., Dizdaroglu, M. & Cooke, M.S. Oxidative DNA damage and disease: induction, repair and significance. *Mutat Res* **567**, 1-61 (2004).
8. Hu, J.J., Dubin, N., Kurland, D., Ma, B.L. & Roush, G.C. The effects of hydrogen peroxide on DNA repair activities. *Mutat Res* **336**, 193-201 (1995).
9. Witz, G. Active oxygen species as factors in multistage carcinogenesis. *Proc Soc Exp Biol Med* **198**, 675-682 (1991).

10. Wu, W.S. The signaling mechanism of ROS in tumor progression. *Cancer Metastasis Rev* **25**, 695-705 (2006).

11. Giles, G.I. The redox regulation of thiol dependent signaling pathways in cancer. *Curr Pharm Des* **12**, 4427-4443 (2006).

12. Toyokuni, S., Okamoto, K., Yodoi, J. & Hiai, H. Persistent oxidative stress in cancer. *FEBS Lett* **358**, 1-3 (1995).

13. Kroemer, G. & Pouyssegur, J. Tumor cell metabolism: cancer's Achilles' heel. *Cancer Cell* **13**, 472-482 (2008).

14. Karihtala, P. & Soini, Y. Reactive oxygen species and antioxidant mechanisms in human tissues and their relation to malignancies. *Apmis* **115**, 81-103 (2007).

15. Mathews, C.K. DNA precursor metabolism and genomic stability. *Faseb J* **20**, 1300-1314 (2006).

16. Hidaka, K., Yamada, M., Kamiya, H., Masutani, C., Harashima, H., Hanaoka, F. & Nohmi, T. Specificity of mutations induced by incorporation of oxidized dNTPs into DNA by human DNA polymerase eta. *DNA Repair (Amst)* **7**, 497-506 (2008).

17. Nakabeppu, Y., Tsuchimoto, D., Furuichi, M. & Sakumi, K. The defense mechanisms in mammalian cells against oxidative damage in nucleic acids and their involvement in the suppression of mutagenesis and cell death. *Free Radic Res* **38**, 423-429 (2004).

18. Nakabeppu, Y., Sakumi, K., Sakamoto, K., Tsuchimoto, D., Tsuzuki, T. & Nakatsu, Y. Mutagenesis and carcinogenesis caused by the oxidation of nucleic acids. *Biol Chem* **387**, 373-379 (2006).

19. Macaluso, M., Paggi, M.G. & Giordano, A. Genetic and epigenetic alterations as hallmarks of the intricate road to cancer. *Oncogene* **22**, 6472-6478 (2003).

20. Furuta, J., Nobeyama, Y., Umebayashi, Y., Otsuka, F., Kikuchi, K. & Ushijima, T. Silencing of Peroxiredoxin 2 and aberrant methylation of 33 CpG islands in putative promoter regions in human malignant melanomas. *Cancer Res* **66**, 6080-6086 (2006).

21. Valinluck, V., Tsai, H.H., Rogstad, D.K., Burdzy, A., Bird, A. & Sowers, L.C. Oxidative damage to methyl-CpG sequences inhibits the binding of the methyl-CpG binding domain (MBD) of methyl-CpG binding protein 2 (MeCP2). *Nucleic Acids Res* **32**, 4100-4108 (2004).

22. Visvardis, E.E., Tassiou, A.M. & Piperakis, S.M. Study of DNA damage induction and repair capacity of fresh and cryopreserved lymphocytes exposed to H2O2 and gamma-irradiation with the alkaline comet assay. *Mutat Res* **383**, 71-80 (1997).

23. Lushchak, V.I. Free radical oxidation of proteins and its relationship with functional state of organisms. *Biochemistry (Mosc)* **72**, 809-827 (2007).

24. Landar, A. & Darley-Usmar, V.M. Nitric oxide and cell signaling: modulation of redox tone and protein modification. *Amino Acids* **25**, 313-321 (2003).

25. England, K. & Cotter, T.G. Direct oxidative modifications of signalling proteins in mammalian cells and their effects on apoptosis. *Redox Rep* **10**, 237-245 (2005).

26. Chakravarti, B. & Chakravarti, D.N. Oxidative modification of proteins: age-related changes. *Gerontology* **53**, 128-139 (2007).

27. Stadtman, E.R. Protein oxidation and aging. *Free Radic Res* **40**, 1250-1258 (2006).

28. Trachootham, D., Lu, W., Ogasawara, M.A., Nilsa, R.D. & Huang, P. Redox regulation of cell survival. *Antioxid Redox Signal* **10**, 1343-1374 (2008).

29. Leonberg, A.K. & Chai, Y.C. The functional role of cysteine residues for c-Abl kinase activity. *Mol Cell Biochem* **304**, 207-212 (2007).

30. Dalle-Donne, I., Scaloni, A., Giustarini, D., Cavarra, E., Tell, G., Lungarella, G., Colombo, R., Rossi, R. & Milzani, A. Proteins as biomarkers of oxidative/nitrosative stress in diseases: the contribution of redox proteomics. *Mass Spectrom Rev* **24**, 55-99 (2005).

31. Girotti, A.W. Lipid hydroperoxide generation, turnover, and effector action in biological systems. *J Lipid Res* **39**, 1529-1542 (1998).

32. Benhar, M., Engelberg, D. & Levitzki, A. ROS, stress-activated kinases and stress signaling in cancer. *EMBO Rep* **3**, 420-425 (2002).

33. Frey, R.S., Ushio-Fukai, M. & Malik, A. NADPH Oxidase-Dependent Signaling in Endothelial Cells: Role in Physiology and Pathophysiology. *Antioxid Redox Signal* (2008).

34. Galanis, A., Pappa, A., Giannakakis, A., Lanitis, E., Dangaj, D. & Sandaltzopoulos, R. Reactive oxygen species and HIF-1 signalling in cancer. *Cancer Lett* **266**, 12-20 (2008).

35. Gregg, D., de Carvalho, D.D. & Kovacic, H. Integrins and coagulation: a role for ROS/redox signaling? *Antioxid Redox Signal* **6**, 757-764 (2004).

36. Rajagopalan, S., Meng, X.P., Ramasamy, S., Harrison, D.G. & Galis, Z.S. Reactive oxygen species produced by macrophage-derived foam cells regulate the activity of vascular matrix metalloproteinases in vitro. Implications for atherosclerotic plaque stability. *J Clin Invest* **98**, 2572-2579 (1996).

37. Wary, K.K., Thakker, G.D., Humtsoe, J.O. & Yang, J. Analysis of VEGF-responsive genes involved in the activation of endothelial cells. *Mol Cancer* **2**, 25 (2003).

38. Wartenberg, M., Donmez, F., Ling, F.C., Acker, H., Hescheler, J. & Sauer, H. Tumor-induced angiogenesis studied in confrontation cultures of multicellular tumor spheroids and embryoid bodies grown from pluripotent embryonic stem cells. *Faseb J* **15**, 995-1005 (2001).

39. Weinberg, R.A. The retinoblastoma protein and cell cycle control. *Cell* **81**, 323-330 (1995).

40. Takahashi, A., Ohtani, N., Yamakoshi, K., Iida, S., Tahara, H., Nakayama, K., Nakayama, K.I., Ide, T., Saya, H. & Hara, E. Mitogenic signalling and the p16INK4a-Rb pathway cooperate to enforce irreversible cellular senescence. *Nat Cell Biol* **8**, 1291-1297 (2006).

41. Hosako, M., Ogino, T., Omori, M. & Okada, S. Cell cycle arrest by monochloramine through the oxidation of retinoblastoma protein. *Free Radic Biol Med* **36**, 112-122 (2004).

42. Liu, B., Chen, Y. & St Clair, D.K. ROS and p53: a versatile partnership. *Free Radic Biol Med* **44**, 1529-1535 (2008).

43. Sun, Y. & Oberley, L.W. Redox regulation of transcriptional activators. *Free Radic Biol Med* **21**, 335-348 (1996).

44. Rainwater, R., Parks, D., Anderson, M.E., Tegtmeyer, P. & Mann, K. Role of cysteine residues in regulation of p53 function. *Mol Cell Biol* **15**, 3892-3903 (1995).

45. Faderl, S., Talpaz, M., Estrov, Z., O'Brien, S., Kurzrock, R. & Kantarjian, H.M. The biology of chronic myeloid leukemia. *N Engl J Med* **341**, 164-172 (1999).

46. Ren, R. Mechanisms of BCR-ABL in the pathogenesis of chronic myelogenous leukaemia. *Nat Rev Cancer* **5**, 172-183 (2005).

47. Melo, J.V. & Barnes, D.J. Chronic myeloid leukaemia as a model of disease evolution in human cancer. *Nat Rev Cancer* **7**, 441-453 (2007).

48. Wong, S. & Witte, O.N. Modeling Philadelphia chromosome positive leukemias. *Oncogene* **20**, 5644-5659 (2001).

49. Zhang, X. & Ren, R. Bcr-Abl efficiently induces a myeloproliferative disease and production of excess interleukin-3 and granulocyte-macrophage colony-stimulating factor in mice: a novel model for chronic myelogenous leukemia. *Blood* **92**, 3829-3840 (1998).

50. Pear, W.S., Miller, J.P., Xu, L., Pui, J.C., Soffer, B., Quackenbush, R.C., Pendergast, A.M., Bronson, R., Aster, J.C., Scott, M.L. & Baltimore, D. Efficient and rapid induction of a chronic myelogenous leukemia-like myeloproliferative disease in mice receiving P210 bcr/abl-transduced bone marrow. *Blood* **92**, 3780-3792 (1998).

51. Pasternak, G., Hochhaus, A., Schultheis, B. & Hehlmann, R. Chronic myelogenous leukemia: molecular and cellular aspects. *J Cancer Res Clin Oncol* **124**, 643-660 (1998).

52. Lin, H., Monaco, G., Sun, T., Ling, X., Stephens, C., Xie, S., Belmont, J. & Arlinghaus, R. Bcr-Abl-mediated suppression of normal hematopoiesis in leukemia. *Oncogene* **24**, 3246-3256 (2005).

53. Valko, M., Rhodes, C.J., Moncol, J., Izakovic, M. & Mazur, M. Free radicals, metals and antioxidants in oxidative stress-induced cancer. *Chem Biol Interact* **160**, 1-40 (2006).

54. Kovacic, P. & Jacintho, J.D. Mechanisms of carcinogenesis: focus on oxidative stress and electron transfer. *Curr Med Chem* **8**, 773-796 (2001).

55. Klaunig, J.E. & Kamendulis, L.M. The role of oxidative stress in carcinogenesis. *Annu Rev Pharmacol Toxicol* **44**, 239-267 (2004).

56. Behrend, L., Henderson, G. & Zwacka, R.M. Reactive oxygen species in oncogenic transformation. *Biochem Soc Trans* **31**, 1441-1444 (2003).

57. Sablina, A.A., Budanov, A.V., Ilyinskaya, G.V., Agapova, L.S., Kravchenko, J.E. & Chumakov, P.M. The antioxidant function of the p53 tumor suppressor. *Nature medicine* **11**, 1306-1313 (2005).

58. Nowicki, M.O., Falinski, R., Koptyra, M., Slupianek, A., Stoklosa, T., Gloc, E., Nieborowska-Skorska, M., Blasiak, J. & Skorski, T. BCR/ABL oncogenic kinase promotes unfaithful repair of the reactive oxygen species-dependent DNA double-strand breaks. *Blood* **104**, 3746-3753 (2004).

59. Koptyra, M., Falinski, R., Nowicki, M.O., Stoklosa, T., Majsterek, I., Nieborowska-Skorska, M., Blasiak, J. & Skorski, T. BCR/ABL kinase induces self-mutagenesis via reactive oxygen species to encode imatinib resistance. *Blood* **108**, 319-327 (2006).

60. Kim, J.H., Chu, S.C., Gramlich, J.L., Pride, Y.B., Babendreier, E., Chauhan, D., Salgia, R., Podar, K., Griffin, J.D. & Sattler, M. Activation of the PI3K/mTOR pathway by BCR-ABL contributes to increased production of reactive oxygen species. *Blood* **105**, 1717-1723 (2005).

61. Koptyra, M., Cramer, K., Slupianek, A., Richardson, C. & Skorski, T. BCR/ABL promotes accumulation of chromosomal aberrations induced by oxidative and genotoxic stress. *Leukemia* **22**, 1969-1972 (2008).

62. Sattler, M., Verma, S., Shrikhande, G., Byrne, C.H., Pride, Y.B., Winkler, T., Greenfield, E.A., Salgia, R. & Griffin, J.D. The BCR/ABL tyrosine kinase induces production of reactive oxygen species in hematopoietic cells. *J Biol Chem* **275**, 24273-24278 (2000).

63. Rodrigues, M.S., Reddy, M.M. & Sattler, M. Cell cycle regulation by oncogenic tyrosine kinases in myeloid neoplasias: from molecular redox

mechanisms to health implications. *Antioxid Redox Signal* **10**, 1813-1848 (2008).

64. Liu, J., Wu, Y., Ma, G.Z., Lu, D., Haataja, L., Heisterkamp, N., Groffen, J. & Arlinghaus, R.B. Inhibition of Bcr serine kinase by tyrosine phosphorylation. *Mol Cell Biol* **16**, 998-1005 (1996).

65. McGahon, A., Bissonnette, R., Schmitt, M., Cotter, K.M., Green, D.R. & Cotter, T.G. BCR-ABL maintains resistance of chronic myelogenous leukemia cells to apoptotic cell death. *Blood* **83**, 1179-1187 (1994).

66. Zou, X. & Calame, K. Signaling pathways activated by oncogenic forms of Abl tyrosine kinase. *J Biol Chem* **274**, 18141-18144 (1999).

67. Fernandez-Luna, J.L. Bcr-Abl and inhibition of apoptosis in chronic myelogenous leukemia cells. *Apoptosis* **5**, 315-318 (2000).

68. Minn, A.J., Kettlun, C.S., Liang, H., Kelekar, A., Vander Heiden, M.G., Chang, B.S., Fesik, S.W., Fill, M. & Thompson, C.B. Bcl-xL regulates apoptosis by heterodimerization-dependent and -independent mechanisms. *Embo J* **18**, 632-643 (1999).

69. Xu, L., Koumenis, I.L., Tilly, J.L. & Giffard, R.G. Overexpression of bcl-xL protects astrocytes from glucose deprivation and is associated with higher glutathione, ferritin, and iron levels. *Anesthesiology* **91**, 1036-1046 (1999).

70. Gouaze, V., Andrieu-Abadie, N., Cuvillier, O., Malagarie-Cazenave, S., Frisach, M.F., Mirault, M.E. & Levade, T. Glutathione peroxidase-1 protects from CD95-induced apoptosis. *J Biol Chem* **277**, 42867-42874 (2002).

71. Hall, A.G. Review: The role of glutathione in the regulation of apoptosis. *Eur J Clin Invest* **29**, 238-245 (1999).

72. Ghibelli, L., Fanelli, C., Rotilio, G., Lafavia, E., Coppola, S., Colussi, C., Civitareale, P. & Ciriolo, M.R. Rescue of cells from apoptosis by inhibition of active GSH extrusion. *Faseb J* **12**, 479-486 (1998).

73. Franco, R., Schoneveld, O.J., Pappa, A. & Panayiotidis, M.I. The central role of glutathione in the pathophysiology of human diseases. *Archives of physiology and biochemistry* **113**, 234-258 (2007).

74. Yi, C.H., Pan, H., Seebacher, J., Jang, I.H., Hyberts, S.G., Heffron, G.J., Vander Heiden, M.G., Yang, R., Li, F., Locasale, J.W., Sharfi, H., Zhai, B., Rodriguez-Mias, R., Luithardt, H., Cantley, L.C., Daley, G.Q., Asara, J.M., Gygi, S.P., Wagner, G., Liu, C.F. & Yuan, J. Metabolic regulation of protein N-alpha-acetylation by Bcl-xL promotes cell survival. *Cell* **146**, 607-620 (2011).

75. Amarante-Mendes, G.P., McGahon, A.J., Nishioka, W.K., Afar, D.E., Witte, O.N. & Green, D.R. Bcl-2-independent Bcr-Abl-mediated resistance to apoptosis: protection is correlated with up regulation of Bcl-xL. *Oncogene* **16**, 1383-1390 (1998).

76. Horita, M., Andreu, E.J., Benito, A., Arbona, C., Sanz, C., Benet, I., Prosper, F. & Fernandez-Luna, J.L. Blockade of the Bcr-Abl kinase activity induces apoptosis of chronic myelogenous leukemia cells by suppressing signal transducer and activator of transcription 5-dependent expression of Bcl-xL. *J Exp Med* **191**, 977-984 (2000).

77. de Groot, R.P., Raaijmakers, J.A., Lammers, J.W. & Koenderman, L. STAT5-Dependent CyclinD1 and Bcl-xL expression in Bcr-Abl-transformed cells. *Mol Cell Biol Res Commun* **3**, 299-305 (2000).

78. Shuai, K., Halpern, J., ten Hoeve, J., Rao, X. & Sawyers, C.L. Constitutive activation of STAT5 by the BCR-ABL oncogene in chronic myelogenous leukemia. *Oncogene* **13**, 247-254 (1996).

79. Nieborowska-Skorska, M., Wasik, M.A., Slupianek, A., Salomoni, P., Kitamura, T., Calabretta, B. & Skorski, T. Signal transducer and activator of transcription (STAT)5 activation by BCR/ABL is dependent on intact Src homology (SH)3 and SH2 domains of BCR/ABL and is required for leukemogenesis. *J Exp Med* **189**, 1229-1242 (1999).

80. Klejman, A., Schreiner, S.J., Nieborowska-Skorska, M., Slupianek, A., Wilson, M., Smithgall, T.E. & Skorski, T. The Src family kinase Hck couples BCR/ABL to STAT5 activation in myeloid leukemia cells. *Embo J* **21**, 5766-5774 (2002).

81. Tao, W.J., Lin, H., Sun, T., Samanta, A.K. & Arlinghaus, R. BCR-ABL oncogenic transformation of NIH 3T3 fibroblasts requires the IL-3 receptor. *Oncogene* **27**, 3194-3200 (2008).

82. Sattler, M., Winkler, T., Verma, S., Byrne, C.H., Shrikhande, G., Salgia, R. & Griffin, J.D. Hematopoietic growth factors signal through the formation of reactive oxygen species. *Blood* **93**, 2928-2935 (1999).

83. Simon, A.R., Rai, U., Fanburg, B.L. & Cochran, B.H. Activation of the JAK-STAT pathway by reactive oxygen species. *Am J Physiol* **275**, C1640-1652 (1998).

84. Gabriele, L., Phung, J., Fukumoto, J., Segal, D., Wang, I.M., Giannakakou, P., Giese, N.A., Ozato, K. & Morse, H.C., 3rd. Regulation of apoptosis in myeloid cells by interferon consensus sequence-binding protein. *J Exp Med* **190**, 411-421 (1999).

85. Diaz-Blanco, E., Bruns, I., Neumann, F., Fischer, J.C., Graef, T., Rosskopf, M., Brors, B., Pechtel, S., Bork, S., Koch, A., Baer, A., Rohr, U.P., Kobbe, G., Haeseler, A., Gattermann, N., Haas, R. & Kronenwett, R. Molecular signature of CD34(+) hematopoietic stem and progenitor cells of patients with CML in chronic phase. *Leukemia* **21**, 494-504 (2007).

86. Ng, C.F., Schafer, F.Q., Buettner, G.R. & Rodgers, V.G. The rate of cellular hydrogen peroxide removal shows dependency on GSH: mathematical insight into in vivo H2O2 and GPx concentrations. *Free Radic Res* **41**, 1201-1211 (2007).

87. Lei, X.G., Cheng, W.H. & McClung, J.P. Metabolic regulation and function of glutathione peroxidase-1. *Annu Rev Nutr* **27**, 41-61 (2007).

88. Griffith, O.W. Biologic and pharmacologic regulation of mammalian glutathione synthesis. *Free Radic Biol Med* **27**, 922-935 (1999).

89. Tew, K.D. Redox in redux: Emergent roles for glutathione S-transferase P (GSTP) in regulation of cell signaling and S-glutathionylation. *Biochem Pharmacol* **73**, 1257-1269 (2007).

90. Druker, B.J., O'Brien, S.G., Cortes, J. & Radich, J. Chronic myelogenous leukemia. *Hematology Am Soc Hematol Educ Program*, 111-135 (2002).

91. Druker, B.J., Talpaz, M., Resta, D.J., Peng, B., Buchdunger, E., Ford, J.M., Lydon, N.B., Kantarjian, H., Capdeville, R., Ohno-Jones, S. & Sawyers, C.L. Efficacy and safety of a specific inhibitor of the BCR-ABL tyrosine kinase in chronic myeloid leukemia. *N Engl J Med* **344**, 1031-1037 (2001).

92. Kantarjian, H., Sawyers, C., Hochhaus, A., Guilhot, F., Schiffer, C., Gambacorti-Passerini, C., Niederwieser, D., Resta, D., Capdeville, R., Zoellner, U., Talpaz, M., Druker, B., Goldman, J., O'Brien, S.G., Russell, N., Fischer, T., Ottmann, O., Cony-Makhoul, P., Facon, T., Stone, R., Miller, C., Tallman, M., Brown, R., Schuster, M., Loughran, T., Gratwohl, A., Mandelli, F., Saglio, G., Lazzarino, M., Russo, D., Baccarani, M. & Morra, E. Hematologic and cytogenetic responses to imatinib mesylate in chronic myelogenous leukemia. *N Engl J Med* **346**, 645-652 (2002).

93. Hughes, T., Deininger, M., Hochhaus, A., Branford, S., Radich, J., Kaeda, J., Baccarani, M., Cortes, J., Cross, N.C., Druker, B.J., Gabert, J., Grimwade, D., Hehlmann, R., Kamel-Reid, S., Lipton, J.H., Longtine, J., Martinelli, G., Saglio, G., Soverini, S., Stock, W. & Goldman, J.M. Monitoring CML patients responding to treatment with tyrosine kinase inhibitors: review and recommendations for harmonizing current methodology for detecting BCR-ABL transcripts and kinase domain mutations and for expressing results. *Blood* **108**, 28-37 (2006).

94. Cortes, J., Giles, F., O'Brien, S., Thomas, D., Garcia-Manero, G., Rios, M.B., Faderl, S., Verstovsek, S., Ferrajoli, A., Freireich, E.J., Talpaz, M. & Kantarjian, H. Result of high-dose imatinib mesylate in patients with Philadelphia chromosome-positive chronic myeloid leukemia after failure of interferon-alpha. *Blood* **102**, 83-86 (2003).

95. Kantarjian, H., Talpaz, M., O'Brien, S., Garcia-Manero, G., Verstovsek, S., Giles, F., Rios, M.B., Shan, J., Letvak, L., Thomas, D., Faderl, S., Ferrajoli, A. & Cortes, J. High-dose imatinib mesylate therapy in newly diagnosed Philadelphia chromosome-positive chronic phase chronic myeloid leukemia. *Blood* **103**, 2873-2878 (2004).

96. Gorre, M.E., Mohammed, M., Ellwood, K., Hsu, N., Paquette, R., Rao, P.N. & Sawyers, C.L. Clinical resistance to STI-571 cancer therapy caused by BCR-ABL gene mutation or amplification. *Science* **293**, 876-880 (2001).

97. Shah, N.P., Nicoll, J.M., Nagar, B., Gorre, M.E., Paquette, R.L., Kuriyan, J. & Sawyers, C.L. Multiple BCR-ABL kinase domain mutations confer polyclonal resistance to the tyrosine kinase inhibitor imatinib (STI571) in chronic phase and blast crisis chronic myeloid leukemia. *Cancer Cell* **2**, 117-125 (2002).

98. Branford, S., Rudzki, Z., Walsh, S., Parkinson, I., Grigg, A., Szer, J., Taylor, K., Herrmann, R., Seymour, J.F., Arthur, C., Joske, D., Lynch, K. & Hughes, T. Detection of BCR-ABL mutations in patients with CML treated with imatinib is virtually always accompanied by clinical resistance, and

mutations in the ATP phosphate-binding loop (P-loop) are associated with a poor prognosis. *Blood* **102**, 276-283 (2003).

99. Yamamoto, M., Kurosu, T., Kakihana, K., Mizuchi, D. & Miura, O. The two major imatinib resistance mutations E255K and T315I enhance the activity of BCR/ABL fusion kinase. *Biochem Biophys Res Commun* **319**, 1272-1275 (2004).

100. Talpaz, M., Shah, N.P., Kantarjian, H., Donato, N., Nicoll, J., Paquette, R., Cortes, J., O'Brien, S., Nicaise, C., Bleickardt, E., Blackwood-Chirchir, M.A., Iyer, V., Chen, T.T., Huang, F., Decillis, A.P. & Sawyers, C.L. Dasatinib in imatinib-resistant Philadelphia chromosome-positive leukemias. *N Engl J Med* **354**, 2531-2541 (2006).

101. Cortes, J., Rousselot, P., Kim, D.W., Ritchie, E., Hamerschlak, N., Coutre, S., Hochhaus, A., Guilhot, F., Saglio, G., Apperley, J., Ottmann, O., Shah, N., Erben, P., Branford, S., Agarwal, P., Gollerkeri, A. & Baccarani, M. Dasatinib induces complete hematologic and cytogenetic responses in patients with imatinib-resistant or -intolerant chronic myeloid leukemia in blast crisis. *Blood* **109**, 3207-3213 (2007).

102. Bradeen, H.A., Eide, C.A., O'Hare, T., Johnson, K.J., Willis, S.G., Lee, F.Y., Druker, B.J. & Deininger, M.W. Comparison of imatinib mesylate, dasatinib (BMS-354825), and nilotinib (AMN107) in an N-ethyl-N-nitrosourea (ENU)-based mutagenesis screen: high efficacy of drug combinations. *Blood* **108**, 2332-2338 (2006).

103. Druker, B.J. Circumventing resistance to kinase-inhibitor therapy. *N Engl J Med* **354**, 2594-2596 (2006).

104. Quintas-Cardama, A., Kantarjian, H. & Cortes, J. Flying under the radar: the new wave of BCR-ABL inhibitors. *Nat Rev Drug Discov* **6**, 834-848 (2007).

105. Ghaffari, S., Jagani, Z., Kitidis, C., Lodish, H.F. & Khosravi-Far, R. Cytokines and BCR-ABL mediate suppression of TRAIL-induced apoptosis through inhibition of forkhead FOXO3a transcription factor. *Proc Natl Acad Sci U S A* **100**, 6523-6528 (2003).

106. Dierov, J., Dierova, R. & Carroll, M. BCR/ABL translocates to the nucleus and disrupts an ATR-dependent intra-S phase checkpoint. *Cancer Cell* **5**, 275-285 (2004).

107. Ahuja, H., Bar-Eli, M., Advani, S.H., Benchimol, S. & Cline, M.J. Alterations in the p53 gene and the clonal evolution of the blast crisis of chronic myelocytic leukemia. *Proc Natl Acad Sci U S A* **86**, 6783-6787 (1989).

108. Maiorino, M., Chu, F.F., Ursini, F., Davies, K.J., Doroshow, J.H. & Esworthy, R.S. Phospholipid hydroperoxide glutathione peroxidase is the 18-kDa selenoprotein expressed in human tumor cell lines. *J Biol Chem* **266**, 7728-7732 (1991).

109. Cilloni, D., Messa, F., Arruga, F., Defilippi, I., Morotti, A., Messa, E., Carturan, S., Giugliano, E., Pautasso, M., Bracco, E., Rosso, V., Sen, A., Martinelli, G., Baccarani, M. & Saglio, G. The NF-kappaB pathway

blockade by the IKK inhibitor PS1145 can overcome imatinib resistance. *Leukemia* **20**, 61-67 (2006).

110. Wei, Y., Stockelberg, D., Hullberg, S., Ricksten, A. & Wadenvik, H. Changes in expression of apoptosis-related genes are linked to the molecular response to imatinib treatment in chronic-phase chronic myeloid leukemia patients. *Acta Haematol* **117**, 83-90 (2007).

111. Donato, N.J., Wu, J.Y., Stapley, J., Gallick, G., Lin, H., Arlinghaus, R. & Talpaz, M. BCR-ABL independence and LYN kinase overexpression in chronic myelogenous leukemia cells selected for resistance to STI571. *Blood* **101**, 690-698 (2003).

112. Konig, H., Hartel, N., Schultheis, B., Schatz, M., Lorentz, C., Melo, J.V., Hehlmann, R., Hochhaus, A. & La Rosee, P. Enhanced Bcr-Abl-specific antileukemic activity of arsenic trioxide (Trisenox) through glutathione-depletion in imatinib-resistant cells. *Haematologica* **92**, 838-841 (2007).

113. Bang, J.H., Han, E.S., Lim, I. & Lee, C.S. Differential response of MG132 cytotoxicity against small cell lung cancer cells to changes in cellular GSH contents. *Biochem Pharmacol* **68**, 659-666 (2004).

114. Zhang, H., Trachootham, D., Lu, W., Carew, J., Giles, F.J., Keating, M.J., Arlinghaus, R.B. & Huang, P. Effective killing of Gleevec-resistant CML cells with T315I mutation by a natural compound PEITC through redox-mediated mechanism. *Leukemia* **22**, 1191-1199 (2008).

115. Lozzio, C.B. & Lozzio, B.B. Human chronic myelogenous leukemia cell-line with positive Philadelphia chromosome. *Blood* **45**, 321-334 (1975).

116. Beran, M., Pisa, P., O'Brien, S., Kurzrock, R., Siciliano, M., Cork, A., Andersson, B.S., Kohli, V. & Kantarjian, H. Biological properties and growth in SCID mice of a new myelogenous leukemia cell line (KBM-5) derived from chronic myelogenous leukemia cells in the blastic phase. *Cancer Res* **53**, 3603-3610 (1993).

117. Wetzler, M., Talpaz, M., Van Etten, R.A., Hirsh-Ginsberg, C., Beran, M. & Kurzrock, R. Subcellular localization of Bcr, Abl, and Bcr-Abl proteins in normal and leukemic cells and correlation of expression with myeloid differentiation. *J Clin Invest* **92**, 1925-1939 (1993).

118. Ricci, C., Scappini, B., Divoky, V., Gatto, S., Onida, F., Verstovsek, S., Kantarjian, H.M. & Beran, M. Mutation in the ATP-binding pocket of the ABL kinase domain in an STI571-resistant BCR/ABL-positive cell line. *Cancer Res* **62**, 5995-5998 (2002).

119. Deng, M. & Daley, G.Q. Expression of interferon consensus sequence binding protein induces potent immunity against BCR/ABL-induced leukemia. *Blood* **97**, 3491-3497 (2001).

120. Shah, N.P., Tran, C., Lee, F.Y., Chen, P., Norris, D. & Sawyers, C.L. Overriding imatinib resistance with a novel ABL kinase inhibitor. *Science* **305**, 399-401 (2004).

121. Samanta, A.K., Lin, H., Sun, T., Kantarjian, H. & Arlinghaus, R.B. Janus kinase 2: a critical target in chronic myelogenous leukemia. *Cancer Res* **66**, 6468-6472 (2006).

122. Zhou, Y., Achanta, G., Pelicano, H., Gandhi, V., Plunkett, W. & Huang, P. Action of (E)-2'-deoxy-2'-(fluoromethylene)cytidine on DNA metabolism: incorporation, excision, and cellular response. *Mol Pharmacol* **61**, 222-229 (2002).

123. Trachootham, D., Zhou, Y., Zhang, H., Demizu, Y., Chen, Z., Pelicano, H., Chiao, P.J., Achanta, G., Arlinghaus, R.B., Liu, J. & Huang, P. Selective killing of oncogenically transformed cells through a ROS-mediated mechanism by beta-phenylethyl isothiocyanate. *Cancer Cell* **10**, 241-252 (2006).

124. Liebes, L., Conaway, C.C., Hochster, H., Mendoza, S., Hecht, S.S., Crowell, J. & Chung, F.L. High-performance liquid chromatography-based determination of total isothiocyanate levels in human plasma: application to studies with 2-phenethyl isothiocyanate. *Anal Biochem* **291**, 279-289 (2001).

125. Wu, S.J., Ng, L.T. & Lin, C.C. Effects of antioxidants and caspase-3 inhibitor on the phenylethyl isothiocyanate-induced apoptotic signaling pathways in human PLC/PRF/5 cells. *Eur J Pharmacol* **518**, 96-106 (2005).

126. Di Bacco, A.M. & Cotter, T.G. p53 expression in K562 cells is associated with caspase-mediated cleavage of c-ABL and BCR-ABL protein kinases. *Br J Haematol* **117**, 588-597 (2002).

127. Barila, D., Rufini, A., Condo, I., Ventura, N., Dorey, K., Superti-Furga, G. & Testi, R. Caspase-dependent cleavage of c-Abl contributes to apoptosis. *Mol Cell Biol* **23**, 2790-2799 (2003).

128. Machuy, N., Rajalingam, K. & Rudel, T. Requirement of caspase-mediated cleavage of c-Abl during stress-induced apoptosis. *Cell Death Differ* **11**, 290-300 (2004).

129. Podar, K., Raab, M.S., Tonon, G., Sattler, M., Barila, D., Zhang, J., Tai, Y.T., Yasui, H., Raje, N., DePinho, R.A., Hideshima, T., Chauhan, D. & Anderson, K.C. Up-regulation of c-Jun inhibits proliferation and induces apoptosis via caspase-triggered c-Abl cleavage in human multiple myeloma. *Cancer Res* **67**, 1680-1688 (2007).

130. Corbin, A.S., Agarwal, A., Loriaux, M., Cortes, J., Deininger, M.W. & Druker, B.J. Human chronic myeloid leukemia stem cells are insensitive to imatinib despite inhibition of BCR-ABL activity. *J Clin Invest* **121**, 396-409 (2011).

131. Hu, Y., Benedict, M.A., Wu, D., Inohara, N. & Nunez, G. Bcl-XL interacts with Apaf-1 and inhibits Apaf-1-dependent caspase-9 activation. *Proc Natl Acad Sci U S A* **95**, 4386-4391 (1998).

132. Huang, D.C., Adams, J.M. & Cory, S. The conserved N-terminal BH4 domain of Bcl-2 homologues is essential for inhibition of apoptosis and interaction with CED-4. *Embo J* **17**, 1029-1039 (1998).

133. Pan, G., O'Rourke, K. & Dixit, V.M. Caspase-9, Bcl-XL, and Apaf-1 form a ternary complex. *J Biol Chem* **273**, 5841-5845 (1998).

134. Yang, J., Liu, X., Bhalla, K., Kim, C.N., Ibrado, A.M., Cai, J., Peng, T.I., Jones, D.P. & Wang, X. Prevention of apoptosis by Bcl-2: release of cytochrome c from mitochondria blocked. *Science* **275**, 1129-1132 (1997).

135. Delia, D., Aiello, A., Soligo, D., Fontanella, E., Melani, C., Pezzella, F., Pierotti, M.A. & Della Porta, G. bcl-2 proto-oncogene expression in normal and neoplastic human myeloid cells. *Blood* **79**, 1291-1298 (1992).

136. Handa, H., Hegde, U.P., Kotelnikov, V.M., Mundle, S.D., Dong, L.M., Burke, P., Rose, S., Gaskin, F., Raza, A. & Preisler, H.D. Bcl-2 and c-myc expression, cell cycle kinetics and apoptosis during the progression of chronic myelogenous leukemia from diagnosis to blastic phase. *Leuk Res* **21**, 479-489 (1997).

137. Hole, P.S., Pearn, L., Tonks, A.J., James, P.E., Burnett, A.K., Darley, R.L. & Tonks, A. Ras-induced reactive oxygen species promote growth factor-independent proliferation in human CD34+ hematopoietic progenitor cells. *Blood* **115**, 1238-1246 (2010).

138. Tweardy, D.J., Morel, P.A., Mott, P.L., Glazer, E.W., Zeh, H.J. & Sakurai, M. Modulation of myeloid proliferation and differentiation by monoclonal antibodies directed against a protein that interacts with the interleukin-3 receptor. *Blood* **80**, 359-366 (1992).

139. Oliver, L., Hue, E., Rossignol, J., Bougras, G., Hulin, P., Naveilhan, P., Heymann, D., Lescaudron, L. & Vallette, F.M. Distinct roles of Bcl-2 and Bcl-Xl in the apoptosis of human bone marrow mesenchymal stem cells during differentiation. *PLoS One* **6**, e19820 (2011).

140. Hockenbery, D.M., Oltvai, Z.N., Yin, X.M., Milliman, C.L. & Korsmeyer, S.J. Bcl-2 functions in an antioxidant pathway to prevent apoptosis. *Cell* **75**, 241-251 (1993).

141. Voehringer, D.W., McConkey, D.J., McDonnell, T.J., Brisbay, S. & Meyn, R.E. Bcl-2 expression causes redistribution of glutathione to the nucleus. *Proc Natl Acad Sci U S A* **95**, 2956-2960 (1998).

142. Chen, Z.X. & Pervaiz, S. BCL-2: pro-or anti-oxidant? *Front Biosci (Elite Ed)* **1**, 263-268 (2009).

143. Friesen, C., Kiess, Y. & Debatin, K.M. A critical role of glutathione in determining apoptosis sensitivity and resistance in leukemia cells. *Cell Death Differ* **11 Suppl 1**, S73-85 (2004).

144. Chen, G., Chen, Z., Hu, Y. & Huang, P. Inhibition of Mitochondrial Respiration and Rapid Depletion of Mitochondrial Glutathione by beta-Phenethyl Isothiocyanate: Mechanisms for Anti-Leukemia Activity. *Antioxid Redox Signal* **15**, 2911-2921 (2011).

145. Hole, P.S., Darley, R.L. & Tonks, A. Do reactive oxygen species play a role in myeloid leukemias? *Blood* **117**, 5816-5826 (2011).

146. Hussain, S.P., Amstad, P., He, P., Robles, A., Lupold, S., Kaneko, I., Ichimiya, M., Sengupta, S., Mechanic, L., Okamura, S., Hofseth, L.J., Moake, M., Nagashima, M., Forrester, K.S. & Harris, C.C. p53-induced up-regulation of MnSOD and GPx but not catalase increases oxidative stress and apoptosis. *Cancer Res* **64**, 2350-2356 (2004).

147. Throm, S.L. & Klemsz, M.J. PU.1 regulates glutathione peroxidase expression in neutrophils. *J Leukoc Biol* **74**, 111-117 (2003).

148. Sen, S., Takahashi, R., Rani, S., Freireich, E.J. & Stass, S.A. Expression of differentially phosphorylated Rb and mutant p53 proteins in myeloid leukemia cell lines. *Leuk Res* **17**, 639-647 (1993).

149. Marinkovic, D., Zhang, X., Yalcin, S., Luciano, J.P., Brugnara, C., Huber, T. & Ghaffari, S. Foxo3 is required for the regulation of oxidative stress in erythropoiesis. *J Clin Invest* **117**, 2133-2144 (2007).

150. Wilson, M.K., McWhirter, S.M., Amin, R.H., Huang, D. & Schlissel, M.S. Abelson virus transformation prevents TRAIL expression by inhibiting FoxO3a and NF-kappaB. *Mol Cells* **29**, 333-341 (2010).

VITA

Hui Zhang was born in Beijing, China on July 30, 1977, the son of Meizhu Yin and Yongliang Zhang. After completing his work at Beijing No. 4 High School, Beijing, China in 1996, he entered Nanjing University in Nanjing, Jiangsu China. He received the degree of Bachelor of Science with a major in biology from Nanjing University in May, 2000. Then, he continued his study in Nanjing University for the next three years and received the degree of Master of Science in May, 2003. In September of 2005 he entered The University of Texas Health Science Center at Houston Graduate School of Biomedical Sciences.